

Analytic and numerical bootstrap for the long-range Ising model

Connor Behan¹, Edoardo Lauria², Maria Nocchi¹, Philine van Vliet³

¹ Mathematical Institute, University of Oxford, Andrew Wiles Building, Radcliffe Observatory Quarter, Woodstock Road, Oxford, OX2 6GG, UK

² LPENS, Département de physique, École Normale Supérieure - PSL
Centre Automatique et Systèmes (CAS), Mines Paris - PSL
Université PSL, Sorbonne Université, CNRS, Inria, 75005 Paris

³ Deutsches Elektronen-Synchrotron DESY, Notkestr. 85, 22607 Hamburg, Germany
Laboratoire de Physique Théorique de l'École Normale Supérieure, PSL University,
CNRS, Sorbonne Universités, UPMC Univ. Paris 06
24 rue Lhomond, 75231 Paris Cedex 05, France

behan@maths.ox.ac.uk, edoardo.lauria@minesparis.psl.eu,
nocchi@maths.ox.ac.uk, philine.vanvliet@phys.ens.fr

Abstract

We combine perturbation theory with analytic and numerical bootstrap techniques to study the critical point of the long-range Ising (LRI) model in two and three dimensions. We use the inversion formula to compute infinitely-many three-loop corrections in the two-dimensional LRI and near the mean-field end. We further exploit the exact OPE relations that follow from bulk locality of the LRI to compute infinitely-many two-loop corrections near the mean-field end, as well as some one-loop corrections near the short-range Ising end. By including such exact OPE relations in the crossing equations for LRI we set up a very constrained bootstrap problem, which we solve numerically using SDPB. We find a family of sharp kinks for two- and three-dimensional theories which we compare with the perturbative predictions for LRI, and with some Monte-Carlo simulations for the two-dimensional LRI.

Contents

| | | |
|----------|--|-----------|
| 1 | Introduction | 2 |
| 2 | Long-range Ising model as a defect CFT | 6 |
| 2.1 | Bulk two-point function of Φ | 6 |
| 2.2 | OPE relations | 10 |
| 3 | Perturbation theory | 13 |
| 3.1 | Review of results in the literature | 14 |
| 3.2 | Using OPE relations from the short-range end | 17 |
| 3.3 | Using OPE relations from the mean-field end | 18 |
| 3.4 | Generalization to long-range $O(N)$ models | 22 |
| 3.5 | Taking stock | 24 |
| 4 | Inversion formula | 25 |
| 4.1 | Overview | 26 |
| 4.2 | Results at two loops | 27 |
| 4.3 | Results at three loops | 30 |
| 4.4 | Further comments | 31 |
| 5 | Numerical results | 31 |
| 5.1 | Warm-up | 32 |
| 5.2 | Kinks in two dimensions | 35 |
| 5.3 | Checks of the critical exponents | 38 |
| 5.4 | Kinks in three dimensions | 42 |
| 6 | Conclusions and outlook | 43 |
| A | Details on the numerics | 45 |
| A.1 | Crossing equations | 45 |
| A.2 | Differences compared to integer codimension | 46 |
| B | Perturbative computations | 47 |
| B.1 | Master integrals | 47 |
| B.2 | Conventions | 47 |
| B.3 | Defect correlators | 49 |
| B.4 | Bulk two-point functions | 53 |

1 Introduction

The importance of studying Conformal Field Theories (CFTs) without a stress tensor can be motivated from various angles. The past decade has seen a surge of interest in Quantum Field Theories (QFTs) that live on a fixed AdS background. Due to the lack of dynamical gravity, the CFT which encodes boundary correlation functions has no stress tensor and is therefore called nonlocal. In particular, one can consider asymptotically heavy operators to recover the flat-space S-matrix [1]. A closely related development is defect CFT [2] dealing with critical systems which have part of their conformal symmetry broken by extended objects. While locality of the bulk places some constraints on the admissible defects, correlators restricted to them will always obey the axioms of a nonlocal CFT. Since the mass of a field in AdS and the co-dimension of a defect can both be varied, it is easy for nonlocal theories to appear in continuous families.

Another motivation comes from the non-perturbative bootstrap [3], which has had a great impact, both practical and philosophical, on the study of CFTs. Much of the bootstrap toolkit works best when traditional assumptions about QFT such as locality are relaxed. One can notice that the works [4, 5], in their efforts to study a local CFT, happened to produce several bounds which were saturated by nonlocal CFTs. In fact, [6] is the only non-supersymmetric numerical bootstrap study to date which has treated locality as an input instead of an output. Hence, a complete picture of the solutions found by most numerical bootstrap studies requires an understanding of nonlocal CFTs.

The goal of this paper is to bootstrap the critical long-range Ising (LRI) model in p dimensions, one of the earliest known examples of a nonlocal CFT and likely one of the simplest. By analogy with its short-range version (SRI) which comes from a classical lattice Hamiltonian with only nearest-neighbour interactions, the critical p -dimensional LRI model is defined as the critical point of

$$H = -J \sum_{i,j} \frac{\sigma_i \sigma_j}{|i - j|^{p+\mathfrak{s}}} , \quad J > 0 , \quad \sigma_i = \pm 1 , \quad (1.1)$$

which has interactions over an infinite distance [7]. Long-range interactions parametrized by \mathfrak{s} in the Hamiltonian above means that the critical point of LRI should correspond to a family of unitary and non-local conformal field theories. Initially, it was thought that the interval which led to non-trivial critical behaviour was $\frac{p}{2} \leq \mathfrak{s} \leq 2$ [8] but it is actually slightly narrower. As we will now discuss, each endpoint allows (1.1) to be reached from a weakly coupled flow, but the bootstrap approach will allow us to move away from this regime.

Following the birth of the perturbative renormalization group [9], Fisher, Ma and Nickel

introduced a continuum description of the LRI based on a quartic deformation of a generalized free field $\hat{\phi}$ with $\Delta_\phi = \frac{p-\mathfrak{s}}{2}$ [8]. A free field ϕ having this scaling dimension must live in $d = p+2-\mathfrak{s}$ dimensions and it is a simple exercise to show that we can go from one to the other by considering a trivial defect of co-dimension $q = 2 - \mathfrak{s}$. Writing bulk co-ordinates as $x^\mu = (\tau^a, y^i)$ with $\mu = 1, \dots, d$, $a = 1, \dots, p$ and $i = 1, \dots, q$, we can define a family of defect operators by

$$\widehat{\phi^m}(\tau) = \frac{1}{\sqrt{m!}} : \phi(\tau, 0)^m : , \quad (1.2)$$

where $: \dots :$ denotes normal ordering. In this notation, the nonlocal action¹

$$S = \mathcal{N}_{\mathfrak{s}} \mathcal{N}_{-\mathfrak{s}} \int d^p \tau_1 d^p \tau_2 \frac{\hat{\phi}(\tau_1) \hat{\phi}(\tau_2)}{|\tau_{12}|^{p+\mathfrak{s}}} + \int d^p \tau \frac{\lambda}{\sqrt{4!}} \widehat{\phi^4} , \quad (1.3)$$

provides a description of the LRI based on a single mean field, henceforth referred to as the *mean-field description*. The interaction in (1.3) becomes irrelevant below $\mathfrak{s} = \frac{p}{2}$, and CFT data at the fixed point can be expanded in powers of $\varepsilon = 2\mathfrak{s} - p$. Normally $0 < \varepsilon \ll 1$ is needed for reliable results but the expansion can truncate in special cases. In particular, $\hat{\phi}$ and $\hat{\phi}^3$ are protected operators with the exact dimensions

$$\Delta_\phi = \frac{p-\mathfrak{s}}{2}, \quad \Delta_{\phi^3} = \frac{p+\mathfrak{s}}{2} . \quad (1.4)$$

For $\hat{\phi}$, this is because local interactions cannot renormalize a nonlocal kinetic term, a rigorous proof of which was given in [10]. For $\hat{\phi}^3$, (1.4) can be seen by applying a nonlocal equation of motion [11]. As we will review shortly, both non-renormalization theorems become automatic when we view the LRI as a defect in co-dimension $2 - \mathfrak{s}$.

If (1.4) held for all $\frac{p}{2} \leq \mathfrak{s} \leq 2$, as originally proposed by [8], the connection between the LRI and SRI models would not be especially strong. Instead, Sak analyzed the weakly irrelevant operator $\hat{\phi} \partial^2 \hat{\phi}$ and concluded that Δ_ϕ stops changing once it reaches the dimension of the short-range spin field Δ_σ^* [12]. Understanding this crossover between two universality classes was a puzzle for many years because the SRI (unlike mean-field theory with $\Delta_\phi = \frac{p}{4}$) does not contain a marginal local operator. The resolution, found in [13, 14], is that the requisite deformation of the SRI by a nonlocal operator is equivalent to the action

$$S = S_{\text{SRI}} + \mathcal{N}_{\mathfrak{s}} \mathcal{N}_{-\mathfrak{s}} \int d^p \tau_1 d^p \tau_2 \frac{\hat{\chi}(\tau_1) \hat{\chi}(\tau_2)}{|\tau_{12}|^{p-\mathfrak{s}}} + \int d^p \tau g \sigma \hat{\chi} , \quad (1.5)$$

henceforth called the *short-range description*. Here, $\hat{\chi}$ is a generalized free field of dimension $\Delta_\chi = \frac{p+\mathfrak{s}}{2}$. This guarantees that $\sigma \hat{\chi}$ becomes irrelevant above $\mathfrak{s} = p - 2\Delta_\sigma^*$. We will again think

¹The overall normalization has been chosen such that $\hat{\phi}$ and all of its powers (1.2) in the undeformed theory are unit-normalized.

of it as a defect mode of a free field χ in dimension $d = p + 2 + \mathfrak{s}$ and define

$$\widehat{\chi^m}(\tau) = \frac{1}{\sqrt{m!}} : \chi(\tau, 0)^m : . \quad (1.6)$$

If one considers the S_{SRI} theory to be known, (1.5) makes it possible to compute CFT data as an expansion in $\delta = \frac{p-\mathfrak{s}}{2} - \Delta_\sigma^*$ for $0 < \delta \ll 1$. By the same arguments as before,

$$\Delta_\chi = \frac{p + \mathfrak{s}}{2}, \quad \Delta_\sigma = \frac{p - \mathfrak{s}}{2} \quad (1.7)$$

are non-perturbative statements.

The dual descriptions (1.3) and (1.5) can help give a flavour for how observables behave as exact functions of \mathfrak{s} . In our study of the critical LRI model, the first half will ensure that more data is available for this purpose. The second half will carry out the numerical bootstrap and show that the LRI at arbitrary values of \mathfrak{s} can be located to high precision. Both parts will make essential use of exact relations between OPE coefficients which involve the basic protected operators. If \mathcal{O}_1 is a scalar and \mathcal{O}_2 is a spin- ℓ tensor of $SO(p)$, they take the form

$$\frac{\lambda_{12\phi}}{\lambda_{12\phi^3}} \propto \frac{\Gamma(\frac{\Delta_\phi + \Delta_{12} + \ell}{2})\Gamma(\frac{\Delta_\phi - \Delta_{12} + \ell}{2})}{\Gamma(\frac{\Delta_{\phi^3} + \Delta_{12} + \ell}{2})\Gamma(\frac{\Delta_{\phi^3} - \Delta_{12} + \ell}{2})}!, \quad \frac{\lambda_{12\sigma}}{\lambda_{12\chi}} \propto \frac{\Gamma(\frac{\Delta_\sigma + \Delta_{12} + \ell}{2})\Gamma(\frac{\Delta_\sigma - \Delta_{12} + \ell}{2})}{\Gamma(\frac{\Delta_\chi + \Delta_{12} + \ell}{2})\Gamma(\frac{\Delta_\chi - \Delta_{12} + \ell}{2})}, \quad (1.8)$$

where the constant of proportionality is independent of \mathcal{O}_1 and \mathcal{O}_2 . The spin-0 and general spin versions of (1.8) were first derived in [11] and [15] respectively. Both of these derivations used the nonlocal equation of motion. It was later realized in [16] that, as a consequence of bulk locality, these relations hold in any defect CFT where the bulk is free, LRI being a particular example as explained in [11]. Recently, [17] showed that they are important for enforcing locality for more general QFTs in AdS. In a perturbative context, we will use the relations to gain an order of perturbation theory which appears to be a new application of them. On the numerical side, we will use the fact that crossing symmetry and unitarity become more powerful when combined with (1.8). For the case of boundaries, which are a type of $q = 1$ defect, this was already demonstrated in [18, 19]. The novelty here is that the LRI model requires us to consider many values of \mathfrak{s} and therefore many co-dimensions (which are all fractional) since $q = 2 \pm \mathfrak{s}$ in the two formulations above.

As a preview of our results, Table 1 compares the CFT data available in the literature to the new batch we are able to compute in two and three dimensions. Along with (1.2) and (1.6), it uses the double-twist notation

$$[\Phi\Phi]_{n,\ell} \propto \Phi \partial^{2n+\ell} \Phi + \dots \quad (1.9)$$

to mean the unique normalized primary with $2n$ contracted and ℓ uncontracted derivatives appearing in the self-OPE of the generalized free field Φ . In addition to the general dimension

| Observable | Loops | Ref | Observable | Loops | Ref |
|--|----------|--------|---|----------|--------|
| Δ_ϕ | ∞ | [8] | Δ_σ | ∞ | [14] |
| Δ_{ϕ^2} | 3 | [20] | Δ_ϵ | 2 | [14] |
| Δ_{ϕ^3} | ∞ | [11] | Δ_χ | ∞ | [14] |
| Δ_{ϕ^4} | 3 | [20] | $\Delta_{\sigma\chi}$ | 2 | [14] |
| $\Delta_{\phi^m}, m > 4$ | 2 | (3.41) | Δ_T | 2 | [14] |
| $\Delta_{[\hat{\phi}\hat{\phi}]_{0,\ell}}, \ell > 0$ | 2 | (3.13) | $\lambda_{\sigma\hat{\chi}\mathcal{O}}, \mathcal{O} \in \text{SRI}$ | 1 | (3.21) |
| $\lambda_{\widehat{\phi\phi^m\phi^{m-1}}}$ | 1 | (3.37) | $\lambda_{\hat{\chi}\hat{\chi}\mathcal{O}}, \mathcal{O} \in \text{SRI}$ | 2 | (3.21) |
| $\lambda_{\widehat{\phi^3\phi^m\phi^{m-1}}}$ | 1 | (3.37) | $\lambda_{\hat{\chi}\hat{\chi}[\hat{\chi}\hat{\chi}]_{n,\ell}}$ | 2 | (4.22) |

Table 1: Scaling dimensions and OPE coefficients in the LRI model which are known to some non-trivial order in both $p = 2$ and $p = 3$. Data in the left hand table, computed from (1.3) with the ϵ expansion, have closed form expressions. Data in the right hand table, computed from (1.5) with the δ expansion, are sometimes numerical. This difficulty comes from the integrals generated by conformal perturbation theory and the lack of an exact solution for the 3d SRI model.

results of Table 1, we also compute anomalous dimensions of $[\hat{\phi}\hat{\phi}]_{n,\ell}$ operators to three loops in $p = 2$ using analytic bootstrap methods [21]. Studying infinitely many operators at once is possible thanks to the Lorentzian inversion formula [22] which is easiest to apply when the conformal blocks are known in closed form.

The rest of this paper is organized as follows. In section 2 we build upon the construction of critical LRI as a conformal defect to gain some exact information on the spectrum of LRI at criticality. Most notably, we solve the bulk-defect bootstrap equation for the bulk two-point function and derive the relations above. These results are non-perturbative, and in particular they are valid regardless of the UV description of LRI. Sections 3 and 4 are devoted to perturbation theory. In section 3 we review some results from the literature about the flows in equations (1.3) and (1.5), as well as derive the new results for the CFT data in Table 1. This is done by combining standard Feynman diagrams with the exact OPE relations, the latter allowing us to gain one order in perturbation theory, as we will explain. We then move onto the inversion formula in section 4 which computes an infinite amount of additional CFT data in two dimensions. In section 5 we turn into the numerical bootstrap machinery, where we use the exact OPE relations as an input for the LRI crossing equations and compare favourably to the inversion and diagrammatic calculations. A summary and suggestions for the future are given in section 6.

2 Long-range Ising model as a defect CFT

The critical point of the p -dimensional long-range Ising model can be realized as a co-dimension $q = d - p$ conformal defect in a theory of a d -dimensional free massless scalar field [11]. As discussed above, q can be either $2 - \mathfrak{s}$ or $2 + \mathfrak{s}$. The fact that the *bulk* theory is free allows us to derive infinitely-many constraints and relations between defect conformal data [16, 18, 19]. This will be the goal of this section. While the LRI spectrum is built out of operators constrained to the p -dimensional defect, one has to be mindful of differences between the original LRI and the defect description. The conformal defect description enjoys a manifest $SO(p+1, 1) \times SO(q)$ symmetry, while in the original LRI there is no $SO(q)$ symmetry. Hence, physical states of the LRI should have zero transverse spin. In this section we discuss the bulk-defect spectrum, the bulk two-point function of a free massless scalar field Φ , and the exact OPE relations derived from bulk locality. We will then interpret results in the context of the LRI where Φ becomes ϕ in one description and χ in the other.

2.1 Bulk two-point function of Φ

In this section we focus on bootstrapping the bulk two-point function of the free massless scalar Φ which can be used to construct the LRI. We start with reviewing the admissible spectrum of defect modes of Φ . We analytically solve the bulk-defect crossing symmetry constraint on this two-point function to compute the relevant defect CFT data. We take both bulk and defect operators to be unit-normalized.

2.1.1 Defect modes of Φ

The bulk-defect OPE of the free massless field is highly constrained by the Laplace equation. For a massless scalar field of dimension Δ_Φ , the symmetry allows the following bulk-defect expansion

$$\Phi(x) = \sum_s \sum_{\psi} b_s^{\Phi, \mathfrak{p}} |y|^{\Delta - \Delta_\Phi} \psi_s(\tau) (w \cdot y)^s + \dots, \quad (2.1)$$

where the ellipsis denotes derivatives with respect to the directions parallel to the defect and we employed the notation of the introduction. In the expression above the ψ_s are defect local primary operators of scaling dimension Δ and transverse spin s (which we will take to be integers) under $SO(q)$ rotations, while w is an $SO(q)$ polarization vector. When Φ is a free field, $\square\Phi = 0$ (away from contact points) fixes the scaling dimensions of the defect modes of Φ to be [2]

$$\begin{aligned} \psi_s^{(+)} : \quad \Delta_s^{(+)} &= \Delta_\Phi + s, \\ \psi_s^{(-)} : \quad \Delta_s^{(-)} &= \Delta_\Phi + 2 - q - s. \end{aligned} \quad (2.2)$$

Notice that $\psi_s^{(+)}$ and $\psi_s^{(-)}$ form a shadow pair on the defect for all s . We will soon identify these defect modes as either $\psi_0^{(+)} = \hat{\phi}$ and $\psi_0^{(-)} = \hat{\phi}^3$, or $\psi_0^{(+)} = \hat{\chi}$ and $\psi_0^{(-)} = \sigma$.

We note that for p and q both integers, the restrictions from unitarity on the values of s for ‘ $-$ ’ modes have been classified in [16]. There, special attention is paid to the cases of $p = 1$ and $p + q = 2$. As explained in the introduction, however, we will take $p = 2, 3$ and q fractional.

2.1.2 Bootstrapping the bulk two-point function for LRI

With the bulk-defect spectrum of Φ at hand, our next task will be to construct the full bulk two-point function of Φ . We should think of $\langle \Phi(x_1)\Phi(x_2) \rangle$ as a deformation of the two-point function with a trivial defect $\langle \Phi(x_1)\Phi(x_2) \rangle_{\text{triv}}$, the latter of which contains only ‘ $+$ ’ modes. Since the interactions (1.3) and (1.5) do not introduce any dependence on the transverse angle with respect to the defect, the only ‘ $-$ ’ mode which can be present is the one with $s = 0$. The same conclusion can be reached in a model independent way if we assume first that all transverse spins are integers, and second that ‘ $-$ ’ modes satisfy $s \leq \frac{4-q}{2}$.²

Together with $SO(p+1, 1) \times SO(q)$ symmetry, these assumptions allow us to write the following expression for the bulk two-point function of Φ in the defect channel:

$$\langle \Phi(x_1)\Phi(x_2) \rangle = \frac{1}{(|y_1||y_2|)^{\Delta_\Phi}} \sum_{s \in \mathbb{N}} \sum_{\mathfrak{p} = \pm} (b_s^{\Phi, \mathfrak{p}})^2 \hat{g}_s^{(\mathfrak{p})}(\hat{r}, \hat{\eta}) , \quad (2.3)$$

where $b_s^{\Phi, \pm}$ are yet unknown, but $b_s^{\Phi, -} = 0$ for $s > 0$. The functions $\hat{g}_s^{(\mathfrak{p})}(\hat{r}, \hat{\eta}) \equiv \hat{g}_{\Delta_s^{(\mathfrak{p})}, s}(\hat{r}, \hat{\eta})$ are the *defect channel* conformal blocks, which read [2, 24]

$$\hat{g}_{\Delta, s}(\hat{r}, \hat{\eta}) = \hat{r}^\Delta {}_2F_1\left(\frac{p}{2}, \Delta, \Delta, -\frac{p}{2} + 1; \hat{r}^2\right) \frac{s!}{2^s \left(\frac{q}{2} - 1\right)_s} C_s^{\frac{q}{2}-1}(\hat{\eta}) , \quad (2.4)$$

with $\hat{r}, \hat{\eta}$ two cross-ratios defined as

$$\hat{\eta} = \cos \theta , \quad \hat{r} = \frac{1}{2} \left(\hat{\chi} - \sqrt{\hat{\chi}^2 - 4} \right) , \quad (2.5)$$

where θ is the transverse angle and the cross-ratio $\hat{\chi}$ is

$$\hat{\chi} = \frac{|\tau_{12}|^2 + |y_1|^2 + |y_2|^2}{|y_1||y_2|} . \quad (2.6)$$

In the Euclidean domain $(\hat{r}, \hat{\eta}) \in [0, 1] \times [-1, 1]$, while $(\hat{\chi}, \cos \theta) \in [2, \infty] \times [-1, 1]$.

Let us now take a closer look at the dynamics of the system. We stated above that the trivial defect two-point function contains only ‘ $+$ ’ modes but the converse is true as well. If we allow

²In the context of [16], this is the unitarity bound for $p > 1$. Referring to it as such here would be an abuse of terminology since unitarity is not guaranteed in fractional dimension; see [23] for a related discussion.

for ‘+’ modes only, the resulting bulk two-point function is simply the unique Klein-Gordon propagator with regular boundary conditions on the defect dictated by the bulk-defect OPE, where the $b_s^{\Phi,+}$ are fixed to reproduce the contact term in the bulk. This two-point function with a trivial defect can be expanded in the defect channel as [25]

$$\langle \Phi(x_1)\Phi(x_2) \rangle_{\text{triv}} = \frac{1}{(x_{12}^2)^{\Delta_\Phi}} = \frac{1}{(|y_1||y_2|)^{\Delta_\Phi}} \sum_{s \geq 0} (b_{s,\text{triv}}^{\Phi,+})^2 \hat{g}_s^{(+)}(\hat{r}, \hat{\eta}) , \quad (b_{s,\text{triv}}^{\Phi,+})^2 = \frac{2^s (\Delta_\Phi)_s}{s!} . \quad (2.7)$$

The non-trivial defect dynamics is entirely encoded in the correlations functions with the scalar ‘−’ modes [16]. We are therefore led to conjecture that the actual LRI two-point function should be³

$$\langle \Phi(x_1)\Phi(x_2) \rangle = \frac{1}{(|y_1||y_2|)^{\Delta_\Phi}} \left((b_0^{\Phi,+})^2 \hat{g}_0^{(+)}(\hat{r}, \hat{\eta}) + (b_0^{\Phi,-})^2 \hat{g}_0^{(-)}(\hat{r}, \hat{\eta}) + \sum_{s > 0} (b_{s,\text{triv}}^{\Phi,+})^2 \hat{g}_s^{(+)}(\hat{r}, \hat{\eta}) \right) , \quad (2.8)$$

for two (yet) unfixed coefficients $(b_0^{\Phi,\pm})^2$, but this is simply:

$$\langle \Phi(x_1)\Phi(x_2) \rangle = \frac{1}{(x_{12}^2)^{\Delta_\Phi}} + \frac{\left((b_0^{\Phi,+})^2 \hat{g}_0^{(+)}(\hat{r}, \hat{\eta}) - \hat{g}_0^{(+)}(\hat{r}, \hat{\eta}) + (b_0^{\Phi,-})^2 \hat{g}_0^{(-)}(\hat{r}, \hat{\eta}) \right)}{(|y_1||y_2|)^{\Delta_\Phi}} . \quad (2.9)$$

Around either endpoint of the LRI, the interactions in (1.3) and (1.5) will perturb the trivial defect bulk two-point function (2.7) in a way that only affects the coefficients of scalar defect blocks. In particular, they can (and will) generate the ‘−’ mode with the expected dimension.

Bulk-defect crossing

The bulk two-point function (2.9) must be bulk-defect crossing symmetric. As we have seen, our ansatz is already written in a basis of defect channel conformal blocks, so in order to check crossing we should verify that (2.9) can be decomposed into bulk channel blocks. Being free, the bulk self-OPE of Φ features only primary operators $[\Phi\Phi]_{0,\ell}$ of even spin ℓ and scaling dimensions $\Delta_\ell = d + \ell - 2$. Using the bulk radial coordinates (r, η) defined in [24], we shall therefore write

$$\langle \Phi(x_1)\Phi(x_2) \rangle = \frac{(r^4 - 4\eta^2 r^2 + 2r^2 + 1)^{\Delta_\Phi}}{(|y_1||y_2|)^{\Delta_\Phi}} (4r)^{-2\Delta_\Phi} \left[1 + \sum_{\ell=\text{even}} \lambda_{\Phi\Phi[\Phi\Phi]_{0,\ell}} a_{[\Phi\Phi]_{0,\ell}} g_\ell(r, \eta) \right] , \quad (2.10)$$

where $a_{[\Phi\Phi]_{0,\ell}}$ are the one-point functions of $[\Phi\Phi]_{0,\ell}$, $g_\ell(r, \eta)$ are given by

$$g_\ell(r, \eta) = (4r)^{\Delta_\ell} \left[\frac{\left(\frac{1-p-\ell}{2}\right)_{\frac{\ell}{2}}}{\left(\frac{\Delta_\ell}{2}\right)_{\frac{\ell}{2}}} {}_2F_1\left(-\frac{\ell}{2}, \frac{\Delta_\ell}{2}; \frac{p+1}{2}; \eta^2\right) + O(r^2) \right] , \quad (2.11)$$

³We are grateful to Balt van Rees for discussions on this point.

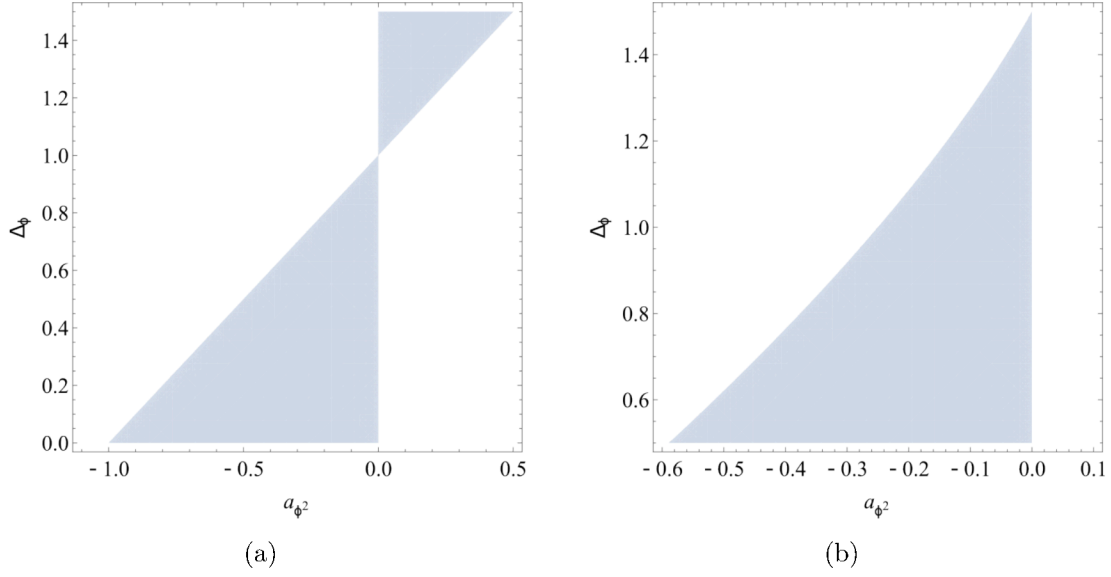


Figure 1: Unitarity region from the bulk-defect bootstrap, in (a) for $p = 2$ and in (b) for $p = 3$.

and higher orders terms can be computing recursively using the results of [24]. Bulk-defect crossing symmetry then dictates:

$$\begin{aligned}
 (b_0^{\Phi,-})^2 &= a_{\Phi^2} \frac{\Gamma(p)\Gamma(\frac{q-2}{2})}{\Gamma(\frac{p}{2})\Gamma(\frac{p+q-2}{2})}, \quad (b_0^{\Phi,+})^2 = 1 - \frac{\Gamma(\frac{p+q-2}{2})\Gamma(\frac{4-q}{2})}{\Gamma(\frac{q}{2})\Gamma(\frac{p-q+2}{2})}(b_0^{\Phi,-})^2, \\
 \lambda_{\Phi\Phi[\Phi\Phi]_{0,\ell}} a_{[\Phi\Phi]_{0,\ell}} &= \frac{\left(\frac{d}{2}-1\right)_{\ell} \left(\frac{q}{2}-1\right)_{\frac{\ell}{2}}}{2^{\ell}(1)_{\frac{\ell}{2}} \left(\frac{1}{2}(d+\ell-3)\right)_{\frac{\ell}{2}} \left(\frac{p+1}{2}\right)_{\frac{\ell}{2}}} a_{\Phi^2}, \quad \ell > 0.
 \end{aligned} \tag{2.12}$$

Note that a_{Φ^2} is further constrained by unitarity, since $(b_0^{\Phi,\pm})^2 \geq 0$ in unitary theories. In particular for $p/2 - 1 \leq \Delta_{\Phi} \leq 3$ these regions are shown in figure 1. We will see how such unitarity regions can be further restricted when specializing to LRI.

It should be clear that (2.9) is no longer a valid ansatz for $q = 1$ because boundaries and interfaces do not have transverse spin. This explains why [26, 27] found a different solution to the bootstrap equations, namely

$$(b_0^{\Phi,+})^2 = 1 + 2^{d-2} a_{\Phi^2}, \quad (b_0^{\Phi,-})^2 = (d-2)(1 - 2^{d-2} a_{\Phi^2}). \tag{2.13}$$

2.1.3 The two endpoints of the flow

Referring to (1.3) and (1.5), we can identify $\Phi = \phi$ when $q = 2 - \mathfrak{s}$ and $\Phi = \chi$ when $q = 2 + \mathfrak{s}$. The trivial defect is then composed of the ‘+’ modes denoted $\hat{\phi}$ or $\hat{\chi}$ and the LRI is defined as

a defect localized interaction away from this point. This is either an interaction with the SRI or a self-interaction depending on the duality frame.

Trivial defects have $b_0^{\Phi,+} = 1$ and $b_0^{\Phi,-} = 0$ which are equivalent to $a_{\Phi^2} = 0$. After a deformation, the allowed one-point functions in figure 1 are negative when $\Delta_\Phi = \Delta_\phi$ and positive when $\Delta_\Phi = \Delta_\chi$. In terms of the small parameters ε and δ , these deformations affect the codimensions as

$$q = 2 - \frac{p + \varepsilon}{2} , \quad q = 2 + p - 2(\delta + \Delta_\sigma^*) , \quad (2.14)$$

respectively. In the former case, we have $a_{\phi^2} \leq 0$ from the $\hat{\phi}^4$ flow while in the latter case we have $a_{\chi^2} \geq 0$ from the $\sigma\hat{\chi}$ flow.

It is interesting to ask what happens to a_{ϕ^2} when $a_{\chi^2} = 0$ or vice versa. This is a question about large ε and δ . In our language, the conjecture of [14] is that $b_0^{\chi,-} = 0$ when $b_0^{\phi,+} = 0$. Instead of the trivial defect, we are therefore dealing with a dual starting point defined by

$$b_0^{\phi,+} = 0 , \quad (b_0^{\phi,-})^2 = \frac{\Gamma(\frac{q}{2}) \Gamma(p - \Delta_\phi)}{\Gamma(\Delta_\phi) \Gamma(\frac{4-q}{2})} = \frac{\Gamma(1 + \frac{p}{2} - \delta - \Delta_\sigma^*) \Gamma(\Delta_\sigma^* + \delta)}{\Gamma(p - \Delta_\sigma^* - \delta) \Gamma(1 - \frac{p}{2} + \delta + \Delta_\sigma^*)} . \quad (2.15)$$

We can equivalently express the results above in terms of a_{ϕ^2} via eq. (2.12) to find

$$a_{\phi^2} = \begin{cases} \delta - 1 + \Delta_\sigma^* = -7/8 + \delta , & p = 2 , \\ \frac{\sqrt{\pi} \cot(\pi(\delta + \Delta_\sigma^*)) \Gamma(\delta + \Delta_\sigma^* - \frac{1}{2})}{4\Gamma(\delta + \Delta_\sigma^* - 2)} = -0.575408 + O(\delta) , & p = 3 , \end{cases} \quad (2.16)$$

where for $p = 2$ we used $\Delta_\sigma^* = 1/8$, while for $p = 3$ we used $\Delta_\sigma^* = 0.5181489$. In order to accommodate both such descriptions of LRI while being consistent with bulk-defect crossing and unitarity, we should allow at least

$$\begin{aligned} -7/8 \leq a_{\phi^2} \leq 0 , \quad p = 2 , \\ -0.575408 \leq a_{\phi^2} \leq 0 , \quad p = 3 . \end{aligned} \quad (2.17)$$

This is the interval in which we will let a_{ϕ^2} vary when looking at the numerical conformal bootstrap in section 5. A very similar calculation could be used to estimate a_{χ^2} at small ε . This result also follows from

$$\frac{\Gamma(\frac{p+2-q}{2})}{\Gamma(\frac{2-q}{2})} \left[a_{\chi^2}^{-1} - \frac{\Gamma(p) \Gamma(\frac{q-2}{2})}{\Gamma(\frac{p}{2}) \Gamma(\frac{p+q-2}{2})} \right] = \frac{\Gamma(\frac{p+q-2}{2})}{\Gamma(\frac{q-2}{2})} \left[a_{\phi^2}^{-1} - \frac{\Gamma(p) \Gamma(\frac{2-q}{2})}{\Gamma(\frac{p}{2}) \Gamma(\frac{p+2-q}{2})} \right] , \quad (2.18)$$

which we will derive in the next subsection.

2.2 OPE relations

In any defect CFT, bulk locality imposes several constraints on the dynamics.⁴ For correlation functions between the bulk field Φ and two defect insertions $\hat{\mathcal{O}}$, \hat{T} , and away from contact points,

⁴Bulk locality plays an important role in the context of general QFTs in AdS, as discussed recently in [17].

it requires the correlator to be an analytic function of the coordinates away. This leads to constraints on defect three-point functions with $\widehat{\mathcal{O}}$, \widehat{T} and the defect modes of Φ which have been written schematically in (1.8). For the LRI specifically, the relations we will use were all derived in [15] following the the special cases considered in [11]. Here, we will review the modern derivation from [16, 18, 19] as it applies to a broader class of models. This will also show how the prefactor of (1.8) is physically related to the one-point function a_{Φ^2} .

2.2.1 Review of the derivation

Consider the case where $\widehat{\mathcal{O}}$ is an $SO(p)$ scalar, and \widehat{T} is a symmetric and traceless tensor of parallel spin ℓ . Both $\widehat{\mathcal{O}}$ and \widehat{T} are taken to be scalars under transverse rotations ($s = 0$). Without loss of generality we can place the third operator at infinity and so we investigate:

$$\langle \Phi(x_1) \widehat{\mathcal{O}}(\tau_2) \widehat{T}^{(\ell)}(\theta, \infty) \rangle . \quad (2.19)$$

We recall that Φ is a free bulk massless scalar field, so its defect modes are written in (2.2) with coefficients $b_s^{\Phi, \pm}$ ($b_s^{\Phi, -} = 0$ for $s > 0$). In the defect channel, the correlator above will be written in terms of the OPE coefficients

$$\langle \psi_0^{(\text{p})}(\tau_1) \widehat{\mathcal{O}}(\tau_2) \widehat{T}^{(\ell)}(\theta, \infty) \rangle = \frac{\lambda_{\psi_0^{(\text{p})} \widehat{\mathcal{O}} \widehat{T}}}{|\tau_{12}|^{\Delta_0^{(\text{p})} + \Delta_{\widehat{\mathcal{O}}} - \Delta_{\widehat{T}}}} . \quad (2.20)$$

We could now resum the bulk-defect OPE to obtain the complete expression for (2.19) in terms of the data in the defect channel, as was done in [16], but we will not need it in the following. The next step is requiring analyticity of (2.19), where we take $\widehat{\mathcal{O}}$ to be either another zero mode $\psi_0^{(\text{p})}$ or a parity-even scalar ε of scaling dimension Δ_ε . Using repeatedly eq. (28) of [16] one finds

$$\begin{aligned} \lambda_{\psi_0^{(+)} \psi_0^{(+)} \widehat{T}} &= \kappa_1(\Delta_{\widehat{T}}, \ell) \lambda_{\psi_0^{(-)} \psi_0^{(+)} \widehat{T}} , & \lambda_{\psi_0^{(-)} \psi_0^{(-)} \widehat{T}} &= \kappa_2(\Delta_{\widehat{T}}, \ell) \lambda_{\psi_0^{(-)} \psi_0^{(+)} \widehat{T}} , \\ \lambda_{\psi_0^{(-)} \varepsilon \widehat{T}} &= \kappa_3(\Delta_{\widehat{T}}, \ell) \lambda_{\psi_0^{(+)} \varepsilon \widehat{T}} , \end{aligned} \quad (2.21)$$

with

$$\begin{aligned} \kappa_1(\Delta_{\widehat{T}}, \ell) &= -R(a_{\Phi^2}) \frac{\Gamma\left(\frac{4-q}{2}\right) \Gamma\left(\frac{\ell+\Delta_{\widehat{T}}}{2}\right) \Gamma\left(\frac{\ell+p+q-2-\Delta_{\widehat{T}}}{2}\right)}{\Gamma\left(\frac{q}{2}\right) \Gamma\left(\frac{\ell+p-\Delta_{\widehat{T}}}{2}\right) \Gamma\left(\frac{\ell+2-q+\Delta_{\widehat{T}}}{2}\right)} , \\ \kappa_2(\Delta_{\widehat{T}}, \ell) &= -\frac{1}{R(a_{\Phi^2})} \frac{\Gamma\left(\frac{q}{2}\right) \Gamma\left(\frac{\ell+\Delta_{\widehat{T}}}{2}\right) \Gamma\left(\frac{\ell+p-q+2-\Delta_{\widehat{T}}}{2}\right)}{\Gamma\left(\frac{4-q}{2}\right) \Gamma\left(\frac{\ell+p-\Delta_{\widehat{T}}}{2}\right) \Gamma\left(\frac{\ell-2+q+\Delta_{\widehat{T}}}{2}\right)} , \\ \kappa_3(\Delta_{\widehat{T}}, \ell) &= -\frac{1}{R(a_{\Phi^2})} \frac{\Gamma\left(\frac{q}{2}\right) \Gamma\left(\frac{2\ell+p-q+2+2\Delta_{\widehat{T}}-2\Delta_\varepsilon}{4}\right) \Gamma\left(\frac{2\ell+p-q+2-2\Delta_{\widehat{T}}+2\Delta_\varepsilon}{4}\right)}{\Gamma\left(\frac{4-q}{2}\right) \Gamma\left(\frac{2\ell+p+q-2+2\Delta_{\widehat{T}}-2\Delta_\varepsilon}{4}\right) \Gamma\left(\frac{2\ell+p+q-2-2\Delta_{\widehat{T}}+2\Delta_\varepsilon}{4}\right)} . \end{aligned} \quad (2.22)$$

We have defined

$$R(a_{\Phi^2}) \equiv b_0^{\Phi,-} / b_0^{\Phi,+} , \quad (2.23)$$

where $b_0^{\Phi,\pm}$ and a_{Φ^2} further satisfy (2.12).

2.2.2 Special cases

For certain special values of the parameters, some of the blocks in the decomposition of (2.19) are already regular before constraints are introduced. These correspond to poles of the gamma functions in (2.21) which cause the exact relations to degenerate. This phenomenon is most interesting when the possibility of operator dimensions infinitesimally close to these special values is disallowed by symmetry. In fractional q models like the LRI, this only happens when

$$\Delta_{\hat{T}} = p + \ell + 2n, \quad \ell \text{ odd}. \quad (2.24)$$

This condition, which guarantees $\kappa_1(\hat{\Delta}_{\hat{T}}, \ell) = \kappa_2(\hat{\Delta}_{\hat{T}}, \ell) = 0$ and hence $\lambda_{\psi_0^{(+)}\psi_0^{(+)}\hat{T}} = \lambda_{\psi_0^{(-)}\psi_0^{(-)}\hat{T}} = 0$, is essential for odd-spin operators because they can only appear in mixed OPEs by Bose symmetry. Importantly, all odd-spin operators in $\psi_0^{(+)} \times \psi_0^{(-)}$ are of this type.

The BCFT setup of [18, 19] also had special cases realized by even-spin operators which were distinguished from the continuum by Ward identities instead of Bose symmetry. These operators, known as the displacement and its higher-spin cousins, satisfied the following conditions.

1. $\Delta_{\hat{T}} = 2\Delta_0^{(+)} + 2n + \ell$ implies $\kappa_1(\Delta_{\hat{T}}, \ell) = \infty$, $\lambda_{\psi_0^{(+)}\psi_0^{(-)}\hat{T}} = 0$ and $\lambda_{\psi_0^{(+)}\psi_0^{(+)}\hat{T}}$ unfixed.
2. $\Delta_{\hat{T}} = 2\Delta_0^{(-)} + 2n + \ell$ implies $\kappa_2(\Delta_{\hat{T}}, \ell) = \infty$, $\lambda_{\psi_0^{(+)}\psi_0^{(-)}\hat{T}} = 0$ and $\lambda_{\psi_0^{(-)}\psi_0^{(-)}\hat{T}}$ unfixed.

For fractional q on the other hand, we cannot construct any $s = 0$ operators out of the bulk currents which obey Ward identities. Algebraically, this reduced freedom can be seen from the fact that $\Delta_0^{(\pm)}$ do not differ by integers meaning there is no way to satisfy both conditions at the same time.

2.2.3 Duality relation

We can now consider a shadow transformation that exchanges $\Delta_0^{(+)}$ and $\Delta_0^{(-)}$. According to (2.2), the one that does the job is $q \leftrightarrow 4 - q$. In terms of LRI parameters, this is equivalent to changing the sign of \mathfrak{s} . The first line of (2.21) then becomes

$$\lambda_{\psi_0^{(-)}\psi_0^{(-)}\hat{T}} = \tilde{\kappa}_1(\Delta_{\hat{T}}, \ell) \lambda_{\psi_0^{(-)}\psi_0^{(+)}\hat{T}} , \quad \lambda_{\psi_0^{(+)}\psi_0^{(+)}\hat{T}} = \tilde{\kappa}_2(\Delta_{\hat{T}}, \ell) \lambda_{\psi_0^{(-)}\psi_0^{(+)}\hat{T}} . \quad (2.25)$$

The $\tilde{\kappa}_i$, however, are not simply the κ_i with $\mathfrak{s} \leftrightarrow -\mathfrak{s}$ applied. This new description of the same LRI has a different bulk so it must use the ‘ \pm ’ modes appropriate to the new co-dimension. This

means that if the original set of relations used $R(a_{\phi^2})$, the new set will have $R(a_{\chi^2})$ in its place. Note that nothing has changed about this physics so it is possible to compare OPE coefficients and find

$$\tilde{\kappa}_1(\Delta_{\hat{T}}, \ell) = \kappa_2(\Delta_{\hat{T}}, \ell) , \quad \tilde{\kappa}_2(\Delta_{\hat{T}}, \ell) = \kappa_1(\Delta_{\hat{T}}, \ell) . \quad (2.26)$$

By comparing to eq. (2.22) we see that

$$R(a_{\phi^2})R(a_{\chi^2}) = 1 , \quad (2.27)$$

which can be rearranged to give (2.18).

A consequence of this fact is that a co-dimension $2-\mathfrak{s}$ defect with one-point function a_{ϕ^2} gives the same numerical bootstrap bounds as a co-dimension $2+\mathfrak{s}$ defect with one-point function a_{χ^2} , as far as this small set of correlators is concerned. Applying this duality to the bounds obtained in refs. [18, 19] should therefore lead to consistent bounds for co-dimension three defects, and it would be interesting to study this further **CB: If we say this now, our next paper will sound less original.EL: better?**

3 Perturbation theory

We can use the exact OPE relations derived in the previous section to study the LRI in perturbation theory. As discussed, the LRI admits two dual descriptions: as a GFF coupled to itself – see eq. (1.3) – and as a GFF coupled to the SRI – see eq. (1.5). When the interaction in (1.1) decays sufficiently slowly or sufficiently quickly, one of these flows becomes weakly coupled and hence describes a perturbation of the trivial defect.

As we will review, at the IR fixed point of (1.3) the critical coupling is $\lambda_* \sim \varepsilon$ with ε being a small parameter. Observables such as the anomalous dimensions and OPE coefficients of (unit-normalized) LRI operators, as well as the ratio R that appears in the OPE relations, can be expanded in powers of ε as

$$\begin{aligned} \Delta &= \Delta^{(0)} + \varepsilon \Delta^{(1)} + \varepsilon^2 \Delta^{(2)} + \varepsilon^3 \Delta^{(3)} + O(\varepsilon^4) , \\ \lambda_{ijk} &= \lambda_{ijk}^{(0)} + \varepsilon \lambda_{ijk}^{(1)} + \varepsilon^2 \lambda_{ijk}^{(2)} + \varepsilon^3 \lambda_{ijk}^{(3)} + O(\varepsilon^4) , \\ R(a_{\phi^2}) &= R^{(0)} + \varepsilon R^{(1)} + \varepsilon^2 R^{(2)} + \varepsilon^3 R^{(3)} + O(\varepsilon^4) . \end{aligned} \quad (3.1)$$

At the IR fixed point of (1.5) the critical coupling is $g_*^2 \sim \delta$ with small δ . Quantities such as the scaling dimensions and the ratio R that are invariant under the \mathbb{Z}_2 symmetry that flips the sign of g_* can be expanded in powers of δ as

$$\begin{aligned} \Delta &= \Delta^{(0)} + \delta \Delta^{(2)} + \delta^2 \Delta^{(4)} + O(\delta^3) , \\ R(a_{\phi^2}) &= R^{(0)} + \delta R^{(2)} + \delta^2 R^{(4)} + O(\delta^3) . \end{aligned} \quad (3.2)$$

Depending on their \mathbb{Z}_2 charges, OPE coefficients will contain either odd or integer powers of $\delta^{1/2}$ (not both) so for them we consider either of:

$$\begin{aligned}\lambda_{ijk} &= \lambda_{ijk}^{(0)} + \delta \lambda_{ijk}^{(2)} + \delta^2 \lambda_{ijk}^{(4)} + O(\delta^3) , \\ \lambda_{ijk} &= \delta^{1/2} \lambda_{ijk}^{(1)} + \delta^{3/2} \lambda_{ijk}^{(3)} + \delta^{5/2} \lambda_{ijk}^{(5)} + O(\delta^{7/2}) .\end{aligned}\tag{3.3}$$

Notice that here $\Delta^{(n)}$ is defined as the shift with respect to the scaling dimension at $\varepsilon = 0$ or $\delta = 0$. Tree-level scaling dimensions can be linear in the small parameter so $\Delta^{(n)}$ is in general different from the anomalous dimension $\gamma^{(n)}$, which is naturally defined in perturbation theory around zero coupling with ε or δ finite.

3.1 Review of results in the literature

In this section we shall review some of the available perturbative results for the LRI model and its $O(N)$ generalization. Starting from the mean-field end we will consider the following perturbations:

$$\begin{aligned}S &= \mathcal{N}_s \mathcal{N}_{-s} \int d^p \tau_1 d^p \tau_2 \frac{\hat{\phi}(\tau_1) \hat{\phi}(\tau_2)}{|\tau_{12}|^{p+s}} + \int d^p \tau \frac{\lambda}{4!} \hat{\phi}^4 , & N = 1 , \\ S &= \mathcal{N}_s \mathcal{N}_{-s} \int d^p \tau_1 d^p \tau_2 \frac{\hat{\phi}(\tau_1) \cdot \hat{\phi}(\tau_2)}{|\tau_{12}|^{p+s}} + \int d^p \tau \frac{\lambda}{4} (\hat{\phi} \cdot \hat{\phi})^2 , & N > 1 ,\end{aligned}\tag{3.4}$$

where (\cdot) denotes the $O(N)$ scalar product and the constant

$$\mathcal{N}_s = \frac{2^{-s} \Gamma(\frac{p-s}{2})}{\pi^{\frac{p}{2}} \Gamma(\frac{s}{2})} ,\tag{3.5}$$

has been chosen in order to have unit-normalized propagator in position space. In complete analogy with the LRI model, the long-range $O(N)$ can be written as a defect for the free, massless $O(N)$ vector model [28]. Since the interaction is marginal when $\varepsilon = 2s - p$ vanishes, loop diagrams can generate inverse powers of ε . Even though we are interested in finite ε , we will treat these as poles to be subtracted. This is a scheme which preserves the property that observables accurate to $O(\varepsilon^n)$ require diagrams with up to n loops. The two-loop fixed point in this scheme is [28] (see [20] for a three-loop result)

$$\begin{aligned}\lambda_* &= \frac{\Gamma(\frac{p}{2})}{3\pi^{p/2}} \varepsilon + \frac{2\Gamma(\frac{p}{2})}{9\pi^{p/2}} [\psi(\frac{p}{2}) - 2\psi(\frac{p}{4}) + \psi(1)] \varepsilon^2 + O(\varepsilon^3) , & N = 1 < \\ \lambda_* &= \frac{\Gamma(\frac{p}{2})}{2\pi^{p/2}(N+8)} \varepsilon + \frac{\Gamma(\frac{p}{2})(5N+22)}{\pi^{p/2}(N+8)^3} [\psi(\frac{p}{2}) - 2\psi(\frac{p}{4}) + \psi(1)] \varepsilon^2 + O(\varepsilon^3) , & N > 1 .\end{aligned}\tag{3.6}$$

Around the short-range end we will only consider the $N = 1$ action:

$$S = S_{\text{SRI}} + \mathcal{N}_s \mathcal{N}_{-s} \int d^p \tau_1 d^p \tau_2 \frac{\hat{\chi}(\tau_1) \hat{\chi}(\tau_2)}{|\tau_{12}|^{p-s}} + \int d^p \tau g \sigma \hat{\chi} ,\tag{3.7}$$

which leads to results depending on the short-range CFT data quoted below [29, 30].

$$\begin{array}{llll} \Delta_\sigma^* = \frac{1}{8} & \Delta_\epsilon^* = 1 & c_T = 1 & (p = 2) \\ \Delta_\sigma^* = 0.518157 & \Delta_\epsilon^* = 1.41265 & c_T = 1.419815 & (p = 3) \end{array} \quad (3.8)$$

Taking $\delta = \frac{p-s}{2} - \Delta_\sigma^*$ to be small, the two-loop beta function for g can be computed numerically with conformal perturbation theory [31]. This was done in [14] leading to the fixed point

$$g_*^2 = \begin{cases} 0.788392\delta + O(\delta^2) , & p = 2 \\ 0.8155(3)\delta + O(\delta^2) , & p = 3 \end{cases} . \quad (3.9)$$

Although separate numerical calculations would be needed for each value of N , it is clear that (3.9) can be generalized to $O(N)$ fixed points in principle.⁵ We will also make speculative comments later on about long-range fixed points based on minimal models. The most optimistic hypothesis one can make from [14] is that *any* Ginzburg-Landau model with a nonlocal kinetic term can be reached by coupling its short-range partner to a GFF.

Anomalous dimensions near the mean-field end

Let us now discuss anomalous dimensions of LRI operators. We shall recall that the fundamental field $\hat{\phi}$ does not renormalize, its scaling dimension being fixed by the non-local equation of motion. For the leading scalar $\hat{\phi}^2 = \hat{\phi} \cdot \hat{\phi} / \sqrt{2N}$ among $O(N)$ singlets, the anomalous dimension is computed at three loops in [20] (two-loop results were originally obtained in [35]) and reads:

$$\begin{aligned} \Delta_{\hat{\phi}^2} = & \frac{p}{2} + \frac{\varepsilon}{2} \frac{N-4}{N+8} - \varepsilon^2 \frac{(N+2)(7N+20)}{(N+8)^3} \left[\psi\left(\frac{p}{2}\right) - 2\psi\left(\frac{p}{4}\right) + \psi(1) \right] \\ & - \varepsilon^3 \frac{(N+2)(7N+20)}{4(N+8)^5} (19N^3 - 60N^2 - 432N - 256) \left[\psi\left(\frac{p}{2}\right) - 2\psi\left(\frac{p}{4}\right) + \psi(1) \right]^2 \\ & + \varepsilon^3 \frac{3(N+2)}{4(N+8)^4} (N^2 - 12N - 16) \left[\psi'(1) - \psi'\left(\frac{p}{2}\right) \right] \\ & - \varepsilon^3 \frac{6(N+2)(5N+22)}{(N+8)^4} \frac{\Gamma(1 + \frac{p}{4})^3 \Gamma(-\frac{p}{4})}{\Gamma(\frac{p}{2})} \left[\psi'(1) - \psi'\left(\frac{p}{4}\right) \right] + O(\varepsilon^4) . \end{aligned} \quad (3.10)$$

The next quantity that is known is the two-loop scaling dimension $\Delta_{[\hat{\phi}\hat{\phi}]_{0,\ell}}$ of the leading spin- ℓ operator $[\hat{\phi}\hat{\phi}]_{0,\ell}$, which was computed in [36] (see also [15]) for the case of $N = 1$. As discussed there, we can compute this quantity by considering the three-point function $\langle \hat{\phi}\hat{\phi}[\hat{\phi}\hat{\phi}]_{0,\ell} \rangle$, and the

⁵The duality between the large N versions of (1.3) and (1.5) has been explored in [32]. References [33, 34] discuss a similar co-dimension one duality between large- N free/critical vector modes coupled to a free massless bulk scalar field with Dirichlet/Neumann boundary conditions.

first correction comes from the two-loop diagram:

Setting for simplicity the insertion of the spinning operator to zero external momentum and repeating the calculations of [36] we obtain the following result for two-loop correction

$$\begin{aligned}
& \frac{6(N+2)(\lambda\mu^\varepsilon)^2}{\mathcal{N}_s^4} \int \frac{dk' dk''}{(2\pi)^{2p}} \frac{k''_{(a_1} \dots k''_{a_\ell)}}{|k'|^s |k - k' - k''|^s |k''|^{2s}} \\
&= \frac{6(N+2)\lambda^2}{(4\pi)^p \mathcal{N}_s^4} \frac{\Gamma(\ell + \frac{p}{2} - s) \Gamma(\frac{p-s}{2})^2 \Gamma(2s - p)}{\Gamma(s) \Gamma(\frac{s}{2})^2 \Gamma(\ell + \frac{3}{2}p - 2s)} \left| \frac{\mu}{k} \right|^\varepsilon \\
&= 6(N+2)\lambda^2 \frac{\pi^p \Gamma(\ell)}{\varepsilon \Gamma(\frac{p}{2}) \Gamma(\frac{p}{2} + \ell)} + O(1) ,
\end{aligned} \tag{3.12}$$

where we divided by the tree-level result.⁶ Since there is no wave-function for $\hat{\phi}$, the $1/\varepsilon$ pole in this diagram is removed by a wave-function renormalization for $[\hat{\phi}\hat{\phi}]_{0,\ell}$, which in turn leads to the following scaling dimension for $[\hat{\phi}\hat{\phi}]_{0,\ell}$ at the IR fixed point

$$\Delta_{[\hat{\phi}\hat{\phi}]_{0,\ell}} = \frac{p+2\ell}{2} - \frac{\varepsilon}{2} - \varepsilon^2 \frac{N+2}{(N+8)^2} \frac{3\Gamma(\frac{p}{2})\Gamma(\ell)}{\Gamma(\frac{p}{2} + \ell)} + O(\varepsilon^3) . \tag{3.13}$$

This generalizes the result in [15, 36] and also corrects a factor of 2 for the $N = 1$ result.

Anomalous dimensions near the short-range end

There are fewer perturbative results near the short-range end. The leading scalar's anomalous dimension was computed at two loops in the δ expansion in [14], which found

$$\Delta_\epsilon = \begin{cases} 1 + O(\delta^2) , & p = 2 , \\ \Delta_\epsilon^* + 0.27\delta + O(\delta^2) , & p = 3 . \end{cases} \tag{3.14}$$

The anomalous dimension of the leading spin-two operator $T_{\mu\nu}$ can be obtained from multiplet recombination [37, 38] (see also [18]), i.e. by exploiting the fact that conservation of SRI's stress-tensor $T_{\mu\nu}$ fails as soon as we turn on g . In turn, this strategy allows us to gain one order in

⁶As the spinning operator does not carry momentum, derivatives will produce the same effect no matter how they are distributed: they simply contribute the same factor of $k''_{a_1} \dots k''_{a_\ell}$. The tree-level diagram is also proportional to the same factor.

perturbation theory. The resulting scaling dimension of T depends on the central charge in (3.8) and is [14, 13]

$$\Delta_T = p + \frac{8\pi^p}{c_T \Gamma(\frac{p}{2})^2} \frac{\Delta_\sigma^*(p - \Delta_\sigma^*)}{p^2 + p - 2} g_*^2 + O(g_*^4) . \quad (3.15)$$

For the specific case of the $p = 2$ LRI we can use Virasoro multiplet recombination methods to compute the anomalous dimensions of higher-spin Virasoro currents in SRI. At spin-4, the dimension of $\Lambda \equiv (L_{-4} - \frac{5}{3}L_{-2}^2)|0\rangle$ has been computed in [15] to be

$$\Delta_\Lambda = 4 + \frac{1335}{2048} \pi^2 g_*^2 + O(g_*^4) . \quad (3.16)$$

Increasing the spin leads to a proliferation of currents and a computationally intensive problem, but for anomalous dimensions up to spin-10 it should become manageable using the techniques of [39]. We leave this problem for future work.

Results in the literature in both perturbative settings have mostly focused on anomalous dimensions and fewer results are available for the OPE coefficients. We will present some new results about OPE coefficients in both settings in the next sections.

3.2 Using OPE relations from the short-range end

Let us first discuss how to use the OPE relations near the short-range end, so that $g_*^2 \sim \delta$ and $0 < \delta \ll 1$. Importantly, the expansion does not start from the trivial defect $b_0^{\phi,-} = 0$ but rather $b_0^{\phi,+} = 0$, see eq. (2.15). The ‘ \pm ’ modes are σ and $\hat{\chi}$ respectively, which means the first two OPE relations in (2.21) read

$$\begin{aligned} \frac{\lambda_{\sigma\sigma\mathcal{O}}}{\lambda_{\sigma\hat{\chi}\mathcal{O}}} &= R(a_{\phi^2}) \frac{\Gamma(p/2 - \Delta_\sigma) \Gamma(\frac{\ell+\Delta}{2}) \Gamma(\frac{\ell+2\Delta_\sigma-\Delta}{2})}{\Gamma(\Delta_\sigma - p/2) \Gamma(\frac{\ell+p-2\Delta_\sigma+\Delta}{2}) \Gamma(\frac{\ell+p-\Delta}{2})} , \\ \frac{\lambda_{\hat{\chi}\hat{\chi}\mathcal{O}}}{\lambda_{\sigma\hat{\chi}\mathcal{O}}} &= R(a_{\phi^2})^{-1} \frac{\Gamma(\Delta_\sigma - p/2) \Gamma(\frac{\ell+\Delta}{2}) \Gamma(\frac{\ell+2p-2\Delta_\sigma-\Delta}{2})}{\Gamma(p/2 - \Delta_\sigma) \Gamma(\frac{\ell-p+2\Delta_\sigma+\Delta}{2}) \Gamma(\frac{\ell+p-\Delta}{2})} . \end{aligned} \quad (3.17)$$

If \mathcal{O} is a primary in the SRI which diagonalizes dilations, then $\lambda_{\hat{\chi}\hat{\chi}\mathcal{O}}$ starts at $O(g_*^2)$ while $\lambda_{\sigma\hat{\chi}\mathcal{O}}$ and $R(a_{\phi^2})^{-1}$ start at $O(g_*)$. The OPE relations can therefore give information about two-loop perturbation theory with one-loop data as input. In practice, the first non-vanishing terms in $\lambda_{\sigma\hat{\chi}\mathcal{O}}$ and $\lambda_{\hat{\chi}\hat{\chi}\mathcal{O}}$ can both be computed from the star-triangle relation in (B.2), using it once for the former and twice for the latter. We will therefore compute the OPE coefficients in (3.17) directly and treat $R(a_{\phi^2})$ as the unknown quantity. If we take \mathcal{O} to be a scalar, the integrals

arising in conformal perturbation theory can now be easily computed to get

$$\begin{aligned}\lambda_{\sigma\hat{\chi}\mathcal{O}} &= \pi^{p/2} g_* \lambda_{\sigma\sigma\mathcal{O}}^* \frac{\Gamma(\Delta_\sigma^* - p/2) \Gamma(\frac{p+\Delta_\sigma^*}{2} - \Delta_\sigma^*) \Gamma(\frac{p-\Delta_\sigma^*}{2})}{\Gamma(p - \Delta_\sigma^*) \Gamma(\Delta_\sigma^*/2) \Gamma(\Delta_\sigma^* - \Delta_\sigma^*/2)} + O(g_*^3) , \\ \lambda_{\hat{\chi}\hat{\chi}\mathcal{O}} &= \pi^p g_*^2 \lambda_{\sigma\sigma\mathcal{O}}^* \frac{\Gamma(\Delta_\sigma^* - p/2)^2 \Gamma(\frac{p+\Delta_\sigma^*}{2} - \Delta_\sigma^*) \Gamma(p - \Delta_\sigma^* - \Delta_\sigma^*/2)}{\Gamma(p - \Delta_\sigma^*)^2 \Gamma(\frac{\Delta_\sigma^* - p}{2} + \Delta_\sigma^*) \Gamma(\Delta_\sigma^* - \Delta_\sigma^*/2)} + O(g_*^4) .\end{aligned}\tag{3.18}$$

Either one of these results is enough to compute $R(a_{\phi^2})$ upon going back to (3.17) and the fact that they agree is a check. We find

$$R(a_{\phi^2})^{-1} = \pi^{p/2} g_* \frac{\Gamma(p/2 - \Delta_\sigma^*)}{\Gamma(p - \Delta_\sigma^*)} + O(g_*^3) .\tag{3.19}$$

Upon plugging in Δ_σ^* and g_* numerically and using (2.12), the result above is equivalent to the following

$$a_{\phi^2} = \begin{cases} -\frac{7}{8} + 9.896\delta + O(\delta^2) , & p = 2 , \\ -0.575408 + 37.13\delta + O(\delta^2) , & p = 3 . \end{cases}\tag{3.20}$$

The power of this approach is that, with (3.19) in hand, the OPE relations can be used to quickly upgrade (3.18) to a spinning version of it. As a result,

$$\begin{aligned}\lambda_{\sigma\hat{\chi}\mathcal{O}} &= \pi^{p/2} g_* \lambda_{\sigma\sigma\mathcal{O}}^* \frac{\Gamma(\Delta_\sigma^* - p/2) \Gamma(\frac{\ell+\Delta_\sigma^*}{2}) \Gamma(\frac{\ell+2\Delta_\sigma^*-\Delta_\sigma^*}{2})}{\Gamma(p - \Delta_\sigma^*) \Gamma(\frac{\ell+p-2\Delta_\sigma^*+\Delta_\sigma^*}{2}) \Gamma(\frac{\ell+p-\Delta_\sigma^*}{2})} + O(g_*^3) , \\ \lambda_{\hat{\chi}\hat{\chi}\mathcal{O}} &= \pi^p g_*^2 \lambda_{\sigma\sigma\mathcal{O}}^* \frac{\Gamma(\Delta_\sigma^* - p/2)^2 \Gamma(\frac{\ell+p-2\Delta_\sigma^*+\Delta_\sigma^*}{2}) \Gamma(\frac{\ell+2p-2\Delta_\sigma^*-\Delta_\sigma^*}{2})}{\Gamma(p - \Delta_\sigma^*)^2 \Gamma(\frac{\ell-p+2\Delta_\sigma^*+\Delta_\sigma^*}{2}) \Gamma(\frac{\ell+2\Delta_\sigma^*-\Delta_\sigma^*}{2})} + O(g_*^4) ,\end{aligned}\tag{3.21}$$

has been concluded using only the (scalar) star-triangle relation. Deriving it directly would have required the more complicated conformal integrals in [40]. We could now apply (3.21) in 3d, inputting the numerically determined CFT data from the SRI, some of which has been bounded rigorously in [30]. In 2d, the caveat requiring \mathcal{O} to diagonalize the generator of dilations becomes important. One way to satisfy this is to find the eigenstates at a given level of the Virasoro ϵ multiplet and choose \mathcal{O} from this set. Conversely, operators in the Virasoro identity multiplet will mix with derivatives of $\sigma\hat{\chi}$ which precludes a diagonalization solely within the SRI.

3.3 Using OPE relations from the mean-field end

Let us now consider the mean-field end, where $g_* \sim \varepsilon$, $0 < \varepsilon \ll 1$ and the expansion starts from the trivial defect. This time the ‘ \pm ’ modes are $\hat{\phi}$ and $\hat{\phi}^3$ respectively, and the first two OPE

relations in (2.21) read:

$$\begin{aligned} \frac{\lambda_{\widehat{\phi\phi\mathcal{O}}}}{\lambda_{\widehat{\phi\phi^3\mathcal{O}}}} &= R(a_{\phi^2}) \frac{\Gamma(p/2 - \Delta_\phi) \Gamma(\frac{\ell+\Delta}{2}) \Gamma(\frac{\ell+2\Delta_\phi-\Delta}{2})}{\Gamma(\Delta_\phi - p/2) \Gamma(\frac{\ell+p-2\Delta_\phi+\Delta}{2}) \Gamma(\frac{\ell+p-\Delta}{2})} , \\ \frac{\lambda_{\widehat{\phi^3\phi^3\mathcal{O}}}}{\lambda_{\widehat{\phi\phi^3\mathcal{O}}}} &= R(a_{\phi^2})^{-1} \frac{\Gamma(\Delta_\phi - p/2) \Gamma(\frac{\ell+\Delta}{2}) \Gamma(\frac{\ell+2p-2\Delta_\phi-\Delta}{2})}{\Gamma(p/2 - \Delta_\phi) \Gamma(\frac{\ell-p+2\Delta_\phi+\Delta}{2}) \Gamma(\frac{\ell+p-\Delta}{2})} . \end{aligned} \quad (3.22)$$

All operators are taken to be unit-normalized. Setting $\Delta_\phi = \frac{p-\varepsilon}{4}$ shows that the OPE relations now constrain the CFT data in a different way. By plugging the λ_{ijk} coefficients at $O(\varepsilon^n)$ into (3.22), we can learn about $R(a_{\phi^2})$ and Δ at $O(\varepsilon^{n+1})$.

We will begin with the concrete example of $\Delta_{\widehat{\phi^2}}$ and $R(a_{\phi^2})$ at $O(\varepsilon^2)$. The process starts by inputting the tree-level OPE coefficients

$$\widehat{\lambda_{\phi\phi\phi^2}^{(0)}} = \sqrt{2}, \quad \widehat{\lambda_{\phi\phi^3\phi^2}^{(0)}} = \sqrt{3}, \quad \widehat{\lambda_{\phi^3\phi^3\phi^2}^{(0)}} = 3\sqrt{2}, \quad (3.23)$$

into the first two OPE relations in eq. (3.22). By further expanding them in ε , it is a simple exercise to show that the OPE relations are satisfied if and only if

$$\Delta_{\phi^2}^{(1)} = -1/6, \quad R^{(0)} = 0, \quad R^{(1)} = \frac{\Gamma(1 - \frac{p}{4}) \Gamma(\frac{p}{2})}{3\sqrt{6}\Gamma(\frac{p}{4} + 1)}. \quad (3.24)$$

In particular, we have reproduced the known anomalous dimension $\gamma_{\phi^2}^{(1)}$ and also $R^{(1)}$ computed directly in appendix B.

At the next-to-leading order we shall need the OPE coefficients at $O(\varepsilon)$. Computing $\lambda_{ijk}^{(1)}$ in position space starts with integrating a GFF four-point function with respect to τ while keeping ε finite. In all cases, this produces an ε^{-1} pole to be subtracted, a logarithmic term associated with anomalous dimensions, and the finite term we are after. As we will see, the latter is always proportional to

$$\mathcal{A}_p \equiv \psi\left(\frac{p}{2}\right) - 2\psi\left(\frac{p}{4}\right) + \psi(1) \ . \quad (3.25)$$

For $\lambda_{\widehat{\phi\phi\phi^2}}^{(1)}$ the unique diagram is:

$$-\frac{\lambda}{\sqrt{2}} \quad (3.26)$$

where the factor $1/\sqrt{2}$ comes from the definition of the empty vertex (i.e. the insertion of $\widehat{\phi}^2$) and we are integrating over all possible insertions of the λ vertex, which is here represented by the full dot. The diagram is computed in appendix B where we find

$$I_{1,1,2} = -\frac{\lambda\pi^{p/2}}{\sqrt{2}} \frac{\Gamma(\frac{p}{2})^{-1}}{|\tau_{13}|^{\frac{p-\varepsilon}{2}} |\tau_{23}|^{\frac{p-\varepsilon}{2}}} \left[\frac{2}{\varepsilon} + \mathcal{A}_p + \log \left| \frac{\tau_{13}\tau_{23}}{\tau_{12}} \right| + O(\varepsilon) \right]. \quad (3.27)$$

For $\lambda_{\widehat{\phi^3\phi^3\phi^2}}^{(1)}$ we have three diagrams:

$$-\frac{3\lambda}{2\sqrt{3}} \text{ (diagram 1)} - \frac{\lambda}{\sqrt{3}} \text{ (diagram 2)} - \frac{3\lambda}{\sqrt{3}} \text{ (diagram 3)} \quad (3.28)$$

Using the results of appendix B we see that the first diagram has no $O(1)$ term, while the second starts at $O(\varepsilon)$. The third diagram has a finite part which is proportional to (3.27) and equals

$$I_{1,3,2} = -\frac{3\lambda\pi^{p/2}}{\sqrt{3}} \frac{\Gamma(\frac{p}{2})^{-1}}{|\tau_{12}|^{\frac{p-\varepsilon}{2}} |\tau_{23}|^{p-\varepsilon}} \left[\frac{4}{\varepsilon} + \mathcal{A}_p + 2 \log \left| \frac{\tau_{12}\tau_{23}^2}{\tau_{13}} \right| + O(\varepsilon) \right]. \quad (3.29)$$

Finishing with $\lambda_{\widehat{\phi^3\phi^3\phi^2}}^{(1)}$, we have five diagrams:

$$-\frac{3\lambda}{\sqrt{2}} \text{ (diagram 1)} - \frac{\lambda}{\sqrt{2}} \left(\text{diagram 2} + \text{diagram 3} \right) \quad (3.30)$$

$$-\frac{6\lambda}{\sqrt{2}} \left(\text{diagram 4} + \text{diagram 5} \right) - \frac{3\lambda}{\sqrt{2}} \text{ (diagram 6)} \quad (3.31)$$

The first one is $72/\varepsilon$ to the desired order, the second and third are zero to the desired order, and all $O(1)$ terms come from the last three diagrams. As shown in appendix B the result is

$$I_{3,3,2} = -\frac{3\lambda\pi^{p/2}}{\sqrt{2}} \frac{\Gamma(\frac{p}{2})^{-1}}{|\tau_{12}|^{p-\varepsilon} |\tau_{13}|^{\frac{p-\varepsilon}{2}} |\tau_{23}|^{\frac{p-\varepsilon}{2}}} \left[\frac{14}{\varepsilon} + 5\mathcal{A}_p + 2 \log |\tau_{12}^5 \tau_{13} \tau_{23}| + O(\varepsilon) \right]. \quad (3.32)$$

Altogether, the $1/\varepsilon$ poles in (3.27), (3.29) and (3.32) can be subtracted by a wave-function renormalization for $\widehat{\phi^2}$ and for $\widehat{\phi^3}$, which in turn give the correct anomalous dimensions at the IR fixed point, and from the finite part we get

$$\lambda_{\widehat{\phi\phi\phi^2}}^{(1)} = -\frac{\mathcal{A}_p}{3\sqrt{2}}, \quad \lambda_{\widehat{\phi\phi^3\phi^2}}^{(1)} = -\frac{\mathcal{A}_p}{\sqrt{3}}, \quad \lambda_{\widehat{\phi^3\phi^3\phi^2}}^{(1)} = -\frac{5\mathcal{A}_p}{\sqrt{2}}. \quad (3.33)$$

We can now plug these results into the OPE relations, and expanding in powers of ε we find that they can be satisfied if and only if

$$\Delta_{\phi^2}^{(2)} = \frac{\mathcal{A}_p}{9}, \quad R^{(2)} = -\frac{\Gamma(1-\frac{p}{4}) \Gamma(\frac{p}{2})}{36\sqrt{6}\Gamma(\frac{p}{4}+1)} [13\psi(\frac{p}{4}) + 3\psi(-\frac{p}{4}) - 8\psi(\frac{p}{2}) - 8\psi(1)]. \quad (3.34)$$

Again, we have reproduced the correct result for $\Delta_{\widehat{\phi^2}}$ – see eq. (3.10) – but this time we have also obtained the next-to-leading order prediction for $R(a_{\phi^2})$. Note that, via eq. (2.12), the latter implies the following expansion for a_{ϕ^2} :

$$\begin{aligned} a_{\phi^2} &= \varepsilon^2 a_{\phi^2}^{(2)} + \varepsilon^3 a_{\phi^2}^{(3)} + O(\varepsilon^4) , \\ a_{\phi^2}^{(2)} &= -\frac{\Gamma\left(\frac{p}{2}\right)^2}{3\sqrt{6}\Gamma(p)} R^{(1)} , \\ a_{\phi^2}^{(3)} &= -\frac{\Gamma\left(\frac{p}{2}\right)^3 \Gamma\left(1 - \frac{p}{2}\right) \Gamma\left(1 - \frac{p}{4}\right)}{216\Gamma\left(\frac{p}{4} + 1\right) \Gamma(p + 1)} \left[4 - \frac{\Gamma\left(\frac{p}{4}\right)^2 \Gamma\left(1 - \frac{p}{4}\right)^2}{\Gamma\left(\frac{p}{2}\right) \Gamma\left(-\frac{p}{2}\right)} - \frac{96\sqrt{6}\Gamma\left(\frac{p}{4} + 1\right)}{\Gamma\left(-\frac{p}{4}\right) \Gamma\left(\frac{p}{2}\right)} R^{(2)} \right] . \end{aligned} \quad (3.35)$$

In particular, for $p = 2$ and $p = 3$ we get

$$\begin{aligned} a_{\phi^2} &= -\frac{1}{27}\varepsilon^2 + \left(\frac{1}{54} - \frac{8\log 4}{81}\right)\varepsilon^3 + O(\varepsilon^4) \quad (p = 2) \\ &= -0.037037\varepsilon^2 - 0.118399\varepsilon^3 + O(\varepsilon^4) , \\ a_{\phi^2} &= -\frac{\pi^{5/2}}{576\sqrt{2}\Gamma\left(\frac{7}{4}\right)^2}\varepsilon^2 + \frac{4\sqrt{2}\pi}{6075}(13\pi - 28 - 64\log 2)\Gamma\left(\frac{9}{4}\right)^2\varepsilon^3 + O(\varepsilon^4) \quad (p = 3) \\ &= -0.0254242\varepsilon^2 - 0.0667824\varepsilon^3 + O(\varepsilon^4) , \end{aligned} \quad (3.36)$$

which are analogous to (3.20).

We can use the OPE relations to compute anomalous dimensions of $\widehat{\phi^m}$ operators. We use the third line of eq. (2.21) with $\hat{T} = \widehat{\phi^m}$, $\varepsilon = \widehat{\phi^{m-1}}$, as well as the ε expansion for $R(a_{\phi^2})$ computed earlier. The relevant OPE coefficients all come from the same integrals which appeared in the derivation of (3.33). Working out the correct combinatorial factors, they read

$$\begin{aligned} \lambda_{\widehat{\phi^3}\widehat{\phi^{m-1}}\widehat{\phi^m}} &= \sqrt{m} \left(1 - \frac{\varepsilon}{6}(m-1)\mathcal{A}_p + O(\varepsilon^2) \right) , \\ \lambda_{\widehat{\phi^3}\widehat{\phi^{m-1}}\widehat{\phi^m}} &= (m-1)\sqrt{\frac{3m}{2}} \left(1 - \frac{\varepsilon}{6}(3m-4)\mathcal{A}_p + O(\varepsilon^2) \right) . \end{aligned} \quad (3.37)$$

Plugging these into the OPE relations and expanding for small ε , at one loop we find that

$$12 \left[\Delta_{\widehat{\phi^{m-1}}}^{(1)} - \Delta_{\widehat{\phi^m}}^{(1)} \right] + 4m - 7 = 0 , \quad (3.38)$$

which allows $\Delta_{\widehat{\phi^0}}^{(1)} = 0$ to be used as a boundary condition. Solving (3.38) and also converting the result to an anomalous dimension yields

$$\Delta_{\widehat{\phi^m}}^{(1)} = \frac{m(2m-5)}{12} , \quad \gamma_{\widehat{\phi^m}}^{(1)} = \frac{m(m-1)}{6} . \quad (3.39)$$

Knowing (3.24), this result can be written as $\gamma_{\widehat{\phi^m}}^{(1)} = \binom{m}{2}\gamma_{\widehat{\phi^2}}^{(1)}$ which is the same relation between one-loop anomalous dimensions that holds in the local Wilson-Fisher fixed point [37]. This is not

surprising because Wick contractions in these theories have the same structure. At two loops we find instead

$$18 \left[\Delta_{\widehat{\phi^{m-1}}}^{(2)} - \Delta_{\widehat{\phi^m}}^{(2)} \right] - (m-1)(3m-8)\mathcal{A}_p = 0 , \quad (3.40)$$

and so

$$\gamma_{\widehat{\phi^m}}^{(2)} = \Delta_{\widehat{\phi^m}}^{(2)} = -\frac{m(m-1)(m-3)}{18}\mathcal{A}_p . \quad (3.41)$$

To our knowledge, for $m > 4$, this quantity has not been computed before since the three-loop results of [20] stop at $m = 4$. Notice that (3.41) vanishes for $m = 1$ and $m = 3$, as it should since the ‘ \pm ’ modes have protected scaling dimensions. The OPE relations allowed us to obtain a two-loop result using only CFT data at lower order.

3.4 Generalization to long-range $O(N)$ models

Long-range $O(N)$ models are on the same conceptual footing as the long-range Ising model. It should therefore be no surprise that the calculations in the previous subsection can be generalized to the $O(N)$ case. We will demonstrate this only for the mean-field end, although we expect the same strategy to work for the short-range end.⁷

This time the defect modes of the free bulk scalar are in the fundamental of $O(N)$ and read

$$\psi_0^{(+,I)} = \hat{\phi}^I , \quad \psi_0^{(-,I)} = \frac{1}{\sqrt{2(N+2)}}(\hat{\phi} \cdot \hat{\phi})\hat{\phi}^I , \quad (3.42)$$

whose overall coefficients are chosen such that they are unit-normalized. For such long-range $O(N)$ models one can recover a set of exact OPE relations that is completely analogous to eq. (2.21) with the same gamma functions. We will exploit such OPE relations to compute anomalous dimensions of (unit-normalized) operators

$$\Sigma_n = \frac{1}{2^n \sqrt{n!(N/2)_n}}(\hat{\phi} \cdot \hat{\phi})^n , \quad \mathcal{W}_n^I = \frac{1}{2^n \sqrt{n!(N/2+1)_n}}(\hat{\phi} \cdot \hat{\phi})^n \hat{\phi}^I . \quad (3.43)$$

The set of perturbative OPE coefficients we need are generalizations of (3.37), which are com-

⁷To this end we would need extensive CFT data for the short-range $O(N)$ models. These are in principle available at large N . It would also be interesting to use the $O(2)$ model data from [41] which was extracted using the techniques of [42].

puted in appendix B up to $O(\varepsilon^2)$ corrections. They read:⁸

$$\begin{aligned}
\lambda_{\mathcal{W}_0 \mathcal{W}_n \Sigma_n} &= \lambda_{\mathcal{W}_0 \mathcal{W}_n \Sigma_n}^{(0)} \left(1 - \varepsilon \frac{3n}{N+8} \mathcal{A}_p + O(\varepsilon^2) \right) , \\
\lambda_{\mathcal{W}_0 \mathcal{W}_n \Sigma_{n+1}} &= \lambda_{\mathcal{W}_0 \mathcal{W}_n \Sigma_{n+1}}^{(0)} \left(1 - \varepsilon \frac{6n+N+2}{2(N+8)} \mathcal{A}_p + O(\varepsilon^2) \right) , \\
\lambda_{\mathcal{W}_1 \mathcal{W}_n \Sigma_n} &= \lambda_{\mathcal{W}_1 \mathcal{W}_n \Sigma_n}^{(0)} \left(1 - \varepsilon \frac{54n+7N-16}{6(N+8)} \mathcal{A}_p + O(\varepsilon^2) \right) , \\
\lambda_{\mathcal{W}_1 \mathcal{W}_n \Sigma_{n+1}} &= \lambda_{\mathcal{W}_1 \mathcal{W}_n \Sigma_{n+1}}^{(0)} \left(1 - \varepsilon \frac{n(54n+17N+28)+3(N+2)}{(N+8)(6n+N+2)} \mathcal{A}_p + O(\varepsilon^2) \right) ,
\end{aligned} \tag{3.44}$$

where the disconnected contributions are

$$\begin{aligned}
\lambda_{\mathcal{W}_0 \mathcal{W}_n \Sigma_n}^{(0)} &= \frac{\sqrt{\left(\frac{N}{2}+1\right)_n}}{\sqrt{\left(\frac{N}{2}\right)_n}} , \quad \lambda_{\mathcal{W}_1 \mathcal{W}_n \Sigma_n}^{(0)} = \frac{3n\sqrt{2\left(\frac{N}{2}+1\right)_n}}{\sqrt{(N+2)\left(\frac{N}{2}\right)_n}} , \\
\lambda_{\mathcal{W}_0 \mathcal{W}_n \Sigma_{n+1}}^{(0)} &= \frac{\sqrt{(n+1)\left(\frac{N}{2}+1\right)_n}}{\sqrt{\left(\frac{N}{2}\right)_{n+1}}} , \quad \lambda_{\mathcal{W}_1 \mathcal{W}_n \Sigma_{n+1}}^{(0)} = \frac{(6n+N+2)\sqrt{2(n+1)\left(\frac{N}{2}\right)_{n+1}}}{N\sqrt{(N+2)\left(\frac{N}{2}+1\right)_n}} .
\end{aligned} \tag{3.45}$$

The calculation again starts with the minimal number of fields. Taking $n = 1$ and $\hat{T} = \Sigma_1$, the first two lines of eq. (2.21) give expressions for the ratios $\lambda_{\mathcal{W}_0 \mathcal{W}_0 \Sigma_1} / \lambda_{\mathcal{W}_0 \mathcal{W}_1 \Sigma_1}$ and $\lambda_{\mathcal{W}_1 \mathcal{W}_1 \Sigma_1} / \lambda_{\mathcal{W}_0 \mathcal{W}_1 \Sigma_1}$. Demanding that they agree with the appropriate cases of (3.45) yields

$$\begin{aligned}
R^{(0)} &= 0 , \quad R^{(1)} = \frac{\sqrt{N+2} \Gamma\left(1 - \frac{p}{4}\right) \Gamma\left(\frac{p}{2}\right)}{\sqrt{2}(N+8)\Gamma\left(\frac{p}{4}+1\right)} , \quad R^{(2)} = \frac{\sqrt{N+2} \Gamma\left(1 - \frac{p}{4}\right) \Gamma\left(\frac{p}{2}\right)}{4\sqrt{2}(N+8)^3\Gamma\left(\frac{p}{4}+1\right)} \\
&\times \left[(N^2 - 64N - 288)\psi\left(\frac{p}{4}\right) - (N+8)^2\psi\left(-\frac{p}{4}\right) + 8(5N+22)\psi\left(\frac{p}{2}\right) + 8(5N+22)\psi(1) \right] .
\end{aligned} \tag{3.46}$$

at $O(\varepsilon^2)$, along with anomalous dimensions of Σ_1 which agree with [28]. This results in the following one-point function of ϕ^2 :

$$\begin{aligned}
a_{\phi^2}^{(2)} &= \frac{(N+2)\Gamma\left(1 - \frac{p}{4}\right) \Gamma\left(\frac{p}{2}\right)^3}{2(N+8)^2\Gamma\left(\frac{p}{4}+1\right)\Gamma(p)} , \quad a_{\phi^2}^{(3)} = -\frac{(N+2)\Gamma\left(1 - \frac{p}{4}\right) \Gamma\left(\frac{p}{2}\right)^3}{8(N+8)^4\Gamma\left(\frac{p}{4}+1\right)\Gamma(p)} \\
&\times \left[(N^2 - 144N - 640)\psi\left(\frac{p}{4}\right) - (N+8)^2\psi\left(-\frac{p}{4}\right) + 16(5N+22)\psi\left(\frac{p}{2}\right) + 16(5N+22)\psi(1) \right] .
\end{aligned} \tag{3.47}$$

To go further and compute anomalous dimensions of (3.43), we shall simply use the third line of eq. (2.21), once with $\hat{T} = \Sigma_n$ and $\varepsilon = \mathcal{W}_n$, and once with $\hat{T} = \Sigma_{n+1}$ and $\varepsilon = \mathcal{W}_n$. Using the known $R^{(1)}$, we obtain the coupled equations

$$\begin{aligned}
\Delta_{\mathcal{W}_n}^{(1)} &= \Delta_{\Sigma_n}^{(1)} + \frac{6n}{N+8} - \frac{1}{4} , \\
0 &= 2(N+8)(\Delta_{\Sigma_n}^{(1)} - \Delta_{\Sigma_{n+1}}^{(1)}) + 24n + N - 4 .
\end{aligned} \tag{3.48}$$

⁸A three-point function with two \mathcal{W}_n^I -type operators is proportional to δ^{IJ} , so we can drop the I label in the the corresponding OPE coefficient.

at one loop. Their solution is:

$$\Delta_{\Sigma_n}^{(1)} = \frac{n(12n + N - 16)}{2(N + 8)} , \quad \Delta_{\mathcal{W}_n}^{(1)} = \frac{24n^2 + 2n(N - 4) - N - 8}{4(N + 8)} . \quad (3.49)$$

Analogous equations can be found at two loops as $R^{(2)}$ is also known. They are solved by:

$$\begin{aligned} \Delta_{\Sigma_n}^{(2)} &= \frac{n[36n^2(N + 8) + 12n(N^2 - N - 54) - N(19N + 58) + 320]}{(N + 8)^3} \mathcal{A}_p , \\ \Delta_{\mathcal{W}_n}^{(2)} &= \frac{6n(n - 1)[6n(N + 8) + N(2N + 13) + 12]}{(N + 8)^3} \mathcal{A}_p . \end{aligned} \quad (3.50)$$

Once again, the virtue of the OPE relations is that they allow to gain one order in perturbation theory, as shown in these examples.

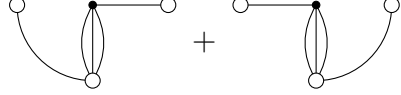
A few comments are in order. First, our results for $\Delta_{\Sigma_1}^{(1)}$ and $\Delta_{\Sigma_1}^{(2)}$ agree with equations (5.6) of [28] and (3.20) of [20]. The quantity $\Delta_{\Sigma_2}^{(2)}$ was also computed in [20], and we agree with their result. Second, both $\Delta_{\mathcal{W}_0}^{(2)}$ and $\Delta_{\mathcal{W}_1}^{(2)}$ vanish as they should, since the corresponding operators are protected defect modes. Finally, for $N = 1$ and any n we recover the results of subsection 3.3.

3.5 Taking stock

Of the new results we have computed so far, the ones which will be used most immediately are (3.20) and (3.35). These express the one-point function a_{ϕ^2} near the short-range and mean-field end of the LRI respectively. Estimates of this quantity will prove to be an important guide for the numerical bootstrap. However, the conceptual novelty of this section is that it is based on new tools for streamlining perturbation theory in the long-range Ising and $O(N)$ models, namely the OPE relations in eq. (2.21). These were powerful enough to provide new two-loop anomalous dimensions for Σ_n and \mathcal{W}_n^I defined in (3.43).

When the special case $\gamma_{\Sigma_1}^{(2)}$ was first found in [28], more standard Feynman diagram calculations were used. It would have also been possible to find all $\gamma_{\Sigma_n}^{(2)}$ in this way because the required number of diagrams stabilizes for sufficiently large n . If desired, one can now turn the process around and predict the $O(\varepsilon^{-1})$ parts of these new diagrams using our scaling dimensions (3.50). One might hope for a further generalization by including derivatives in (3.43). The OPE relations explored here hold for operators with spin and they can certainly be used to compute their anomalous dimensions. The main obstacle one faces is that the linear combinations of derivatives which lead to a conformal primary are non-trivial. Finding a way around this was possible when we computed (3.13) but only because the operator $[\hat{\phi}\hat{\phi}]_{0,\ell}$ was limited to two fields. With arbitrarily many fields, the presence of derivatives introduces a book-keeping exercise which seems hard to avoid with either the OPE relations or pre-bootstrap methods.

On the other hand, one statement of this form that we can make is $\lambda_{\hat{\phi}\hat{\phi}\hat{\mathcal{O}}}^{(1)} = 0$ when $\hat{\mathcal{O}}$ is an operator involving four fields $\hat{\phi}$ and potentially many derivatives. This result will become important in the next section which discusses a method for extracting CFT data along a trajectory of operators in a four-point function. When computing $\langle \hat{\phi}(x_1)\hat{\phi}(x_2)\hat{\mathcal{O}}(x_3) \rangle$ to one loop, each distribution of derivatives is handled using the diagrams


(3.51)

Following the steps used for (3.13), these are computed using either

$$\int \frac{d^p \tau_0 \tau_{03}^{a_1} \dots \tau_{03}^{a_l}}{|\tau_{01}|^{\frac{1}{2}(p-\varepsilon)} |\tau_{03}|^{\frac{3}{2}(p-\varepsilon)+2l}} = \frac{\Gamma(p+l-\varepsilon)}{\Gamma(\frac{1}{4}(p-\varepsilon))\Gamma(\frac{3}{4}(p-\varepsilon)+l)} \quad (3.52)$$

$$\times \int_0^1 dx \int d^p \tau_0 \frac{x^{\frac{1}{4}(p-\varepsilon)-1} (1-x)^{\frac{3}{4}(p-\varepsilon)+l-1}}{[\tau_0^2 + x(1-x)\tau_{13}^2]^{p+l-\varepsilon}} (\tau_0 + x\tau_{13})^{a_1} \dots (\tau_0 + x\tau_{13})^{a_l},$$

or its image under $(1 \leftrightarrow 2)$. Without loss of generality, we have taken the factors of τ_{03}^a (if they are contracted at all) to be contracted with the factors of τ_{23}^a outside the integral rather than each other. While (3.52) clearly vanishes when l is odd, a simple calculation shows that all $l/2$ terms of it are $O(\varepsilon)$ when l is even. This means that the three-point function, which includes λ_* , is $O(\varepsilon^2)$.

4 Inversion formula

One of our perturbative results in the previous section applies to an infinite family of operators labelled by spin — namely $[\hat{\phi}\hat{\phi}]_{0,\ell}$ for $\ell > 0$. This is the leading trajectory of double-twist operators built from the fundamental field. Many studies in recent years have computed analogous families of anomalous dimensions using an efficient technique which sidesteps most of the need for diagrammatic computations. This is the Lorentzian inversion formula [22] designed to yield CFT data in a form which is analytic in spin down to a critical value determined by the growth of the correlator in the Regge limit. Moreover, detailed knowledge of the correlator is optional for applying it as long as one has access to a simpler piece called the double discontinuity. Specializing to identical external scalars Φ in $p = 2$, the Lorentzian inversion formula is

$$\begin{aligned} c(\Delta, \ell) &= \frac{1 + (-1)^\ell}{4} \frac{\Gamma(\frac{\Delta+\ell}{2})^4}{2\pi^2 \Gamma(\Delta+\ell) \Gamma(\Delta+\ell-1)} \int_0^1 \frac{dz}{z^2} \int_0^1 \frac{d\bar{z}}{\bar{z}^2} g_{\Delta-1, \ell+1}(z, \bar{z}) d\text{Disc}[G(z, \bar{z})] \\ &= \frac{\Gamma(\frac{\Delta+\ell}{2})^4}{2\pi^2 \Gamma(\Delta+\ell) \Gamma(\Delta+\ell-1)} \int_0^1 \frac{dz}{z^2} \int_0^1 \frac{d\bar{z}}{\bar{z}^2} k_{\ell-\Delta+2}(z) k_{\Delta+\ell}(\bar{z}) d\text{Disc}[G(z, \bar{z})], \end{aligned} \quad (4.1)$$

where

$$\text{dDisc}[G(z, \bar{z})] = G(z, \bar{z}) - \frac{1}{2}G^\odot(z, \bar{z}) - \frac{1}{2}G^\odot(z, \bar{z}) , \quad (4.2)$$

is the double discontinuity and the spectral density is defined so that

$$c(\Delta, \ell) = - \sum_{\mathcal{O}} \frac{\lambda_{\Phi\Phi\mathcal{O}}^2}{\Delta - \Delta_{\mathcal{O}}} . \quad (4.3)$$

Our main goal in this section is to improve upon the $p = 2$ case of our results for $[\hat{\phi}\hat{\phi}]_{n,\ell}$ by extending them to three loops and all $n \geq 0$.

4.1 Overview

When applying the Lorentzian inversion formula, a useful fact is that double-twist operators produce integer powers of $1 - \bar{z}$ in the crossed channel which have a vanishing double discontinuity. This means that if Φ is a generalized free field, all contributions to (4.1) come from $(1 - \bar{z})^{-\Delta_\Phi}$ associated with the identity operator. As we turn on deformations however, other non-trivial terms (referred to as Casimir singular in [29]) start to appear. These include other fractional powers of $1 - \bar{z}$ and logarithms appearing quadratically or higher. These satisfy

$$\begin{aligned} \text{dDisc}[(1 - \bar{z})^\xi] &= (1 - \bar{z})^\xi 2 \sin^2(\pi\xi) , \\ \text{dDisc}[\log(1 - \bar{z})^2] &= 4\pi^2 , \\ \text{dDisc}[\log(1 - \bar{z})^3] &= 12\pi^2 \log(1 - \bar{z}) . \end{aligned} \quad (4.4)$$

We will take $\Phi = \hat{\phi}$ which allows the deformation to be parameterized by ε . CFT data will then be expanded as

$$\begin{aligned} a_{\mathcal{O}} &= a_{\mathcal{O}}^{(0)} + \varepsilon a_{\mathcal{O}}^{(1)} + \varepsilon^2 a_{\mathcal{O}}^{(2)} + \varepsilon^3 a_{\mathcal{O}}^{(3)} + O(\varepsilon^4) , \\ \Delta_{\mathcal{O}} &= \Delta_{\mathcal{O}}^{(0)} + \varepsilon \gamma_{\mathcal{O}}^{(1)} + \varepsilon^2 \gamma_{\mathcal{O}}^{(2)} + \varepsilon^3 \gamma_{\mathcal{O}}^{(3)} + O(\varepsilon^4) , \end{aligned} \quad (4.5)$$

where $a_{\mathcal{O}} = \lambda_{\Phi\Phi\mathcal{O}}^2$ and we remind the reader that $\Delta_{\mathcal{O}}^{(0)}$ and $a_{\mathcal{O}}^{(0)}$ in this expansion depend on ε . Plugging (4.5) into (4.3),

$$\begin{aligned} -c(\Delta, \ell) &\sim \frac{\langle a_{\mathcal{O}}^{(0)} \rangle}{\Delta - \Delta_{\mathcal{O}}^{(0)}} + \varepsilon \left[\frac{\langle a_{\mathcal{O}}^{(1)} \rangle}{\Delta - \Delta_{\mathcal{O}}^{(0)}} + \frac{\langle a_{\mathcal{O}}^{(0)} \gamma_{\mathcal{O}}^{(1)} \rangle}{(\Delta - \Delta_{\mathcal{O}}^{(0)})^2} \right] \\ &+ \varepsilon^2 \left[\frac{\langle a_{\mathcal{O}}^{(2)} \rangle}{\Delta - \Delta_{\mathcal{O}}^{(0)}} + \frac{\langle a_{\mathcal{O}}^{(0)} \gamma_{\mathcal{O}}^{(2)} + a_{\mathcal{O}}^{(1)} \gamma_{\mathcal{O}}^{(1)} \rangle}{(\Delta - \Delta_{\mathcal{O}}^{(0)})^2} + \frac{\langle a_{\mathcal{O}}^{(0)} \gamma_{\mathcal{O}}^{(1)2} \rangle}{(\Delta - \Delta_{\mathcal{O}}^{(0)})^3} \right] \\ &+ \varepsilon^3 \left[\frac{\langle a_{\mathcal{O}}^{(3)} \rangle}{\Delta - \Delta_{\mathcal{O}}^{(0)}} + \frac{\langle a_{\mathcal{O}}^{(0)} \gamma_{\mathcal{O}}^{(3)} + a_{\mathcal{O}}^{(1)} \gamma_{\mathcal{O}}^{(2)} + a_{\mathcal{O}}^{(2)} \gamma_{\mathcal{O}}^{(1)} \rangle}{(\Delta - \Delta_{\mathcal{O}}^{(0)})^2} + \frac{\langle 2a_{\mathcal{O}}^{(0)} \gamma_{\mathcal{O}}^{(1)} \gamma_{\mathcal{O}}^{(2)} + a_{\mathcal{O}}^{(1)} \gamma_{\mathcal{O}}^{(1)2} \rangle}{(\Delta - \Delta_{\mathcal{O}}^{(0)})^3} + \frac{\langle a_{\mathcal{O}}^{(0)} \gamma_{\mathcal{O}}^{(1)3} \rangle}{(\Delta - \Delta_{\mathcal{O}}^{(0)})^4} \right] , \end{aligned} \quad (4.6)$$

is the behaviour of the spectral density as $\Delta \rightarrow \Delta_{\mathcal{O}}^{(0)}$. Since there will generically be many operators with dimension $\Delta_{\mathcal{O}}^{(0)} + O(\varepsilon)$, we have used the $\langle \dots \rangle$ notation to refer to a sum over this degenerate eigenspace. One can now go through the same procedure and find

$$\begin{aligned}
G(z, \bar{z}) = \sum_{\Delta_{\mathcal{O}}^{(0)}, \ell_{\mathcal{O}}} & \left[\langle a_{\mathcal{O}}^{(0)} \rangle + \varepsilon \langle a_{\mathcal{O}}^{(1)} + a_{\mathcal{O}}^{(0)} \gamma_{\mathcal{O}}^{(1)} \partial_{\Delta} \rangle + \varepsilon^2 \langle a_{\mathcal{O}}^{(2)} + (a_{\mathcal{O}}^{(1)} \gamma_{\mathcal{O}}^{(1)} + a_{\mathcal{O}}^{(0)} \gamma_{\mathcal{O}}^{(2)}) \partial_{\Delta} + \frac{1}{2} a_{\mathcal{O}}^{(0)} \gamma_{\mathcal{O}}^{(1)2} \partial_{\Delta}^2 \rangle \right. \\
& + \varepsilon^3 \langle a_{\mathcal{O}}^{(3)} + (a_{\mathcal{O}}^{(2)} \gamma_{\mathcal{O}}^{(1)} + a_{\mathcal{O}}^{(1)} \gamma_{\mathcal{O}}^{(2)} + a_{\mathcal{O}}^{(0)} \gamma_{\mathcal{O}}^{(3)}) \partial_{\Delta} + \left(\frac{1}{2} a_{\mathcal{O}}^{(1)} \gamma_{\mathcal{O}}^{(1)2} + a_{\mathcal{O}}^{(0)} \gamma_{\mathcal{O}}^{(1)} \gamma_{\mathcal{O}}^{(2)} \right) \partial_{\Delta}^2 + \frac{1}{6} a_{\mathcal{O}}^{(0)} \gamma_{\mathcal{O}}^{(1)3} \partial_{\Delta}^3 \rangle \\
& \left. + O(\varepsilon^4) \right] \left| \frac{z}{1-z} \right|^{2\Delta_{\phi}} g_{\mathcal{O}}(1-z, 1-\bar{z}) , \tag{4.7}
\end{aligned}$$

for the crossed channel conformal block expansion. If we temporarily focus on double-twist operators, all contributions to the double discontinuity come from terms with two or more ∂_{Δ} derivatives. Their coefficients at $O(\varepsilon^n)$ only involve CFT data up to $O(\varepsilon^{n-1})$. A naive reading of (4.7) therefore suggests an iterative procedure wherein the results of the inversion formula at one order are fed back into it at the next. At high enough orders, this logic breaks down for three reasons:

1. multi-twist operators will eventually be exchanged which can produce a double-discontinuity without two derivatives;
2. even for double-twist operators, those of low spin are not captured by the inversion formula and need to be put in by hand;
3. averages like $\langle a_{\mathcal{O}}^{(0)} \gamma_{\mathcal{O}}^{(1)2} \rangle$ are only known in terms of $\langle a_{\mathcal{O}}^{(0)} \rangle$ and $\langle a_{\mathcal{O}}^{(0)} \gamma_{\mathcal{O}}^{(1)} \rangle$ if one works with a large system of correlators to resolve the degeneracy.

For us, new types of operators will appear in a controlled way and degeneracy will not be an obstacle until after three loops. This differs from the situation in holographic theories which are more severely affected by degeneracy because they involve infinitely many generalized free fields [43–46].

4.2 Results at two loops

We will now make the above statements more precise. To start, the $\varepsilon = 0$ OPE (apart from the identity) contains only double-twist operators $[\hat{\phi}\hat{\phi}]_{n,\ell}$ labelled by $n \geq 0$ and $\ell \geq 0$. These have $\Delta_{n,\ell}^{(0)} = 2\Delta_{\phi} + 2n + \ell$ and

$$a_{n,\ell}^{(0)} = \frac{1 + (-1)^{\ell}}{n!(n+\ell)!} \frac{\Gamma(\Delta_{\phi} + n)^2 \Gamma(\Delta_{\phi} + n + \ell)^2}{\Gamma(\Delta_{\phi})^4} \frac{\Gamma(2\Delta_{\phi} + n - 1) \Gamma(2\Delta_{\phi} + n + \ell - 1)}{\Gamma(2\Delta_{\phi} + 2n - 1) \Gamma(2\Delta_{\phi} + 2n + 2\ell - 1)} . \tag{4.8}$$

We can derive (4.8) by inverting the identity or by using the original brute force methods of [47]. It is now possible to say that $a_{\mathcal{O}}^{(0)}$ and $a_{\mathcal{O}}^{(1)}$ are only non-zero for double-twist operators but we can actually make a stronger statement. After inserting $\lambda_{\hat{\phi}^4}$ once, the naive expectation is that a quadruple-twist operator \mathcal{O} will be seen to have $\lambda_{\hat{\phi}\hat{\phi}\mathcal{O}} = O(\varepsilon)$. In fact, our calculation in the last section showed that $\lambda_{\hat{\phi}\hat{\phi}\mathcal{O}} = O(\varepsilon^2)$ which means that also $a_{\mathcal{O}}^{(2)}$ and $a_{\mathcal{O}}^{(3)}$ are only non-zero for double-twist operators. The second major simplification is that $\gamma_{n,\ell}^{(1)}$ is only non-zero for $n = \ell = 0$. The necessity of $\ell = 0$ is already clear from the fact that there is no double discontinuity at $O(\varepsilon)$. To prove the more general claim, consider

$$\langle [\hat{\phi}\hat{\phi}]_{n,\ell}(\tau_1) [\hat{\phi}\hat{\phi}]_{n,\ell}(\tau_2) \phi^4(\tau_3) \rangle = \sum_{i,j} \langle D_A^{(i)} \phi D_B^{(i)} \phi(\tau_1) D_A^{(j)} \phi D_B^{(j)} \phi(\tau_2) \phi^4(\tau_3) \rangle, \quad (4.9)$$

where the D_A and D_B are differential operators. They ultimately act on $|\tau_{13}|^{-2\Delta_\phi}$ and $|\tau_{23}|^{-2\Delta_\phi}$ after we apply Wick's theorem to the right hand side of (4.9). This 3pt function is therefore regular as $\tau_1 \rightarrow \tau_2$. This property is only consistent with the Polyakov form

$$\langle [\hat{\phi}\hat{\phi}]_{n,\ell}(\tau_1) [\hat{\phi}\hat{\phi}]_{n,\ell}(\tau_2) \phi^4(\tau_3) \rangle = \frac{\lambda_{[\hat{\phi}\hat{\phi}]_{n,\ell}[\hat{\phi}\hat{\phi}]_{n,\ell}\phi^4}}{|\tau_{12}|^{4n+2\ell} |\tau_{13}|^{4\Delta_\phi} |\tau_{23}|^{4\Delta_\phi}}, \quad (4.10)$$

if $\lambda_{[\hat{\phi}\hat{\phi}]_{n,\ell}[\hat{\phi}\hat{\phi}]_{n,\ell}\phi^4}$ vanishes whenever n and ℓ are not both zero. First order perturbation theory then implies that the same holds for $\gamma_{n,\ell}^{(1)}$. An alternative way to prove that $\gamma_{n,\ell}^{(1)} \propto \delta_{n,0}\delta_{\ell,0}$ is discussed in appendix C.

Returning to (4.7), we now only need to input two quantities to solve for the double discontinuity at $O(\varepsilon^2)$. These are

$$a_{\hat{\phi}^2}^{(0)} = 2, \quad \gamma_{\hat{\phi}^2}^{(1)} = \frac{1}{3}. \quad (4.11)$$

If we now let ∂_Δ^2 act on the overall power law in $\left| \frac{z}{1-z} \right|^{2\Delta_\phi} g_{\Delta,0}(1-z, 1-\bar{z}) \Big|_{\Delta=2\Delta_\phi}$ (as opposed to the hypergeometric functions), it follows that the desired term in the spectral density is

$$c^{(2)}(\Delta, \ell) = \frac{\Gamma(\frac{\Delta+\ell}{2})^4}{18\Gamma(\Delta+\ell)\Gamma(\Delta+\ell-1)} \int_0^1 \frac{dz}{z^2} \int_0^1 \frac{d\bar{z}}{\bar{z}^2} k_{\ell-\Delta+2}(z) k_{\Delta+\ell}(\bar{z}) \left| \frac{z}{1-z} \right|^{1-\frac{\varepsilon}{2}} |k_{1-\frac{\varepsilon}{2}}(1-z)|^2. \quad (4.12)$$

If we are content with extracting CFT data to an accuracy of $O(\varepsilon^2)$, it is consistent to set $\varepsilon = 0$ in the integrand and evaluate

$$\begin{aligned} \varepsilon^2 c^{(2)}(\Delta, \ell) &= \frac{\varepsilon^2}{9} \frac{\Gamma(\frac{\Delta+\ell}{2})^4}{2\Gamma(\Delta+\ell)\Gamma(\Delta+\ell-1)} \int_0^1 \frac{d\bar{z}}{\bar{z}^2} z^{\frac{\Delta+\ell}{2}} {}_2F_1\left(\frac{\Delta+\ell}{2}, \frac{\Delta+\ell}{2}; \Delta+\ell; \bar{z}\right) \bar{z}^{\frac{1}{2}} {}_2F_1\left(\frac{1}{2}, \frac{1}{2}; 1; 1-\bar{z}\right) \\ &\quad \int_0^1 \frac{dz}{z^2} z^{\frac{\ell-\Delta+2}{2}} {}_2F_1\left(\frac{\ell-\Delta+2}{2}, \frac{\ell-\Delta+2}{2}; \ell-\Delta+2; z\right) z^{\frac{1}{2}} {}_2F_1\left(\frac{1}{2}, \frac{1}{2}; 1; 1-z\right). \end{aligned} \quad (4.13)$$

The factored integrals can be done in at least three ways.

1. By Taylor expanding the hypergeometric functions and integrating termwise, it is possible to resum and find $\frac{\Gamma(\Delta+\ell)}{\Gamma(\frac{1}{2}(\Delta+\ell)+1)^2} \left(\frac{\Delta+\ell}{\Delta+\ell-1}\right)^2$ for the first integral. The second is simply the shadow with $\Delta \mapsto 2 - \Delta$.
2. One can get the same result by exploiting the inner product which makes the quadratic Casimir D of $\mathfrak{sl}(2)$ self-adjoint [48]. Since each integral is an inner product of two eigenfunctions, one with eigenvalue $-\frac{1}{4}$ and the other with eigenvalue $h(h-1)$ for $h \in \{\frac{\Delta+\ell}{2}, \frac{\ell-\Delta+2}{2}\}$, we can use $\langle f, g \rangle = \frac{1}{h(h-1)+\frac{1}{4}} [\langle Df, g \rangle - \langle f, Dg \rangle]$ which localizes to a boundary term.
3. Finally, (4.12) is nothing but $\frac{\Gamma(\frac{\Delta+\ell}{2})^4}{18\Gamma(\Delta+\ell)\Gamma(\Delta+\ell-1)} \mathcal{I}(\ell - \Delta + 2, \frac{2-\varepsilon}{2}, \frac{2-\varepsilon}{4}) \mathcal{I}(\Delta + \ell, \frac{2-\varepsilon}{2}, \frac{2-\varepsilon}{4})$ where $\mathcal{I}(\Delta_s, \Delta_t, \Delta_\phi)$ is the crossing kernel in one dimension [48–50].

It is worth reviewing the crossing kernel since this is the approach which worked for evaluating (4.12) even with $\varepsilon \neq 0$. This will be crucial for the three-loop considerations in the next subsection.

Conformal blocks for $\mathfrak{sl}(2)$ are simply $k_{\Delta_s}(z)$ for the s -channel and $(\frac{z}{1-z})^{\Delta_\phi} k_{\Delta_t}(1-z)$ for the t -channel. The crossing kernel projects one onto the other. Using the techniques of [50], it becomes

$$\begin{aligned} \mathcal{I}(\Delta_s, \Delta_t, \Delta_\phi) &= \int_0^1 \frac{dz}{z^2} k_{\Delta_s}(z) \left(\frac{z}{1-z}\right)^{\Delta_\phi} k_{\Delta_t}(1-z) \\ &= \frac{\Gamma(\Delta_s)\Gamma(\Delta_t)}{\Gamma(\frac{\Delta_s}{2})^2\Gamma(\frac{\Delta_t}{2})^2} \int_{-i\infty}^{i\infty} \frac{dsdt}{2\pi i} K(s, t) \delta(\Delta_\phi + \frac{\Delta_s - \Delta_t}{2} - 1 + s - t), \end{aligned} \quad (4.14)$$

where

$$K(s, t) \equiv \Gamma(-s)\Gamma(-t) \frac{\Gamma(\frac{\Delta_s}{2} + s)^2 \Gamma(\frac{\Delta_t}{2} + t)^2}{\Gamma(\Delta_s + s) \Gamma(\Delta_t + t)}, \quad (4.15)$$

which leaves a single Mellin-Barnes integral. The formula

$$\begin{aligned} {}_7F_6 &\left[\begin{matrix} a & 1 + \frac{1}{2}a & b & c & d & e & f \\ \frac{1}{2}a & 1 + a - b & 1 + a - c & 1 + a - d & 1 + a - e & 1 + a - f; & 1 \end{matrix} \right] \\ &= \frac{\Gamma(1+a-b)\Gamma(1+a-c)\Gamma(1+a-d)\Gamma(1+a-e)\Gamma(1+a-f)}{\Gamma(1+a)\Gamma(b)\Gamma(c)\Gamma(d)\Gamma(1+a-c-d)\Gamma(1+a-b-d)\Gamma(1+a-b-c)\Gamma(1+a-e-f)} \\ &\times \int_{-i\infty}^{i\infty} \frac{du}{2\pi i} \frac{\Gamma(-u)\Gamma(1+a-b-c-d-u)\Gamma(b+u)\Gamma(c+u)\Gamma(d+u)\Gamma(1+a-e-f+u)}{\Gamma(1+a-e+u)\Gamma(1+a-f+u)}, \end{aligned} \quad (4.16)$$

is then available for turning (4.14) into a single very well poised hypergeometric function evaluated at 1. This can be done in four different ways. One can choose $1+a-e-f+u$ to be either

$\frac{\Delta_s}{2} + s$ or $\frac{\Delta_t}{2} + t$ and also eliminate either s or t in (4.14). We will make $\frac{\Delta_s}{2} + s$ privileged and eliminate t since this is the only choice whose hypergeometric function approaches 1 as $\varepsilon \rightarrow 0$. The others would significantly disguise the simplicity of the final result. Accordingly, we will write

$$\mathcal{I}(\Delta_s, \Delta_t, \Delta_\phi) = \frac{\Gamma(\Delta_t)\Gamma(\frac{\Delta_s}{2} + \Delta_\phi - 1)^2\Gamma(\frac{\Delta_t}{2} - \Delta_\phi + 1)\Gamma(\Delta_s + \frac{\Delta_t}{2} + \Delta_\phi - 1)}{\Gamma(\frac{\Delta_s + \Delta_t}{2})^2\Gamma(\frac{\Delta_s + \Delta_t}{2} + \Delta_\phi - 1)^2} \quad (4.17)$$

$${}_7F_6 \left[\begin{matrix} \frac{2\Delta_s + \Delta_t + 2\Delta_\phi - 4}{2} & \frac{2\Delta_s + \Delta_t + 2\Delta_\phi}{4} & \frac{\Delta_s + 2\Delta_\phi - 2}{2} & \frac{\Delta_s + 2\Delta_\phi - 2}{2} & \frac{\Delta_s}{2} & \frac{\Delta_s}{2} & \frac{\Delta_t + 2\Delta_\phi - 2}{2} \\ \frac{2\Delta_s + \Delta_t + 2\Delta_\phi - 4}{4} & \Delta_s & \frac{\Delta_s + \Delta_t}{2} & \frac{\Delta_s + \Delta_t}{2} & \frac{\Delta_s + \Delta_t + 2\Delta_\phi - 2}{2} & \frac{\Delta_s + \Delta_t + 2\Delta_\phi - 2}{2} & 1 \end{matrix} ; \right] .$$

Mixed correlators have more than a four-fold ambiguity and sometimes it is even best to forgo (4.16) altogether and instead simplify the crossing kernel by manipulating the Mellin-Barnes integral directly [51].

The purely two-loop result

$$\begin{aligned} \varepsilon^2 c^{(2)}(\Delta, \ell) &= \frac{\varepsilon^2}{9} \frac{\Gamma(\frac{\Delta + \ell}{2})^4}{2\Gamma(\Delta + \ell)\Gamma(\Delta + \ell - 1)} \mathcal{I}(\ell - \Delta + 2, 1, \frac{1}{2}) \mathcal{I}(\Delta + \ell, 1, \frac{1}{2}) \\ &= \frac{\varepsilon^2}{9} \frac{\Gamma(\frac{\Delta + \ell}{2})^4}{2\Gamma(\Delta + \ell)\Gamma(\Delta + \ell - 1)} \frac{\Gamma(\Delta + \ell)\Gamma(\ell - \Delta + 2)}{\Gamma(\frac{\Delta + \ell}{2} + 1)^2\Gamma(\frac{\ell - \Delta + 2}{2} + 1)^2} \frac{(\Delta + \ell)^2(\ell - \Delta + 2)^2}{(\Delta + \ell - 1)^2(\ell - \Delta + 1)^2} , \end{aligned} \quad (4.18)$$

has a double pole as $\Delta \rightarrow \ell + 1$. Expanding around it and comparing to (4.6) gives

$$a_{0,\ell}^{(2)} = -\frac{2}{9} \frac{\Gamma(\ell + \frac{1}{2})^2}{\pi \ell^2 \Gamma(2\ell)} [\psi(2\ell) - \psi(\ell) - 4 \log 2 - \ell^{-1}] , \quad \gamma_{0,\ell}^{(2)} = -\frac{1}{9\ell} . \quad (4.19)$$

The anomalous dimension (which required us to divide by (4.8)) agrees with the diagrammatic result. Interestingly, (4.18) only has single poles at $\ell + 2n + 1$ for $n > 0$. We therefore see that the subleading double twists $[\hat{\phi}\hat{\phi}]_{n,\ell}$, despite being independent operators not subject to any equation of motion, have vanishing anomalous dimensions to two loops. On the other hand, their OPE coefficients receive the correction

$$a_{n,\ell}^{(2)} = -\frac{1}{18} \frac{n^{-2}(n + \ell)^{-2}\Gamma(n + \ell + \frac{1}{2})^2}{\Gamma(2n)\Gamma(2n + 2\ell)\Gamma(\frac{1}{2} - n)^2} , \quad (4.20)$$

which can be seen from the coefficient of the single pole.

4.3 Results at three loops

Since the anomalous dimension of $\hat{\phi}^2$ is known at $O(\varepsilon^3)$ and we always have the option of applying more derivatives to the crossing kernel, it might seem that a four-loop spectral density is within reach. The main conceptual hurdle here is that the double discontinuity will involve an infinite sum of double-twist conformal blocks in the crossed channel which are weighted by

$a_{0,\ell}^{(0)}\gamma_{0,\ell}^{(2)2}$. For the local Wilson-Fisher CFTs studied in [21], a formula for this weighted sum over ℓ was conjectured by appealing to a transcendentality principle. More recently, an algorithm was developed in [52] which can extract CFT data from this sum without any extra assumptions.

4.4 Further comments

The analytic bootstrap is most powerful when applied to theories that have a weakly broken degeneracy in their spectrum of twists [53]. Generalized free theories provide the simplest examples. In this section, we have applied the Lorentzian inversion formula to the 4pt function of $\hat{\phi}$ which is the fundamental field of the LRI near the mean-field end. What about going to the short-range end and considering the 4pt function of $\hat{\chi}$?

The main difference in this case is that no double-twist operator has an anomalous dimension at $O(\delta)$. It is easy to compute a few renormalized integrals like

$$\int d^p\tau_2 d^p\tau_3 \langle \hat{\chi}^2(0) \sigma \hat{\chi}(\tau_2) \sigma \hat{\chi}(\tau_3) \hat{\chi}^2(\infty) \rangle, \quad (4.21)$$

and see why — the integrand completely vanishes after power-law divergences are subtracted. This is a straightforward repetition of the argument in [14] for why $\hat{\chi}$ itself does not renormalize. This can be physically understood from the fact that, at $O(\delta)$, the Ising model coupled to a generalized free field by $\sigma \hat{\chi}$ is indistinguishable from *two* generalized free fields coupled by $\sigma \hat{\chi}$. The statements made in [54], about certain operators having no anomalous dimension in this theory, can be extended to all operators because quadratic actions cannot produce loop diagrams which are logarithmically divergent. The $O(\delta)$ correction to the 4pt function as a whole (which indeed has no logarithmic terms) can be computed as

$$\begin{aligned} \langle \hat{\chi}(\tau_1) \hat{\chi}(\tau_2) \hat{\chi}(\tau_3) \hat{\chi}(\tau_4) \rangle &= [(|\tau_{12}||\tau_{34}|)^{-2\Delta_\chi} + (|\tau_{13}||\tau_{24}|)^{-2\Delta_\chi} + (|\tau_{14}||\tau_{23}|)^{-2\Delta_\chi}] \\ &\times \left[1 + 2g_*^2 \pi^p \frac{\Gamma(\frac{p}{2} - \Delta_\sigma)}{\Gamma(\Delta_\sigma)} \frac{\Gamma(\frac{p}{2} - \Delta_\chi)}{\Gamma(\Delta_\chi)} + O(g_*^4) \right], \end{aligned} \quad (4.22)$$

using only the chain integral. This shows that all OPE coefficients for $[\hat{\chi}\hat{\chi}]_{n,\ell}$ undergo the same shadow symmetric rescaling.

5 Numerical results

Up until this point, we have been focused on perturbative results. Although these are only strictly valid close to $\mathfrak{s} = \frac{p}{2}$ or $\mathfrak{s} = p - 2\Delta_\sigma^*$, they improve our expectations for where non-trivial long-range Ising models should be found in the space of scaling dimensions. When this space is cut down to a manageable size, it can be searched with the numerical bootstrap [3]. In the most

favourable cases, one can force the theory of interest to live in an “island” by rigorously excluding the possibility that a consistent CFT lives at any of the surrounding points [55–60, 42, 61, 62]. More commonly, a precursor to this type of result called a “kink” is what provides evidence that a theory has been found. The goal of this section is to produce kinks for general \mathfrak{s} which agree with perturbation theory near the two endpoints and therefore give non-perturbative predictions for LRI critical exponents in between.

It is worth explaining how our approach differs from that of [15] which ignored all of the OPE relations except:

$$\lambda_{11\mathcal{O}}\lambda_{22\mathcal{O}} = \frac{\Gamma(\frac{\ell+\Delta}{2})^2\Gamma(\frac{\ell+p+q-2-\Delta}{2})\Gamma(\frac{\ell+p-q+2-\Delta}{2})}{\Gamma(\frac{\ell+p-\Delta}{2})^2\Gamma(\frac{\ell+2-q+\Delta}{2})\Gamma(\frac{\ell-2+q+\Delta}{2})}\lambda_{12\mathcal{O}}^2, \quad (\Delta \equiv \Delta_{\mathcal{O}}), \quad (5.1)$$

which is the same relation whether we take $1 \equiv \psi_0^{(+)}$ and $2 \equiv \psi_0^{(-)}$ or vice versa. This was done to remove dependence on $R(a_{\phi^2}) = R(a_{\chi^2})^{-1}$ but the studies [18, 19] later showed that it is better to keep this ratio in the problem and vary it manually, within the unitarity region depicted in figure 1. Besides allowing us to impose more OPE relations, scanning over a parameter other than a scaling dimension is necessary for making progress on the two-dimensional LRI. Indeed, it is known that single-correlator exclusion plots for the dimensions of relevant operators (which have no LRI kink) are not improved by extra correlators unless one imposes model-dependent gaps [63]. Fortunately, we will see that this new type of scan is also sufficient for finding the LRI in $p = 2$. As such, we will spend most of our time on this case and be more terse for $p = 3$. For a different bootstrap study which benefited from scanning over more than just scaling dimensions, see [64].

EL: Comments:

1. **PvV: Add pert results as dots in plot?** **CB: Sure.**

5.1 Warm-up

For a given external dimension Δ_ϕ , we can bound the scaling dimensions of exchanged operators. As discussed above, we will bound them as functions of the unknown ratio $R(a_{\phi^2})$. We will use a_{ϕ^2} as a proxy for this ratio and label our bounds by Δ_ϕ . If one prefers a_{χ^2} , which vanishes at $\mathfrak{s} = p - 2\Delta_\phi^*$ instead of $\mathfrak{s} = \frac{p}{2}$, it is easy to convert between them using eq. (2.18). The crossing equations used throughout, given explicitly in appendix A, are the ones appropriate for a three-correlator system involving $\hat{\phi} \equiv \psi_0^{(+)}$ and its shadow $\psi_0^{(-)}$. Imposing the OPE relations (2.21) on odd-spin operators forces them to have scaling dimensions in the discrete set $p + \ell + 2n$ for $n \geq 0$. We will treat $\ell = 1$ as an exception and demand that there is no spin-1 operator of dimension

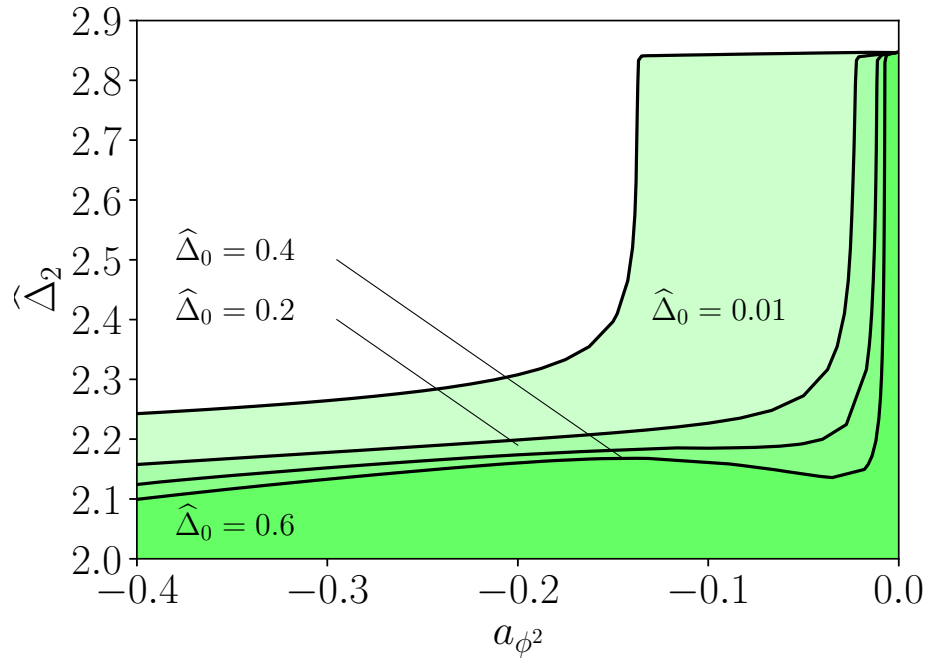


Figure 2: Bounds on the dimension of the leading spin-2 operator for $\Delta_\phi = 0.425$. The lightest region shows a nearly universal bound with only a spin-0 gap of 0.01 imposed for stability. The darker regions impose more restrictive spin-0 gaps and are needed to see evidence of the long-range Ising model for this value of Δ_ϕ .

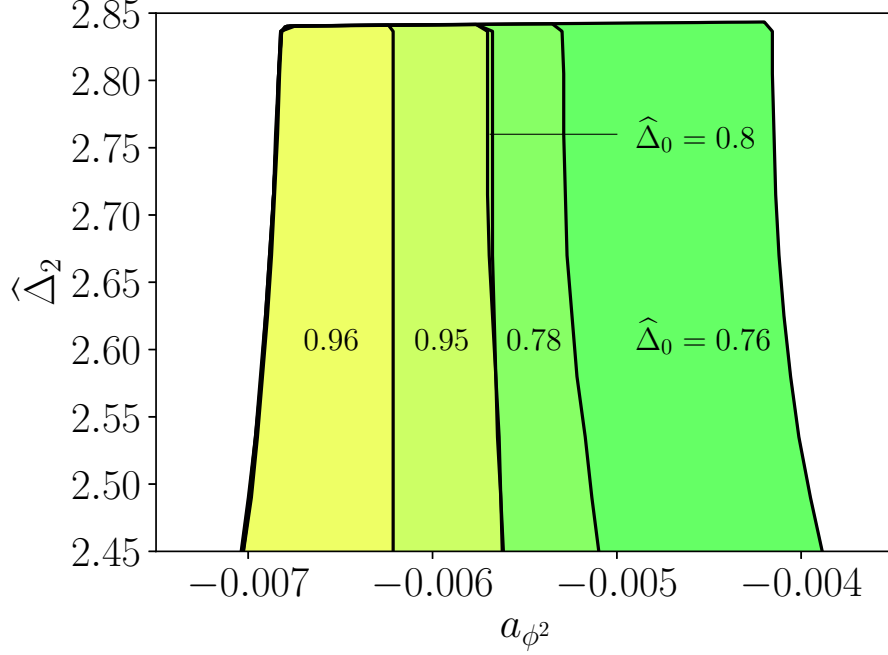


Figure 3: Bounds on the spin-2 gap for larger values of the imposed spin-0 gap which would be hard to see on the scale of figure 2. Yellow regions correspond to more stringent gaps and the smallest one, which fixes a_{ϕ^2} to 0.1%, is a good candidate for where the $\Delta_\phi = 0.425$ long-range Ising model should live.

$p + 1$. A primary with these quantum numbers cannot exist in the LRI near either endpoint. At the mean-field end the only candidate is a descendant of $\hat{\phi}^4$ while at the short-range end the only candidate is a descendant of $T_{\mu\nu}$, see e.g. the discussion in ref. [14].⁹ Finally, we will impose (2.21) for all operators with $\ell = 0, 2$. This is a slight simplification compared to the BCFT setup in [18, 19] which required there to be a discrete set of even-spin operators (like the displacement) which evade the OPE relations.

The type of plot made in [18, 19], which maximizes the gap $\hat{\Delta}_2$ for spin-2 operators, will be a useful starting point. Whenever a non-trivial upper bound on $\hat{\Delta}_2$ exists, a theory saturating it is guaranteed to be nonlocal. The plot is shown in figure 2 for an external dimension of $\Delta_\phi = 0.425$. The most permissive region in this plot has a kink at around $a_{\phi^2} = -0.15$. This is an order of magnitude off from where it should be if we estimate a_{ϕ^2} in the $\Delta_\phi = 0.425$ LRI by plugging $\varepsilon = 0.3$ into the perturbative results of eq. (3.35). As noted in [19] however, plots of this type

⁹In the case of unitary and local BCFTs, [18] proved that a vector of dimension d is absent from the spectrum of boundary primaries. One can find counter-examples when unitarity is given up [65]. Via the same reasoning one can prove that for unitary and local p -dimensional conformal defects a vector of dimension $p + 1$ should be absent from the spectrum of defect primaries.

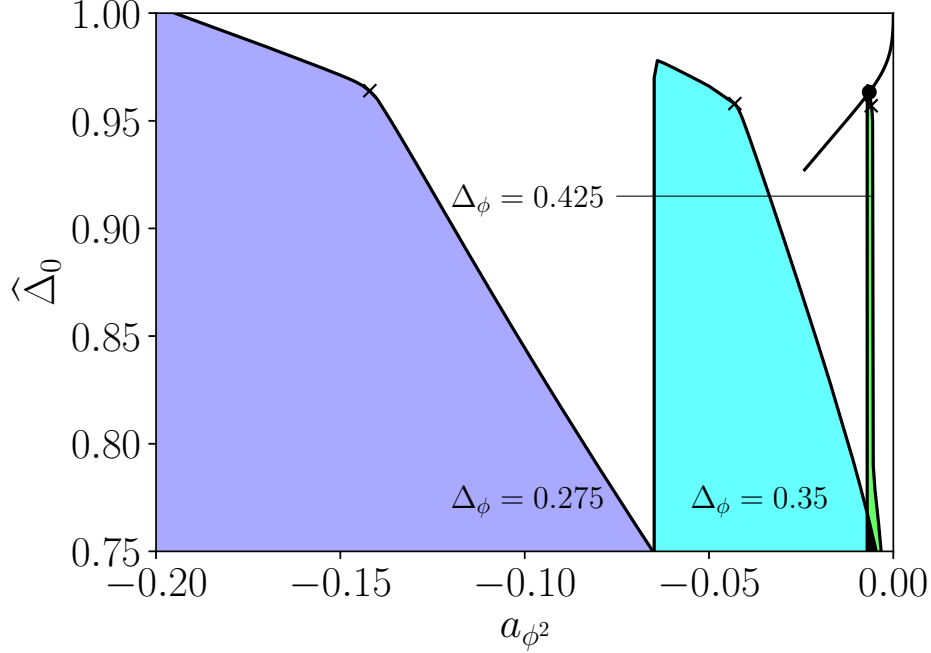


Figure 4: Bounds on the dimension of the leading exchanged scalar for $\Delta_\phi = 0.425$ (narrowest), $\Delta_\phi = 0.35$ and $\Delta_\phi = 0.275$ (widest). For cosmetic reasons, these bounds were made subject to the constraints $\hat{\Delta}_2 \geq 2.4$, $\hat{\Delta}_2 \geq 2.3$ and $\hat{\Delta}_2 \geq 2.2$ respectively. The rightmost kinks, indicated on the plot, are stable with respect to the spin-2 gap and serve as candidates for the LRI.

can show more interesting features once we restrict our search to CFTs obeying a certain gap $\hat{\Delta}_0$ on internal operators of spin-0. As we raise this gap in figure 2, the vertical wall moves rapidly at first but then slows down. By $\hat{\Delta}_0 = 0.6$, which is well below the mean-field value of $\hat{\Delta}_0 = 1$, it has already stabilized at a position close to the right hand side. As we continue to raise $\hat{\Delta}_0$, something even more interesting happens. A second vertical wall starts moving to the *left*. The zoomed in plot figure 3 shows the spike which is obtained in this way. The leftward motion stops as well at around $\hat{\Delta}_0 = 0.8$ making the spike temporarily stable. At about $\hat{\Delta}_0 = 0.95$, the leftward motion starts again resulting in complete disappearance once we get to $\hat{\Delta}_0 = 0.97$. This is strikingly close to the scalar gap for the LRI with $\Delta_\phi = 0.425$ as predicted by perturbation theory.

5.2 Kinks in two dimensions

As the spin-0 gap is varied, the bounds above sometimes change quickly and sometimes change slowly. Plots bounding $\hat{\Delta}_0$ should therefore be just as interesting as those bounding $\hat{\Delta}_2$. Our main conjecture regarding numerics is that this exercise allows one to find a kink corresponding

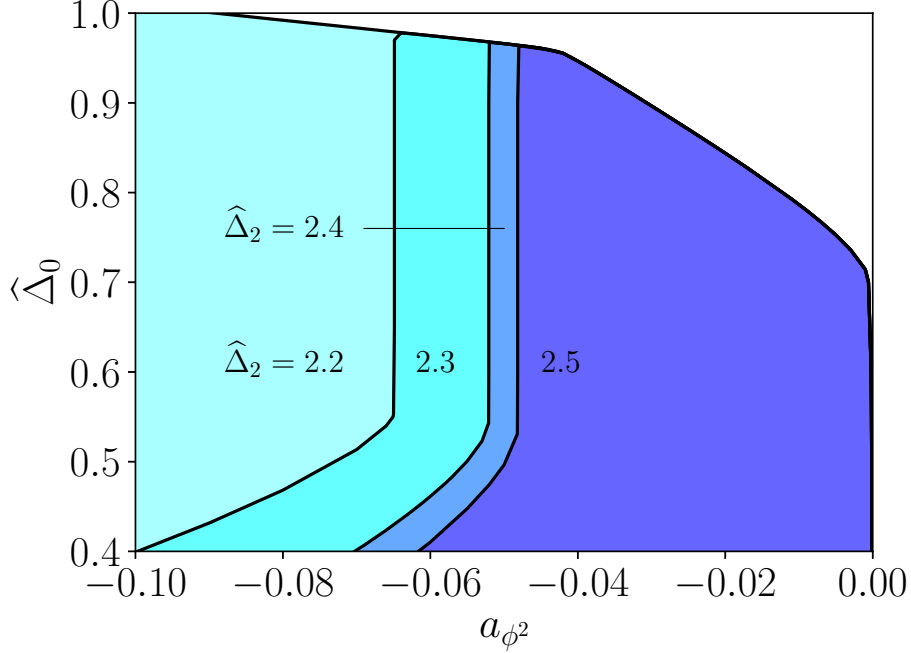


Figure 5: Allowed regions in $(a_{\phi^2}, \hat{\Delta}_0)$ space for $\Delta_\phi = 0.35$. These include the region from figure 4 with $\hat{\Delta}_2 \geq 2.3$ but also three other versions of it with different spin-2 gaps. The prevailing trend is that the left edge moves while the right edge (which contains the LRI kink) does not. This happens for all external dimensions so we have chosen $\Delta_\phi = 0.35$ as a “generic” example not close to $\frac{p}{4}$.

to the long-range Ising model for arbitrary Δ_ϕ without any assumption on the spin-2 gap. Figure 4 shows almost this result except with a modest spin-2 gap for readability. Specifically, we have imposed

$$\hat{\Delta}_2 \geq \frac{4}{3}\Delta_\phi - \frac{1}{6}, \quad (5.2)$$

to prevent the allowed regions from overlapping heavily. This arbitrary gap is easily obeyed by the long-range Ising model and the features we will now discuss would still be visible without it. Two of the allowed regions in Figure 4 show one kink on the left and another on the right. The third region would as well if the horizontal axis were extended. It turns out that the solution to crossing at the leftmost kink has a spin-2 operator saturating (5.2) whereas the leading spin-2 operator dimension at the rightmost kink is much higher. This can be seen in figure 5 which compares four different allowed regions for $\Delta_\phi = 0.35$ with each one having a different constraint on $\hat{\Delta}_2$. Evidently, there is some critical spin-2 gap which makes the allowed region have only one kink. For $\Delta_\phi = 0.425$, this is about $\hat{\Delta}_2 = 2.84$ in agreement with figure 3. As the spin-2 constraint is relaxed, making the region wider, the single kink splits into two with one staying still and the other moving to the left. Based on this pattern, the stationary kink on the right should

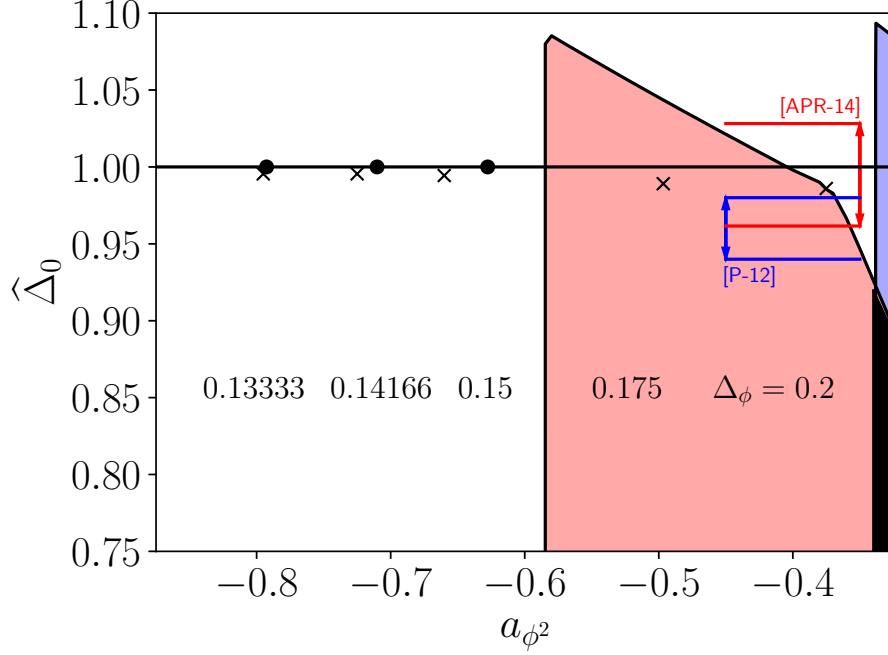


Figure 6: Kinks attributed to the long-range Ising model for five more values of Δ_ϕ . For $\Delta_\phi = 0.2$, the full allowed region subject to $\hat{\Delta}_2 \geq 2.1$ is shown as well. The error bars close to this kink denote the findings for the ν exponent from the Monte Carlo studies [66, 67]. Closer to the left, dots are given so that the kinks at $\Delta_\phi = 0.15$, $\Delta_\phi = 0.14166$ and $\Delta_\phi = 0.13333$ may be compared to the results of $O(\delta)$ perturbation theory.

be the one associated with the long-range Ising model. Figure 4 shows that it is about 0.2% below the perturbative prediction around the mean-field end despite having much less noticeable error in the horizontal position. Reasons for this will be discussed in the next subsection which deals with resummations. The moving kink bears some resemblance to the one in [19] which was associated with minimal models. To check whether the same might be true here, we can follow the kink to the leftmost most edge of $a_{\phi^2} = -\frac{7}{8}$ where the theory becomes local. Interestingly, this gives it an approximate spin-0 gap of

$$\hat{\Delta}_0 = \frac{8}{3}\Delta_\phi + \frac{2}{3}. \quad (5.3)$$

This is precisely the relation between $\Delta_{(1,2)}$ and $\Delta_{(1,3)}$ for the m 'th Virasoro minimal model if we eliminate m to express one scaling dimension in terms of the other. As remarked in [14], there is no reason why these other models cannot be coupled to a generalized free field in the same vein as the Ising model to generate many nonlocal CFTs. The match with (5.3) can then be taken as evidence that these “long-range minimal models” are being singled out by the numerical bootstrap. To put it another way, the kink for Δ_ϕ which saturates the imposed spin-2 gap might

be constructed by taking the m 'th minimal model for some m and coupling its $\phi_{(1,2)}$ operator to a generalized free field of dimension $2 - \Delta_\phi$. The precise value of m will be difficult to determine in general but we believe that many checks of this proposal can be done in perturbation theory. As usual, it will be important to consider non-integer values of m and construct these RG flows using generalized minimal models. Generalized minimal models are non-unitary but it is known that their low-lying correlators manifest this in a very limited way [68].

As shown in eq. (2.17), bulk-defect crossing symmetry and unitarity implies that $-\frac{7}{8} \leq a_{\phi^2} \leq 0$. Our conclusions so far have been based on values of a_{ϕ^2} in the upper half of this range. We have also computed a bound on $\hat{\Delta}_0$ for $\Delta_\phi = 0.2$ and still found a kink in the upper half of this range. The basic structure of perturbation theory makes it clear that four evenly spaced values of Δ_ϕ in the range $\frac{1}{8} \leq \Delta_\phi \leq \frac{1}{2}$ will be far from evenly spaced with respect to a_{ϕ^2} . After all, the expansion of the latter starts at $O(1)$ around the short-range end but $O(\varepsilon^2)$ around the mean-field end. We have therefore picked another four values of Δ_ϕ between $\frac{1}{8}$ and 0.2 for testing how well the putative LRI kinks agree with the δ expansion. The kinks themselves are shown in figure 6. Their positions were computed from the second derivative of a bound on $\hat{\Delta}_0$ but the rest of the bound has been omitted to avoid clutter. The perturbative line (which always has $\hat{\Delta} = 1$ since $\Delta_\varepsilon = 1 + O(\delta^2)$) shows the desired convergence between the numerical and analytic values of a_{ϕ^2} on the left hand side. The right hand side of figure 6 shows partially overlapping error bars obtained by Monte Carlo simulations which both considered $\mathfrak{s} = 1.6$ or $\Delta_\phi = 0.2$. After using the standard relation

$$\Delta_{\hat{\phi}^2} = p - \nu^{-1} , \quad (5.4)$$

it becomes clear that our kink is compatible with $\nu^{-1} = 0.996(33)$ found by [67] but not $\nu = 0.96(2)$ found by [66].

5.3 Checks of the critical exponents

The most important next step is to verify that the numerical bootstrap, beyond simply “knowing” about the long-range Ising model, can actually be used to derive its critical exponents to high precision. To do this, we should address the fact that the data in figures 4 and 6 only agree with the ε and δ expansions respectively within a narrow window. It is also clear that the kinks demonstrating the best agreement still lie noticeably below the perturbative line. These discrepancies can be diminished with simple improvements to both the numerics and perturbation theory.

On the numerical side, we should refine the discrete grid of points discussed in appendix A. In all previous plots, the OPE relations have been imposed for 3000 closely spaced values of Δ . Increasing this number appears to make all of the kinks move monotonically upwards. This is

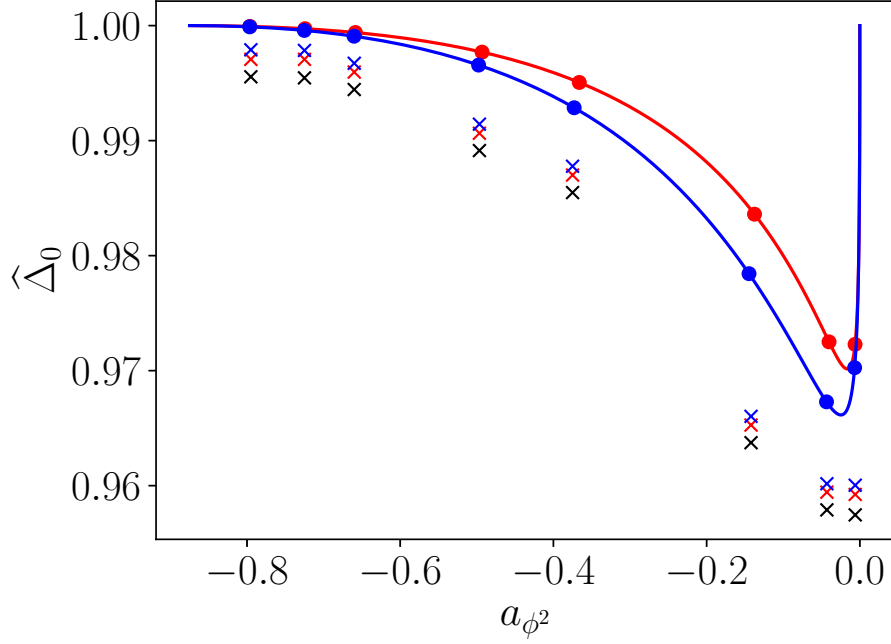


Figure 7: Comparison between perturbative and non-perturbative estimates of the leading internal scalar dimension in the long-range Ising model. The blue line is a Padé approximant based on all known perturbative data while the red one omits $O(\epsilon^3)$. The dots on them correspond to the eight external dimensions considered throughout this section ranging from $\Delta_\phi = 0.13333$ on the left to $\Delta_\phi = 0.425$ on the right. The x's denote kinks from the numerical runs which are sensitive to the number of grid points. We show results for 3000, 6000 and 12000 points in black, red and blue respectively.

expected in the numerical bootstrap since constraints at the new points make it harder to find functionals for ruling out CFTs. We have gone to 12000 which appears to be large enough that further errors are dominated by the resolution in a_{ϕ^2} . On the perturbative side, we will use the approximants $\text{Pade}_{[m,n]}$ which are rational functions with $m+n+1$ coefficients designed to resum an asymptotic series. While this can be done for either the ε or δ expansions individually, it is much better to use a two-sided approximant. Picking the same one for both axes, we will write

$$\hat{\Delta}_0(\mathfrak{s}) = \frac{\sum_{j=0}^m a_j \mathfrak{s}^j}{1 + \sum_{j=1}^n b_j \mathfrak{s}^j}, \quad a_{\phi^2}(\mathfrak{s}) = \frac{\sum_{j=0}^m a'_j \mathfrak{s}^j}{1 + \sum_{j=1}^n b'_j \mathfrak{s}^j}, \quad (5.5)$$

and fix the coefficients by demanding that $\mathfrak{s} = 1 + \frac{\varepsilon}{2}$ and $\mathfrak{s} = 2(1 - \Delta_\sigma^* - \delta)$ reproduce the expected behaviour around the mean-field and short-range ends respectively. Solutions for the coefficients (if they exist) are admissible if they lead to real valued functions that have no poles between $\varepsilon = 0$ and $\delta = 0$. If we perturb up to $O(\delta)$ and $O(\varepsilon^{m-1})$, the $\text{Pade}_{[m,1]}$ approximant has admissible solutions for $m = 3$ and $m = 4$. As shown in figure 7, the latter gets us significantly closer to where the kinks are.

While Padé approximants indicate that the kinks are trustworthy, it is also important to see how well the bootstrap agrees with other non-perturbative methods. The Monte Carlo estimates of ν from [66, 67], mentioned briefly in the last subsection, are ideal for this purpose. Figure 6 shows that our kink for $\Delta_\phi = 0.2$ lies slightly outside the error bars predicted for this LRI in [66]. This becomes even more true after increasing the number of sample points to 12000. Conversely, [67] found a larger value of ν and explained the discrepancy by noting that the LRI has significant finite size effects which can be mitigated by simulating a different Hamiltonian in the same universality class. An intriguing possibility is using the numerical bootstrap to derive, not just upper bounds on $\hat{\Delta}_0$, but lower bounds as well since these could conceivably exclude the earlier Monte Carlo result. We have not been able to find lower bounds that are strong enough but it is instructive to see how close they come.

The key is that the LRI (and the SRI as well) has one relevant operator that is \mathbb{Z}_2 -even. This is of course $\hat{\phi}^2$ in one description and ϵ in the other. A bound on the spin-0 gap $\hat{\Delta}_0$ says nothing about how many scalars there are with $\hat{\Delta}_0 < \Delta < 2$. A better strategy is to demand that all scalars exchanged in our crossing equations have $\Delta > 2$ except for one with dimension $\hat{\Delta}_0$. Tuning this value and testing for feasibility of the crossing equations every time is what produces upper and lower bounds. The lower bound we find with no extra assumption is well below the bottom of the blue error bar in figure 6 but more interesting things happen when we raise the spin-2 gap $\hat{\Delta}_2$. When doing simple gap maximization, it has already been seen in figure 5 that the upper bound in the vicinity of the kink is insensitive to $\hat{\Delta}_2$. When we take $\hat{\Delta}_0$ to be isolated, this continues to hold for the upper bound but not the lower bound. The lower bound

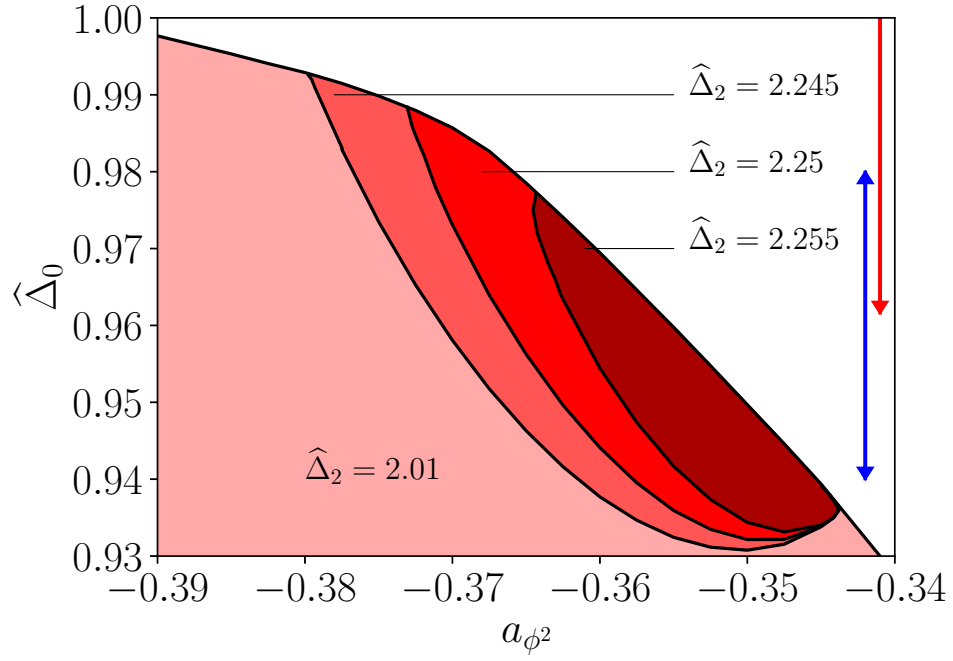


Figure 8: The vicinity of the $\Delta_\phi = 0.2$ kink in $(a_{\phi^2}, \hat{\Delta}_0)$ space when we scan over the dimension of a single exchanged relevant scalar instead of maximizing the scalar gap. The lightest region is essentially the one seen in figure 6 while the darker islands start to form after a significant spin-2 gap $\hat{\Delta}_2$ is imposed. The blue and red error bars follow from the Monte Carlo results of [66] and [67] respectively.

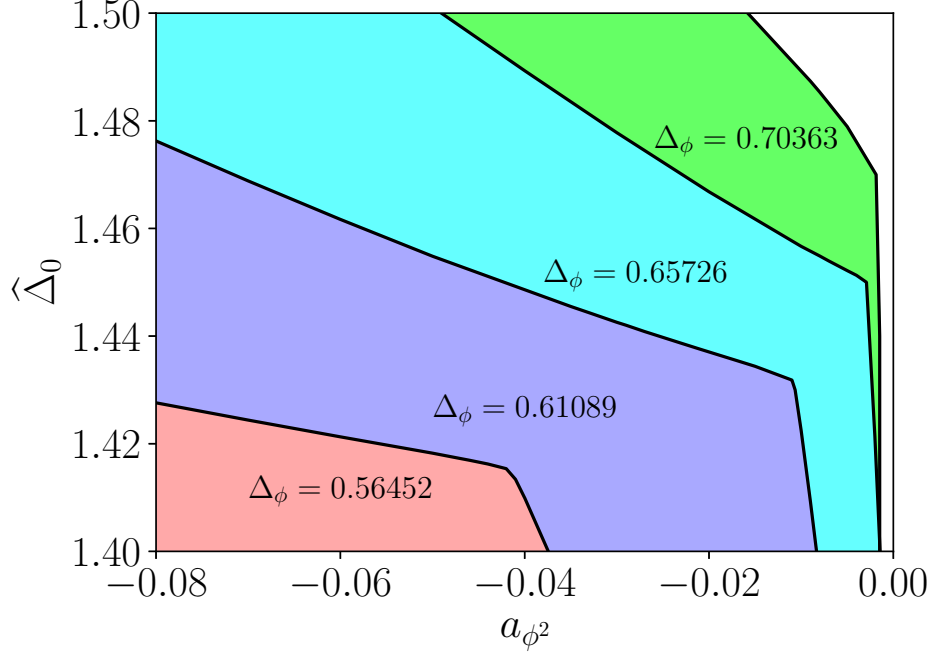


Figure 9: Allowed regions in $(a_{\phi^2}, \hat{\Delta}_0)$ space for three dimensions and four equally spaced external dimensions between $\Delta_\phi = \frac{3}{4}$ and $\Delta_\phi = \Delta_\sigma^*$. Again, we conjecture that each kink is a long-range Ising model.

becomes increasingly restrictive and turns the allowed region into an island. Figure 8 shows three of these islands starting with $\hat{\Delta}_2 = 2.245$ which is almost large enough to rule out the kink. By the time we reach $\hat{\Delta}_2 = 2.255$, the kink has become disallowed but the island is still large enough to be compatible with the error bars of both [66] and [67]. Unfortunately, the lower bounds do not improve significantly when we add the \mathbb{Z}_2 -even scalar as a third external operator using the larger system of crossing equations in (A.3).

5.4 Kinks in three dimensions

It remains to be seen that finding the long-range Ising model numerically works equally well in three dimensions. This time, it is harder to get a point of comparison perturbatively. In figure 7, the red and blue curves had similar values of a_{ϕ^2} because the ε and δ expansions approximated each other fairly well. For example, $\delta = 0$ corresponds to $\varepsilon = \frac{3}{2}$ in two dimensions and this underestimates a_{ϕ^2} by about a factor of 2. In three dimensions, this is instead a factor of 7 leading to predictions which fluctuate wildly upon using different Padé approximants. Improving this with higher-loop perturbation theory around the short-range end will lead to integrals with more than four insertions of σ in the 3d Ising model. Approximating one of these correlators will

require higher-point CFT data and techniques for extracting them are currently in their infancy [69].

Although the checks we can do are limited, it is plausible that the kinks plotted in figure 9 describe the long-range Ising model once again. For one thing, their vertical co-ordinates interpolate between $\hat{\Delta}_0 = \frac{3}{2}$ and $\hat{\Delta}_0 = \Delta_\epsilon^*$ as expected. Their horizontal co-ordinates all appear to be an order of magnitude smaller than the short-range value $a_{\phi^2} = -0.575408$ but we know that the $O(\delta)$ deformation changes this rapidly. Numerical runs for Δ_ϕ very close to Δ_σ^* indeed show that the motion of the kink becomes almost completely horizontal so that the right limiting behavior is recovered.

A final point is that the regions in figure 9 do not change after imposing a spin-2 gap. The moving kinks in figures 4 and 6, which depend on this gap, are therefore unique to two dimensions. This supports the interpretation that they arise as a deformation of Virasoro minimal models which almost all have an upper critical dimension below $p = 3$.

6 Conclusions and outlook

In this work we have investigated the long-range Ising model, a particular and well-known example of a nonlocal CFT, which plays an important role in condensed matter physics. We have used different techniques, both perturbative and non-perturbative, to determine various CFT data. A central role is played by the use of exact relations between OPE coefficients, which can be implemented in the numerical bootstrap as well as employed in perturbative computations to gain an extra loop order in the results. These OPE relations emerge from the setup chosen in this paper, where we consider the p -dimensional LRI as a defect in a free bulk CFT. The relations were derived for both the mean-field and SRI ends of the LRI perturbative regime, although we mostly focused on new results on the mean-field end.

Besides combining the OPE relations with standard Feynman diagram techniques to obtain anomalous dimensions and OPE coefficients, as computed in section 3, one can also use techniques such as the Lorentzian inversion formula to obtain CFT data perturbatively. This was done in section 4 and resulted in an infinite amount of CFT data at three loops from the mean-field end. In section 5 the LRI was studied nonperturbatively using the numerical bootstrap. The numerics showed a number of kinks corresponding to both perturbative and non-perturbative (Monte Carlo) predictions for the LRI in two and three dimensions. This shows that the LRI, and possibly other long-range models, are within reach of the numerical bootstrap in both two and three dimensions.

Interestingly, as shown in figure 6, the Monte-Carlo results of [67] are consistent with the position of our kink, while [66] are not. In our preliminary attempt to isolate LRI by making

significant spin-2 gap assumptions we have obtained figure 8, which shows an island that starts to form to the *right* of the kink. This island is still compatible with the error bars of both [66] and [67], so in order to make progress we should either make less conservative gap assumptions or include more correlators. These numerical bootstrap studies will involve many parameters and are generally expected to be very time-consuming, so a good strategy would be to implement them within the newest frameworks of [70, 71] or [72]. Secondly, we have not tried to extract the extremal spectrum for LRI, although that can be done with the EFM [73]. The obtained spectrum can then be used as input for the inversion formula away from the perturbative regime, as was explored before in [29, 41]. Besides Monte Carlo and the numerical bootstrap, nonperturbative predictions can also be obtained through fuzzy sphere methods CITE. It would be interesting to compare this method to the results of this work.

Currently the results in two dimensions in section 5 also show hints of a different family of long-range models: the long-range minimal models. It would be interesting to investigate these models further, through perturbative computations and comparing those to the numerical spectrum which can be extracted using EFM [73]. Another possible extension would be to consider long-range $O(N)$ models. In this work we have already presented some perturbative results for these models, which could then readily be compared to the numerics.

For the study of the LRI we have focused on integer-dimensional defects in a free bulk, with possible fractional codimension. Instead we can also consider defects with fixed codimension, such as monodromy defects. A future direction would be to explore those defects using the same techniques and strategies that have been employed here for the LRI, see e.g. [16, 74].

Lastly, in [75] level repulsion was shown numerically for CFTs of the Wilson-Fisher fixed point. A similar feature can be expected to appear when studying the LRI. Varying the parameter \mathfrak{s} between $p/2$ and $p - 2\Delta_{\sigma\text{SRI}}$, exploring the region between the two perturbative ends, and extracting the spectrum using EFM, one could find hints of level repulsion, shedding more light on how the $\sigma\chi$ -type operators of the SRI end map onto the ϕ^4 operators at the mean-field end beyond the known lowest-lying cases.

Acknowledgements

We would like to thank B. van Rees, D. Mazáč, J. Henriksson, P. Liendo, M. Meineri, M. Paulos, G. Gori and A. Tilloy for discussions. Numerical calculations in this paper were done on the University of Oxford Advanced Research Computing (ARC) facility [76]. EL is funded by the European Union (ERC, QFT.zip project, Grant Agreement no. 101040260, held by A. Tilloy). PvV is funded by the European Union (ERC, FUNBOOTS prject, project number 101043588) and acknowledges support from the DFG through the Emmy Noether research group ‘The Con-

formal Bootstrap Program' project number 400570283, and through the German-Israeli Project Cooperation (DIP) grant 'Holography and the Swampland'. Views and opinions expressed are however those of the author(s) only and do not necessarily reflect those of the European Union or the European Research Council Executive Agency. Neither the European Union nor the granting authority can be held responsible for them.

A Details on the numerics

A.1 Crossing equations

We want to bootstrap the system of four-point functions involving two scalars operators. In p spatial dimensions, the external scaling dimensions should sum to p so we can write them as $\frac{p \pm \mathfrak{s}}{2}$ with $\mathfrak{s} > 0$. In the crossing equations written below, operators 1 and 2 are on equal footing so it does not yet matter which has dimension $\frac{p-\mathfrak{s}}{2}$ and which has dimension $\frac{p+\mathfrak{s}}{2}$. The 5 inequivalent crossing equations are

$$\begin{aligned}
0 &= \sum_{\mathcal{O}} \lambda_{11\mathcal{O}}^2 F_{-,\Delta,l}^{11,11}(u,v) , \\
0 &= \sum_{\mathcal{O}} \lambda_{22\mathcal{O}}^2 F_{-,\Delta,l}^{22,22}(u,v) , \\
0 &= \sum_{\mathcal{O}} \lambda_{12\mathcal{O}}^2 F_{-,\Delta,l}^{12,12}(u,v) , \\
0 &= \sum_{\mathcal{O}} (-1)^\ell \lambda_{12\mathcal{O}}^2 F_{\mp,\Delta,l}^{12,21}(u,v) \pm \lambda_{11\mathcal{O}} \lambda_{22\mathcal{O}} F_{\mp,\Delta,l}^{11,22}(u,v) .
\end{aligned} \tag{A.1}$$

The operators must also obey the OPE relations (2.21) and this makes it important to specify them more precisely. Operator 1 will be the one with dimension $\frac{p-\mathfrak{s}}{2}$ called $\hat{\phi}$ or σ in the LRI. Operator 2 will be the one with dimension $\frac{p+\mathfrak{s}}{2}$ called $\hat{\phi}^3$ or $\hat{\chi}$ in the LRI. There is now one choice to make.

1. If we wish to express results as functions of a_{ϕ^2} , we must take $q = 2 - \mathfrak{s}$ and use OPE relations with $\psi_0^{(+)}$ as operator 1 and $\psi_0^{(-)}$ as operator 2.
2. If we wish to express results as functions of a_{χ^2} , we must take $q = 2 + \mathfrak{s}$ and use OPE relations with $\psi_0^{(-)}$ as operator 1 and $\psi_0^{(+)}$ as operator 2.

This work makes the former choice.

When the OPE relations are imposed for all spins, the crossing equations can be rewritten as follows

$$0 = \vec{V}_{\mathbb{I}} + \sum_{\ell=\text{even}} \lambda_{12\mathcal{O}}^2 \vec{V}_{+,\Delta,\ell} + \sum_{\ell=\text{odd}} \sum_{n=0}^{\infty} \lambda_{12\mathcal{O}}^2 \vec{V}_{-,p+2n+\ell,\ell} . \tag{A.2}$$

One can also add a third external scalar to the setup and find

$$\begin{aligned}
0 = & \vec{V}_{\mathbb{1}} + \sum_{\ell=\text{even}} \begin{pmatrix} \lambda_{12\mathcal{O}} & \lambda_{13\mathcal{O}} \end{pmatrix} \vec{V}_{+,\Delta,\ell} \begin{pmatrix} \lambda_{12\mathcal{O}} \\ \lambda_{13\mathcal{O}} \end{pmatrix} \\
& + \sum_{\ell=\text{odd}} \lambda_{13\mathcal{O}}^2 \vec{V}_{0,\Delta,\ell} + \sum_{\ell=\text{odd}} \sum_{n=0}^{\infty} \lambda_{12\mathcal{O}}^2 \vec{V}_{-,p+2n+\ell,\ell} .
\end{aligned} \tag{A.3}$$

In practice, we keep all spins in the range $0 \leq \ell \leq \ell_{\text{max}} = 30$ but only impose the relations for $\ell = 0, \ell = 2$ and the odd spins. To transform (A.1) into a finite problem, we have replaced each functional equation with 45 component equations obtained by evaluating its derivatives at the crossing symmetric point $u = v = \frac{1}{4}$. In the conventions of [73], these derivatives are the ones selected by $n_{\text{max}} = 8$.

A.2 Differences compared to integer codimension

We use the semidefinite program solver **SDPB** [56, 77] which is designed for crossing equations that depend on Δ through rational functions. The algorithm in [55] can produce rational approximations of conformal blocks to any desired order but the OPE relations pose more of a challenge. The prefactors in (2.21) contain ratios of the form

$$\Gamma(\Delta + \delta_1)/\Gamma(\Delta + \delta_2) . \tag{A.4}$$

When $\delta_1 - \delta_2$ is an integer, (A.4) is manifestly rational. When $\delta_1 - \delta_2$ is a half-integer, (A.4) is not a rational function but its *square* is to a high degree of precision [18]. These are the only two cases which arise for integer codimension q . By contrast, this work considers continuously varying q with each one corresponding to a different long-range Ising model between the non-trivial endpoints.

Without a rational function at our disposal, we have opted to approximate crossing equations by a large number of constant functions. As such, we do not demand that the OPE relations hold for all $\hat{\Delta}_0 < \Delta < \infty$ and $\hat{\Delta}_2 < \Delta < \infty$ when imposing the spin-0 gap $\hat{\Delta}_0$ and the spin-2 gap $\hat{\Delta}_2$. Instead, we demand that they hold for many closely spaced scaling dimensions in $(\hat{\Delta}_0, d + 18)$ for spin-0 operators and $(\hat{\Delta}_2, d + 20)$ for spin-2 operators. Most results in section 5 were obtained with 3000 points but for the high precision results of subsection (5.3) we have sampled 12000. As the gaps are varied, the number of points stays constant rather than the grid spacing. This allows us to take advantage of the checkpoint feature of **SDPB**. We also recommend passing `--writeSolution=y` since files from old runs can take a non-trivial amount of time to delete without this.

B Perturbative computations

B.1 Master integrals

The massless integrals we will use can all be derived from Symanzik's formula for an integral with exponents α_i summing to p [78]. This reads

$$\pi^{-p/2} \int d^p \tau_0 \prod_{i=1}^n \frac{\Gamma(\alpha_i)}{|\tau_{i0}|^{2\alpha_i}} = \prod_{i < j} \int_{-i\infty}^{i\infty} \frac{d\delta_{ij}}{2\pi i} \Gamma(\delta_{ij}) |\tau_{ij}|^{-2\delta_{ij}}, \quad (\text{B.1})$$

where the variables on the right hand side obey the constraint $\sum_{i \neq j} \delta_{ij} = \alpha_i$. For $n = 3$ and $n = 4$, eq. (B.1) gives

$$\begin{aligned} \int \frac{d^p \tau_0}{|\tau_{01}|^{2\alpha_1} |\tau_{02}|^{2\alpha_2} |\tau_{03}|^{2\alpha_3}} &= \prod_{i=1}^3 \frac{\Gamma(\frac{p}{2} - \alpha_i)}{\Gamma(\alpha_i)} \frac{\pi^{p/2}}{|\tau_{12}|^{p-2\alpha_3} |\tau_{13}|^{p-2\alpha_2} |\tau_{23}|^{p-2\alpha_1}}, \quad (\text{B.2}) \\ \int \frac{d^p \tau_0}{|\tau_{01}|^{2\alpha_1} |\tau_{02}|^{2\alpha_2} |\tau_{03}|^{2\alpha_3} |\tau_{04}|^{2\alpha_4}} &= \left| \frac{\tau_{24}}{\tau_{14}} \right|^{\alpha_{12}} \left| \frac{\tau_{14}}{\tau_{13}} \right|^{\alpha_{34}} \frac{\pi^{p/2}}{|\tau_{12}|^{\alpha_1+\alpha_2} |\tau_{34}|^{\alpha_3+\alpha_4}} \int_{-i\infty}^{i\infty} \frac{ds dt}{(2\pi i)^2} U^s V^{t-\frac{1}{2}(\alpha_2+\alpha_3)} \\ &\quad \times \Gamma\left(\frac{\alpha_1+\alpha_2-2s}{2}\right) \Gamma\left(\frac{\alpha_3+\alpha_4-2s}{2}\right) \Gamma\left(\frac{\alpha_2+\alpha_3-2t}{2}\right) \Gamma\left(\frac{\alpha_1+\alpha_4-2t}{2}\right) \Gamma\left(\frac{\alpha_1+\alpha_3-2u}{2}\right) \Gamma\left(\frac{\alpha_2+\alpha_4-2u}{2}\right), \end{aligned}$$

where $s + t + u = p$. We will refer to the first line as the star-triangle relation. If we multiply these expressions by $|\tau_n|^{2\alpha_n}$ and take $\tau_n \rightarrow \infty$, we find related lower-point integrals where the exponents no longer sum to p .

$$\begin{aligned} \int \frac{d^p \tau_0}{|\tau_{01}|^{2\alpha_1} |\tau_{02}|^{2\alpha_2}} &= \frac{\Gamma(\alpha_1 + \alpha_2 - \frac{p}{2})}{\Gamma(p - \alpha_1 - \alpha_2)} \prod_{i=1}^2 \frac{\Gamma(\frac{p}{2} - \alpha_i)}{\Gamma(\alpha_i)} \frac{\pi^{p/2}}{|\tau_{12}|^{2\alpha_1+2\alpha_2-p}}, \quad (\text{B.3}) \\ \int \frac{d^p \tau_0}{|\tau_{01}|^{2\alpha_1} |\tau_{02}|^{2\alpha_2} |\tau_{03}|^{2\alpha_3}} &= \pi^{p/2} |\tau_{13}|^{p-2\alpha_1-2\alpha_2-2\alpha_3} \int_{-i\infty}^{i\infty} \frac{ds dt}{(2\pi i)^2} \left| \frac{\tau_{12}}{\tau_{13}} \right|^{2s-\alpha_1-\alpha_2} \left| \frac{\tau_{23}}{\tau_{13}} \right|^{2t-\alpha_2-\alpha_3} \\ &\quad \times \Gamma\left(\frac{\alpha_1+\alpha_2-2s}{2}\right) \Gamma\left(\frac{\alpha_3+\alpha_4-2s}{2}\right) \Gamma\left(\frac{\alpha_2+\alpha_3-2t}{2}\right) \Gamma\left(\frac{\alpha_1+\alpha_4-2t}{2}\right) \Gamma\left(\frac{\alpha_1+\alpha_3-2u}{2}\right) \Gamma\left(\frac{\alpha_2+\alpha_4-2u}{2}\right). \end{aligned}$$

We will refer to the first line as the chain integral. Note that the second lines of (B.2) and (B.3) can be expressed in terms of the so-called \bar{D} functions [79].

When looking at bulk correlators at the end of this appendix, we will encounter “massive” integrals with transverse distances playing the role of mass. For these, it is helpful to use the identity

$$(\tau^2 + y^2)^{-\alpha} = |y|^{-2\alpha} \int_{-i\infty}^{i\infty} \frac{du}{2\pi i} \frac{\Gamma(u) \Gamma(\alpha - u)}{\Gamma(\alpha)} \left| \frac{y}{\tau} \right|^{2u}. \quad (\text{B.4})$$

B.2 Conventions

We recall here our conventions. We denote bulk coordinates with $x^\mu = (\tau^a, x^i)$, where a labels the parallel directions with respect to the flat p -dimensional defect. The bulk dimension is $d = p + q$.

Perturbation theory is based on two nonlocal actions which involve the constant

$$\mathcal{N}_{\mathfrak{s}} = \frac{2^{-\mathfrak{s}} \Gamma(\frac{p-\mathfrak{s}}{2})}{\pi^{\frac{p}{2}} \Gamma(\frac{\mathfrak{s}}{2})} . \quad (\text{B.5})$$

For the mean-field end description we use

$$S = \mathcal{N}_{\mathfrak{s}} \mathcal{N}_{-\mathfrak{s}} \int d^p \tau_1 d^p \tau_2 \frac{\hat{\phi}(\tau_1) \cdot \hat{\phi}(\tau_2)}{|\tau_{12}|^{p+\mathfrak{s}}} + \int d^p \tau \frac{\lambda}{4} (\hat{\phi} \cdot \hat{\phi})^2 \quad (\text{B.6})$$

with ϕ^I transforming as a vector of $O(N)$. The small parameter is $\varepsilon \equiv 2\mathfrak{s} - p$, and the IR fixed point is

$$\lambda_* = \frac{\Gamma(\frac{p}{2})}{2\pi^{p/2}} \frac{\varepsilon}{(N+8)} + O(\varepsilon^2) . \quad (\text{B.7})$$

For the short-range end description we use

$$S = S_{\text{SRI}} + \mathcal{N}_{\mathfrak{s}} \mathcal{N}_{-\mathfrak{s}} \int d^p \tau_1 d^p \tau_2 \frac{\hat{\chi}(\tau_1) \hat{\chi}(\tau_2)}{|\tau_{12}|^{p-\mathfrak{s}}} + \int d^p \tau g \sigma \hat{\chi} . \quad (\text{B.8})$$

The small parameter is $\delta = \frac{p-\mathfrak{s}}{2} - \Delta_{\sigma}^*$ and the IR fixed point is

$$g_*^2 = \begin{cases} 0.788392\delta + O(\delta^2), & p = 2 \\ 0.8155(3)\delta + O(\delta^2), & p = 3 \end{cases} . \quad (\text{B.9})$$

To realize these actions on a p -dimensional defect, we will take the codimension to be $q = 2 - \mathfrak{s}$ so that the bulk propagator is given by

$$\langle \phi^I(x_1) \phi^J(x_2) \rangle = \frac{\delta^{IJ}}{(x_{12}^2)^{\Delta_{\phi}}} , \quad \Delta_{\phi} = \frac{d}{2} - 1 \equiv \frac{p - \mathfrak{s}}{2} . \quad (\text{B.10})$$

When $\varepsilon \ll 1$, making the long-range $O(N)$ model a perturbation of the trivial defect, $\hat{\phi}^I$ will be the ‘+’ mode of the bulk field i.e. $\hat{\phi}^I(\tau) = \phi^I(\tau, x^i = 0)$. This allows the defect propagator to easily be written down. When $\delta \ll 1$ (and $N = 1$), we will keep the codimension the same rather than changing the sign of \mathfrak{s} which would make the starting defect trivial again. In this case, σ becomes the ‘+’ mode of ϕ .

It is worth emphasizing that kinetic terms with $\mathcal{N}_{\mathfrak{s}} \mathcal{N}_{-\mathfrak{s}}$ have been chosen to give $\hat{\phi}$ and $\hat{\chi}$ unit-normalized two-point functions in position space. As we will see in examples, a nice property of our convention is that operator norms stay the same at next-to-leading order for arbitrary powers of both $\hat{\phi}$ and $\hat{\chi}$. This can be seen by using the chain integral from (B.3) once and twice respectively. In the case of $\hat{\phi}$, we can observe that all $O(\lambda_*)$ corrections to $\langle \widehat{\phi^m} \widehat{\phi^m} \rangle$ involve the subdiagram

$$\text{bubble} = \int \frac{d^p \tau_0}{|\tau_{01}|^{p-\varepsilon} |\tau_{02}|^{p-\varepsilon}} = \frac{\pi^{p/2}}{|\tau_{12}|^{p-2\varepsilon}} \frac{\Gamma(\frac{\varepsilon}{2})^2 \Gamma(\frac{p}{2} - \varepsilon)}{\Gamma(\varepsilon) \Gamma(\frac{p-\varepsilon}{2})^2} = \frac{\pi^{p/2}}{|\tau_{12}|^{p-2\varepsilon}} \Gamma\left(\frac{p}{2}\right)^{-1} \left[\frac{4}{\varepsilon} + O(\varepsilon) \right] . \quad (\text{B.11})$$

This has an $O(\varepsilon^{-1})$ term, which is compatible with the anomalous dimensions of these operators, but there is no $O(1)$ term which would lead to a correction of the normalization. This also applies to powers of $\hat{\chi}$, for which the universal subdiagram at $O(g_*^2)$ is given by:

$$-\bullet-\bullet- = \int \frac{d^p \tau_2 d^p \tau_3}{|\tau_{12}|^{2\Delta_\chi} |\tau_{23}|^{2\Delta_\sigma^*} |\tau_{34}|^{2\Delta_\chi}} = \frac{\Gamma(\frac{p}{2} + \delta) \Gamma(\frac{p}{2} - \delta) \Gamma(\frac{p}{2} - \Delta_\sigma^*) \Gamma(\frac{p}{2} - \Delta_\sigma^* - 2\delta) \Gamma(\Delta_\sigma^* - \frac{p}{2} + \delta)^2}{|\tau_{14}|^{2\Delta_\chi - 2\delta} \pi^{-p} \Gamma(\delta) \Gamma(-\delta) \Gamma(\Delta_\sigma^*) \Gamma(\Delta_\sigma^* + \delta) \Gamma(p - \Delta_\sigma^* - \delta)^2} . \quad (\text{B.12})$$

This lacks not only an $O(1)$ term, but an $O(\delta^{-1})$ pole as well. This reflects the very simple behaviour of $\hat{\chi}$ correlators under $O(\delta)$ perturbations seen in (4.22).

B.3 Defect correlators

In this section we compute the following defect correlation functions:

$$\begin{aligned} & \langle S_n(\tau_1) S_n(\tau_2) \rangle , \quad \langle W_n(\tau_1) W_n(\tau_2) \rangle , \\ & \langle W_0(\tau_1) W_n(\tau_2) S_n(\tau_3) \rangle , \quad \langle W_0(\tau_1) W_n(\tau_2) S_{n+1}(\tau_3) \rangle , \\ & \langle W_1(\tau_1) W_n(\tau_2) S_n(\tau_3) \rangle , \quad \langle W_1(\tau_1) W_n(\tau_2) S_{n+1}(\tau_3) \rangle . \end{aligned} \quad (\text{B.13})$$

where

$$S_n \equiv (\hat{\phi} \cdot \hat{\phi})^n , \quad W_n \equiv (\hat{\phi} \cdot \hat{\phi})^n \hat{\phi}^I , \quad (\text{B.14})$$

and we suppressed $O(N)$ indices for simplicity. We will often abbreviate integrals in this section with $G_{ij} \equiv |\tau_{ij}|^{-2\Delta_\phi}$.

B.3.1 Two-point functions

We start from the two-point function of S_n . At tree-level we have

$$\langle S_n(\tau_1) S_n(\tau_2) \rangle^{(0)} = 2^{2n} n! (N/2)_n G_{12}^{2n} \quad (\text{B.15})$$

The first correction appears at $O(\lambda)$ and it is given by

$$\begin{aligned} \langle S_n(\tau_1) S_n(\tau_2) \rangle &= Z_{S_n}^2 \langle S_n(\tau_1) S_n(\tau_2) \rangle^{(0)} \\ &\quad - \frac{\lambda}{4} n! 4^{n+1} n (6n + N - 4) (N/2)_n G_{12}^{2n-2} \int d^p \tau_3 G_{13}^2 G_{23}^2 + O(\lambda^2) . \end{aligned} \quad (\text{B.16})$$

The $1/\varepsilon$ divergent piece from the integral

$$\int d^p \tau_3 G_{13}^2 G_{23}^2 = \frac{\pi^{p/2}}{\varepsilon \Gamma(\frac{p}{2})} G_{12}^2 \left(\frac{4}{\varepsilon} + 4 \log \tau_{12} + O(\varepsilon) \right) , \quad (\text{B.17})$$

is cancelled by the wave-function counterterm

$$Z_{S_n} \equiv 1 + \delta Z_{S_n} = 1 + \frac{2n\pi^{p/2}(6n + N - 4)}{\Gamma\left(\frac{p}{2}\right)} \frac{\lambda}{\varepsilon} + O(\lambda^2) , \quad (\text{B.18})$$

and at the IR fixed point we find

$$\langle S_n(\tau_1) S_n(\tau_2) \rangle \equiv \frac{C_{S_n}}{(\tau_{12}^2)^{\hat{\Delta}_{S_n}}} = \frac{4^n n! (N/2)_n (1 + O(\varepsilon^2))}{(\tau_{12}^2)^{2n\Delta_\phi + \frac{n(6n+N-4)}{N+8}\varepsilon}} . \quad (\text{B.19})$$

In particular we obtain that $\hat{\Delta}_{S_n} = \frac{np}{2} + \frac{n(12n+N-16)}{2(N+8)}\varepsilon + O(\varepsilon^2)$.

For the two-point function of W_n we have that, at tree-level (we suppress indices for simplicity)

$$\langle W_n(\tau_1) W_n(\tau_2) \rangle^{(0)} = 2^{2n} n! (N/2 + 1)_n G_{12}^{2n+1} . \quad (\text{B.20})$$

At one loop we find

$$\begin{aligned} \langle W_n(\tau_1) W_n(\tau_2) \rangle &= Z_{W_n}^2 \langle W_n(\tau_1) W_n(\tau_2) \rangle_0 \\ &- \frac{\lambda}{2} \frac{n(2\pi)^{n+1} n! (6n + N + 2) (N/2)_{n+1}}{N} G_{12}^{2n-1} \int d^p \tau_3 G_{13}^2 G_{23}^2 + O(\lambda^2) , \end{aligned} \quad (\text{B.21})$$

hence we choose

$$Z_{W_n} \equiv 1 + \delta Z_{W_n} = 1 + \frac{2n\pi^{p/2}(6n + N + 2)}{\Gamma\left(\frac{p}{2}\right)} \frac{\lambda}{\varepsilon} + O(\lambda^2) , \quad (\text{B.22})$$

and at the IR fixed point we find

$$\langle W_n(\tau_1) W_n(\tau_2) \rangle \equiv \frac{C_{W_n}}{(\tau_{12}^2)^{\hat{\Delta}_{W_n}}} = \frac{4^n n! (N/2 + 1)_n (1 + O(\varepsilon^2))}{(\tau_{12}^2)^{(2n+1)\Delta_\phi + \frac{n(6n+N+2)}{N+8}\varepsilon}} . \quad (\text{B.23})$$

In particular we obtain that $\hat{\Delta}_{W_n} = \frac{p}{4}(2n + 1) - \frac{\varepsilon(-24n^2 - 2n(N-4) + N+8)}{4(N+8)} + O(\varepsilon^2)$.

B.3.2 Three-point functions

Let us start with the three-point function with W_0 and S_n , which at tree level reads

$$\langle W_0(\tau_1) W_n(\tau_2) S_n(\tau_3) \rangle^{(0)} = 2^{2n} n! (N/2 + 1)_n G_{12} G_{23}^{2n} . \quad (\text{B.24})$$

The one-loop correction reads

$$\langle W_0(\tau_1) W_n(\tau_2) S_n(\tau_3) \rangle^{(1)} = (\delta Z_{W_n} + \delta Z_{S_n}) \langle W_0(\tau_1) W_n(\tau_2) S_n(\tau_3) \rangle^{(0)} - \frac{\lambda}{4} I_{0,n,n} , \quad (\text{B.25})$$

where the integral $I_{0,n,n}$ has the following form

$$I_{0,n,n} = \int d^p \tau_4 \left(a_n^{(1)} G_{14} G_{23}^{2n-1} G_{24}^2 G_{34} + a_n^{(2)} G_{13} G_{24}^3 G_{34} G_{23}^{2n-2} + a_n^{(3)} G_{12} G_{24}^2 G_{34}^2 G_{23}^{2n-2} \right) , \quad (\text{B.26})$$

for some combinatorial coefficients which we will fix shortly. Using the master formulae given in section B.1 it is not difficult to verify that

$$\int d^p \tau_4 G_{14} G_{24}^2 G_{34} = \frac{\pi^{p/2} G_{12} G_{23}}{\Gamma\left(\frac{p}{2}\right)} \left(\frac{2}{\varepsilon} + \mathcal{A}_p - 2 \log \left(\frac{\tau_{13}}{\tau_{12} \tau_{23}} \right) + O(\varepsilon) \right) , \quad (\text{B.27})$$

with $\mathcal{A}_p \equiv \psi\left(\frac{p}{2}\right) - 2\psi\left(\frac{p}{4}\right) + \psi(1)$. The second addend in the integrand above is $O(\varepsilon)$, and is therefore subleading at the IR fixed point. The last addend was computed in eq. (B.17). We also have that

$$a_n^{(1)} = 3 \times 2^{2n+3} n! n (N/2 + 1)_n , \quad a_n^{(3)} = 4^{n+1} n! n (6n + N - 4) (N/2 + 1)_n . \quad (\text{B.28})$$

When plugging these results into eq. (B.25) and using (B.22), (B.18) we find that the $1/\varepsilon$ poles cancel out, as they should. At the IR fixed point the renormalized result becomes a conformal three-point correlation function with overall coefficient given by

$$C_{W_0 W_n S_n} = 4^n n! (N/2 + 1)_n \left(1 - \varepsilon \frac{3n}{N+8} \mathcal{A}_p + O(\varepsilon^2) \right) . \quad (\text{B.29})$$

Dividing this by the normalizations of the operators we find the first line of (3.44).

For the three-point function with S_{n+1} , at tree-level we have

$$\langle W_0(\tau_1) W_n(\tau_2) S_{n+1}(\tau_3) \rangle^{(0)} = 2^{2n+1} (n+1)! (N/2 + 1)_n G_{13} G_{23}^{2n+1} . \quad (\text{B.30})$$

The one-loop correction reads

$$\langle W_0(\tau_1) W_n(\tau_2) S_{n+1}(\tau_3) \rangle^{(1)} = (\delta Z_{W_n} + \delta Z_{S_{n+1}}) \langle W_0(\tau_1) W_n(\tau_2) S_{n+1}(\tau_3) \rangle^{(0)} - \frac{\lambda}{4} I_{0,n,n+1} , \quad (\text{B.31})$$

where the integral $I_{0,n,n+1}$ has the following form

$$I_{0,n,n+1} = \int d^p \tau_4 \left(a_n^{(1)} G_{14} G_{23}^{2n} G_{24}^2 G_{34}^2 + a_n^{(2)} G_{13} G_{24}^2 G_{34}^2 G_{23}^{2n-1} + a_n^{(3)} G_{12} G_{24} G_{34}^3 G_{23}^{2n-1} \right) . \quad (\text{B.32})$$

The integrals are the same that we have computed in (B.27), in particular the third addend above is again $O(\varepsilon)$. The combinatorial coefficients are found to be

$$\begin{aligned} a_n^{(1)} &= 2^{2n+3} (n+1)! (6n + N + 2) (N/2 + 1)_n , \\ a_n^{(2)} &= 2^{2n+3} (n+1)! n (6n + N + 2) (N/2 + 1)_n . \end{aligned} \quad (\text{B.33})$$

When plugging these results into eq. (B.31) and using (B.22), (B.18) we find that the $1/\varepsilon$ poles cancel out, as they should. At the IR fixed point the renormalized result becomes a conformal three-point correlation function with overall coefficient given by

$$C_{W_0 W_n S_{n+1}} = 2^{2n+1} (n+1)! (N/2+1)_n \left(1 - \varepsilon \frac{2+6n+N}{2(N+8)} \mathcal{A}_p + O(\varepsilon^2) \right). \quad (\text{B.34})$$

Dividing this by the normalizations of the operators we find the second line of (3.44).

Next, we compute the three-point function with W_1 and S_n . At tree level we have

$$\langle W_1(\tau_1) W_n(\tau_2) S_n(\tau_3) \rangle^{(0)} = 3 \times 2^{2n+1} n! n (N/2+1)_n G_{12}^2 G_{12} G_{23}^{2n-1}, \quad (\text{B.35})$$

while the one-loop correction reads

$$\langle W_1(\tau_1) W_n(\tau_2) S_n(\tau_3) \rangle^{(1)} = (\delta Z_{W_1} + \delta Z_{W_n} + \delta Z_{S_n}) \langle W_1(\tau_1) W_n(\tau_2) S_n(\tau_3) \rangle^{(0)} - \frac{\lambda}{4} I_{1,n,n}. \quad (\text{B.36})$$

The quantity $I_{1,n,n}$ is (we disregarded a tadpole diagram which vanishes in dimreg)

$$\begin{aligned} I_{1,n,n} = \int d^p \tau_4 & \left(a_n^{(1)} G_{12} G_{14}^2 G_{23}^{2n-1} G_{24} G_{34} + a_n^{(2)} G_{12} G_{13} G_{14} G_{24}^2 G_{23}^{2n-2} G_{34} + a_n^{(3)} G_{12} G_{13}^2 G_{23}^{2n-3} G_{24}^3 G_{34} \right. \\ & + a_n^{(4)} G_{12}^2 G_{14} G_{23}^{2n-4} G_{24} G_{34}^2 + a_n^{(5)} G_{12}^2 G_{13} G_{23}^{2n-3} G_{24}^2 G_{34}^2 + a_n^{(6)} G_{12}^3 G_{23}^{2n-3} G_{24} G_{34}^3 \\ & \left. + a_n^{(7)} G_{13} G_{23}^{2n-1} G_{14}^2 G_{24}^2 + a_n^{(8)} G_{13}^2 G_{23}^{2n-2} G_{14} G_{24}^3 + a_n^{(9)} G_{24} G_{23}^{2n} G_{14}^3 \right), \end{aligned} \quad (\text{B.37})$$

for some combinatorial coefficients $a_n^{(k)}$. As it turns out upon using the master formulae of section B.1, in the expression above the terms proportional to $a_n^{(3)}$, $a_n^{(6)}$, $a_n^{(8)}$ and $a_n^{(9)}$ are all $O(\varepsilon)$. The relevant integrals were computed earlier, and for the combinatorial coefficients we find

$$\begin{aligned} a_n^{(1)} &= 4^{2+n} n! n (8+N) (N/2+1)_n, \\ a_n^{(2)} &= 4^{n+2} n! n (18n+N-10) (N/2+1)_n, \\ a_n^{(4)} &= 3 \times 2^{2n+3} n! n (6n+N-4) (N/2+1)_n, \\ a_n^{(5)} &= 3 \times 2^{2n+3} n! (n-1) n (6n+N-4) (N/2+1)_n, \\ a_n^{(7)} &= 2^{2n+3} n! n (N+8) (N/2+1)_n. \end{aligned} \quad (\text{B.38})$$

When plugging these results into eq. (B.36) and using (B.22), (B.18) the $1/\varepsilon$ poles cancel. At the IR fixed point the renormalized result becomes a conformal three-point correlation function with coefficient

$$C_{W_1 W_n S_{n+1}} = \frac{3 \times 2^{2n+1} n \Gamma(n+1) \Gamma(n+1 + \frac{N}{2})}{\Gamma(\frac{N}{2}+1)} \left(1 - \varepsilon \frac{54n+7N-16}{6(N+8)} \mathcal{A}_p + O(\varepsilon^2) \right). \quad (\text{B.39})$$

Dividing this by the normalizations of the operators we find the third line of (3.44).

With no extra complications we can also compute the one-loop correction to the three-point function with S_{n+1} . The final result reads

$$C_{W_1 W_n S_{n+1}} = \frac{1}{N} 4^{1+n} (6n + N + 2) \Gamma(n + 2) \left(\frac{N}{2} \right)_{n+1} \times \left(1 - \varepsilon \frac{n(54n + 17N + 28) + 3(N + 2)}{(N + 8)(6n + N + 2)} \mathcal{A}_p + O(\varepsilon^2) \right). \quad (\text{B.40})$$

Dividing this by the normalizations of the operators we find the fourth line of (3.44).

B.4 Bulk two-point functions

Finally, we will verify that (3.35) and (3.20) can be found with traditional perturbation theory for the two-point function of the bulk field. This will require us to perturb around a trivial defect at the mean-field end and a non-trivial defect at the short-range end. Had we taken $\Phi = \chi$, the roles of the trivial and non-trivial defects would have been exchanged. It will be convenient to work with the connected two-point function

$$\langle \phi(x_1) \phi(x_2) \rangle_c = \langle \phi(x_1) \phi(x_2) \rangle - |x_{12}|^{-2\Delta_\phi} \quad (\text{B.41})$$

which has a well defined limit as $x_1 \rightarrow x_2$. The subtracted term $|x_{12}|^{-2\Delta_\phi} = (\tau^2 + y^2)^{-\Delta_\phi}$ is the only piece whose decomposition into defect channel blocks has non-zero transverse spin.

B.4.1 Around the mean-field end

The tree-level contribution is just the correlator in the presence of a trivial defect of co-dimension $q = 2 - \mathfrak{s}$, which has $b_0^{\phi,+} = 1$ and $b_0^{\phi,-} = 0$. The first non-trivial correction to the connected correlator comes at $O(\lambda^2)$, and reads

$$\begin{aligned} \langle \phi^I(x_1) \phi^J(x_2) \rangle_c^{(2)} &= 2(N + 2) \delta^{IJ} \lambda^2 \int \frac{d^p \tau_3 d^p \tau_4}{|x_{13}|^{2\Delta_\phi} |\tau_{34}|^{6\Delta_\phi} |x_{24}|^{2\Delta_\phi}} \\ &= 2(N + 2) \delta^{IJ} \lambda^2 \frac{\pi^p \Gamma\left(\frac{p}{2} - 3\Delta_\phi\right)}{|y_1|^{2\Delta_\phi} |y_2|^{2\Delta_\phi} |\tau_{12}|^{6\Delta_\phi - 2p} \Gamma(\Delta_\phi)^2 \Gamma(3\Delta_\phi)} \\ &\quad \times \int_{-i\infty}^{+i\infty} \frac{dt du}{(2\pi i)^2} \frac{\Gamma\left(\frac{p}{2} - t\right) \Gamma\left(\frac{p}{2} - u\right) \Gamma(\Delta_\phi - t) \Gamma(\Delta_\phi - u) \Gamma(-p + t + u + 3\Delta_\phi)}{\Gamma\left(-3\Delta_\phi + \frac{3p}{2} - t - u\right) |\tau_{12}|^{2(t+u)} |y_1|^{-2t} |y_2|^{-2u}}. \end{aligned} \quad (\text{B.42})$$

In the second line, we have used (B.4). To compute this integral, we can deform the contours such that poles for positive t, u and negative t, u are separated, and then close to the left, picking up the poles with negative t, u . This yields a result which can be decomposed into only the $s = 0$ blocks of eq. (2.4) because there is no dependence on the transverse angle as expected. Adding

back the tree-level contribution, this function is

$$\langle \phi^I(x_1) \phi^J(x_2) \rangle = \frac{\delta^{IJ}}{(|y_1||y_2|)^{p/2}} \left((b_0^{\phi,+})^2 \hat{g}_0^{(+)}(\hat{r}, \hat{\eta}) + (b_0^{\phi,-})^2 \hat{g}_0^{(-)}(\hat{r}, \hat{\eta}) \right) + O(\varepsilon^3), \quad (\text{B.43})$$

where

$$(b_0^{\phi,+})^2 = 1 + \frac{(N+2)\Gamma(-\frac{p}{4})\Gamma(\frac{p}{2})^2}{2(N+8)^2\Gamma(\frac{3p}{4})}\varepsilon^2, \quad (b_0^{\phi,-})^2 = \frac{(N+2)\Gamma(1-\frac{p}{4})^2\Gamma(\frac{p}{2})^2}{2(N+8)^2\Gamma(\frac{p}{4}+1)^2}\varepsilon^2. \quad (\text{B.44})$$

The ratio

$$(b_0^{\phi,-})^2/(b_0^{\phi,+})^2 = \frac{(N+2)\Gamma(1-\frac{p}{4})^2\Gamma(\frac{p}{2})^2}{2(N+8)^2\Gamma(\frac{p}{4}+1)^2}\varepsilon^2 + O(\varepsilon^3), \quad (\text{B.45})$$

can then be used to see that we get precisely (3.35) to $O(\varepsilon^2)$. Another way to extract a_{ϕ^2} quickly is to use the fact that it is the coefficient of $|y|^{-2\Delta_\phi}$ in the connected correlator when we set $y_1 = y_2 = y$ and take $\tau_{12} \rightarrow 0$. In this limit, only the residues with $t + u = p - 3\Delta_\phi$ contribute.

B.4.2 Around the short-range end

The other extreme for a defect with $q = 2 - \mathfrak{s}$ is to take $b_0^{\phi,+} = 0$. This choice, which is required to reach the short-range end, implies $(b_0^{\phi,-})^2 = \frac{\Gamma(\frac{2-\mathfrak{s}}{2})\Gamma(\frac{p+\mathfrak{s}}{2})}{\Gamma(\frac{2+\mathfrak{s}}{2})\Gamma(\frac{p-\mathfrak{s}}{2})}$. When these two coefficients are specified, we know the defect channel decomposition of the connected two-point function. We can therefore take $x_1 \rightarrow x_2$ (meaning $\hat{r} \rightarrow 1$) to get

$$\begin{aligned} |y|^{2\Delta_\phi} \langle \phi(\tau, y) \phi(\tau, y) \rangle_c^{(0)} &= (b_0^{\phi,-})^2 {}_2F_1(p - \Delta_\phi, p/2; 1 - \Delta_\phi + p/2; 1) - {}_2F_1(\Delta_\phi, p/2; 1 + \Delta_\phi - p/2; 1) \\ &= \begin{cases} -\frac{7}{8} + \delta, & p = 2 \\ -0.575 + 0.749\delta, & p = 2 \end{cases}, \end{aligned} \quad (\text{B.46})$$

matching (2.16). This is the one-point function without any interactions. Accounting for two $\sigma\hat{\chi}$ insertions is very similar to what we did before except now the defect will have one $\hat{\chi}$ propagator instead of three $\hat{\phi}$ propagators. Going through the same steps

$$\begin{aligned} \langle \phi(x_1) \phi(x_2) \rangle_c^{(2)} &= \frac{g^2(b_0^{\phi,-})^2}{2} \int \frac{d^p \tau_3 d^p \tau_4}{|x_{13}|^{2\Delta_\sigma^*} |\tau_{34}|^{2\Delta_\chi} |x_{24}|^{2\Delta_\sigma^*}} \\ &= \frac{g^2(b_0^{\phi,-})^2}{2} \frac{\pi^p \Gamma(\frac{p}{2} - \Delta_\sigma^*)}{|y_1|^{\Delta_\sigma^* + \Delta_\chi} |y_2|^{\Delta_\sigma^* + \Delta_\chi} |\tau_{12}|^{2\Delta_\sigma^* - 2p} \Gamma(\Delta_\chi)^2 \Gamma(\Delta_\sigma^*)} \\ &\quad \times \int_{-i\infty}^{+i\infty} \frac{dt du}{(2\pi i)^2} \frac{\Gamma(\frac{p}{2} - t) \Gamma(\frac{p}{2} - u) \Gamma(\Delta_\chi - t) \Gamma(\Delta_\chi - u) \Gamma(-p + t + u + \Delta_\sigma^*)}{\Gamma(-\Delta_\sigma^* + \frac{3p}{2} - t - u) |\tau_{12}|^{2(t+u)} |y_1|^{-2t} |y_2|^{-2u}}. \end{aligned} \quad (\text{B.47})$$

We can now take the residue at $u = p - \Delta_\sigma^* - t$ and use the first Barnes lemma to conclude

$$|y|^{2\Delta_\phi} \langle \phi(\tau, y) \phi(\tau, y) \rangle_c^{(2)} = \frac{g^2 (b_0^{\phi, -})^2}{2} \frac{\Gamma(\frac{p}{2} - \Delta_\sigma^*) \Gamma(\Delta_\sigma^* + 2\Delta_\chi - p) \Gamma(\Delta_\sigma^* + \Delta_\chi - \frac{p}{2})^2}{\Gamma(\frac{p}{2}) \Gamma(2\Delta_\sigma^* + 2\Delta_\chi - p) \Gamma(\Delta_\chi)^2} . \quad (\text{B.48})$$

It is now a simple matter to plug in the fixed point and the numerical Δ_σ^* . Doing so and adding (B.46) recovers the result (3.20) originally obtained from the OPE relations.

C More bulk two-point function at one loop

In this section we consider composite bulk operators $S_n = (\phi \cdot \phi)^n$ and compute their two-point function at one-loop in perturbation theory around the mean-field end of long-range $O(N)$ models. As we discuss this correlator exchanges infinitely-many defect primaries, whose scaling dimensions receive corrections at $O(\varepsilon)$. Hence we have access to further perturbative data for LRI composite operators.

Preliminaries: decomposition of the GFF-trivial defect

Consider the bulk-two point function for a bulk scalar operator with scaling dimension Δ_O in the presence of a trivial defect. With the defect blocks of (2.4) we find

$$\langle O(x_1) O(x_2) \rangle_{\text{triv}} = \frac{1}{(x_{12}^2)^{\Delta_O}} = \frac{1}{(|y_1||y_2|)^{\Delta_O}} \sum_{s, m \in \mathbb{N}} (b_{s, m}^O)^2 \hat{g}_{\Delta_O + s + 2m, s}(\hat{r}, \hat{\eta}) , \quad (\text{C.1})$$

where [80]

$$(b_{s, m}^O)^2 = \frac{2^s \Gamma(\frac{q}{2} + s) \Gamma(-\frac{d}{2} + m + \Delta_O + 1) \Gamma(2m + s + \Delta_O) \Gamma(m + s + \Delta_O - \frac{p}{2})}{\Gamma(\Delta_O) \Gamma(m + 1) \Gamma(s + 1) \Gamma(-\frac{d}{2} + \Delta_O + 1) \Gamma(m + \frac{q}{2} + s) \Gamma(2m + s + \Delta_O - \frac{p}{2})} . \quad (\text{C.2})$$

These coefficients are seen to be positive for Δ_O above the unitarity bound and integer s , as they should. As a check, when $\Delta_O = \Delta_\phi = d/2 - 1$ all but $(b_{s, 0}^\phi)^2$ vanish, and we recover (2.9). Note that for $\Delta_O \neq d/2 - 1$ there are infinitely-many $s = 0$ defect blocks that contribute.

Computation

Using the conventions of appendix B we have that, at tree-level

$$\langle S_n(x_1) S_n(x_2) \rangle^{(0)} = 2^{2n} n! (N/2)_n G_{12}^{2n} . \quad (\text{C.3})$$

The conformal block expansion of this bulk two-point function can be obtained from the result of eq. (C.1). We therefore find a family of defect primaries of the following form

$$\psi_{s, k} \sim S_n(\partial_\perp^2)^k \partial_\perp^{i_1} \dots \partial_\perp^{i_s} S_n - \text{traces}, \quad (\text{C.4})$$

with spin s and with tree-level scaling dimensions

$$\hat{\Delta}_{s,k} = 2n\Delta_\phi + 2k + s . \quad (\text{C.5})$$

The first correction appears at $O(\lambda)$ and it is given by

$$\begin{aligned} \langle S_n(x_1) S_n(x_2) \rangle &= \langle S_n(x_1) S_n(x_2) \rangle^{(0)} \\ &\quad - \underbrace{\frac{\lambda}{4} n! 4^{n+1} n(6n + N - 4) (N/2)_n G_{12}^{2n-2}}_{\equiv \mathcal{C}_S} \int d^d \tau_3 G_{13}^2 G_{23}^2 + O(\lambda^2) . \end{aligned} \quad (\text{C.6})$$

Note that there is no wave-function renormalization for S_n . From the integral alone we get

$$\frac{1}{(x_{12}^2)^{-2\Delta_\phi(n-1)}} \sum_{i,j=0}^{\infty} \left[\frac{A_{ij}(\Delta_\phi)}{(\tau_{12}^2)^{2\Delta_\phi+i+j}} (|y_1|^{2j} |y_2|^{-4\Delta_\phi+2i+p} + (1 \leftrightarrow 2)) + \frac{B_{ij}(\Delta_\phi)}{(\tau_{12}^2)^{(4\Delta_\phi+i+j-p/2)}} |y_2|^{2i} |y_1|^{2j} \right] , \quad (\text{C.7})$$

with

$$\begin{aligned} A_{ij}(\Delta_\phi) &= \frac{\pi^{p/2} (-1)^{i+j} \Gamma(i+j+2\Delta_\phi) \Gamma(-i+2\Delta_\phi - \frac{p}{2}) \Gamma(-j+\frac{p}{2} - 2\Delta_\phi)}{i! j! \Gamma(2\Delta_\phi)^2 \Gamma(-i-j+\frac{p}{2} - 2\Delta_\phi)} , \\ B_{ij}(\Delta_\phi) &= \frac{\pi^{p/2} (-1)^{i+j} \Gamma(-i+\frac{p}{2} - 2\Delta_\phi) \Gamma(-j+\frac{p}{2} - 2\Delta_\phi) \Gamma(i+j+4\Delta_\phi - \frac{p}{2})}{i! j! \Gamma(2\Delta_\phi)^2 \Gamma(-i-j+p-4\Delta_\phi)} . \end{aligned} \quad (\text{C.8})$$

Upon including all the prefactors, evaluating at the IR fixed point and expanding in ε we get

$$\begin{aligned} \delta \langle S_n(x_1) S_n(x_2) \rangle^{(1)} &= \frac{2\pi^{p/2} \mathcal{C}_S \log(\zeta) \zeta^{-\frac{p}{2}} {}_2F_1\left(\frac{1}{2}, \frac{p}{2}; 1; -\frac{4}{\zeta}\right)}{\Gamma\left(\frac{p}{2}\right) |y_1|^{np} (2 - 2\hat{\eta} + \zeta)^{\frac{1}{2}(n-1)p}} \\ &\quad - \mathcal{C}_S \sum_{k=0}^{\infty} \frac{(-1)^k 2^{2k+1} \pi^{\frac{p-1}{2}} \Gamma\left(k+\frac{1}{2}\right) \Gamma\left(k+\frac{p}{2}\right)}{\Gamma(k+1)^2 \Gamma\left(\frac{p}{2}\right)^2} \left(-2H_k + H_{k-\frac{1}{2}} + \psi\left(k+\frac{p}{2}\right) + \gamma + \log 4 \right) \\ &\quad \times |y_1|^{-np} \zeta^{-k-\frac{p}{2}} (2 - 2\hat{\eta} + \zeta)^{-\frac{1}{2}(n-1)p} + O(\varepsilon^2) , \end{aligned} \quad (\text{C.9})$$

where we have set $|y_2| = |y_1|$ for simplicity, $\hat{\eta}$ is defined in (2.5) and $\zeta = |\tau_{12}|^2/|y_1|^2 = \hat{\chi} - 2$ ($\hat{\chi}$ is defined in (2.6)).

From the coefficient of the logarithmic piece in the first line above we obtain the $O(\varepsilon)$ correction to the scaling dimensions in eq. (C.5), i.e.

$$\hat{\Delta}_{s,k}^{1\text{-loop}} = \hat{\Delta}_{s,k} + \varepsilon \hat{\gamma}_{s,k} + O(\varepsilon^2) . \quad (\text{C.10})$$

Indeed

$$\frac{d}{d \log \hat{r}} \hat{g}_{\hat{\Delta}+g\gamma,s}(\hat{r}, \hat{\eta}) \Big|_{g=0} = -\gamma \hat{g}_{\hat{\Delta},s}(\hat{r}, \hat{\eta}) , \quad (\text{C.11})$$

and so

$$\frac{d}{d \log \zeta} \delta \langle S_n(x_1) S_n(x_2) \rangle = - \sum_{s,k \in \mathbb{N}} (b_{s,k}^{S_n})^2 \hat{\gamma}_{s,k} \hat{g}_{\Delta_{s,k},s}(\zeta, \hat{\eta}) \Big|_{\varepsilon=0} , \quad (\text{C.12})$$

being $(b_{s,k}^{S_n})^2$ the coefficients of (C.2). We find:

$$\hat{\gamma}_{s,k} = \left(f_{s,k} \frac{(n-1)(6n+N-4)\Gamma\left(\frac{1}{4}(2n-1)p\right)\Gamma\left(\frac{np}{2}+1\right)\Gamma\left(k+\frac{np+s}{2}-\frac{p}{2}\right)}{2^{4k}k!(N+8)\Gamma\left(k+\frac{1}{4}(2n-1)p\right)\Gamma\left(\frac{np-p}{2}+1\right)\Gamma\left(2k+\frac{np}{2}+s\right)} \right) , \quad (\text{C.13})$$

where $f_{s,k}$ are complicated polynomials of (n, p, s) , which for $k \leq 3$ are found to be

$$\begin{aligned} f_{s,0} &= 1 , \\ f_{s,1} &= 4n^2p^2 + np(8s+8-6p) + p^2(4s+8-p) - 12p(s+1) , \\ f_{s,2} &= 32n^4p^4 + 32n^3p^3(4s+12-3p) \\ &\quad - 8n^2p^2[2p^3 - p^2(8s+33) + 12p(4s+11) - 16(s^2+7s+11)] \\ &\quad + 8np(3p-4s-12)[p^3 - 4p^2(s+3) + 6p(2s+5) - 8(s+2)] \\ &\quad + p(p-4)[16(p^2-4p+6)s^2 - 8(p(p^2-12p+44)-60)s + (p-6)^2(p-4)^2] , \\ f_{s,3} &= 384n^6p^6 - 576n^5p^5(3p-4(s+5)) \\ &\quad - 96n^4p^4(3p^3 - 3p^2(4s+25) + 36p(3s+14) - 16(3s(s+11)+85)) \\ &\quad + 48n^3p^3(3p-4(s+5))(6p^3 - 3p^2(8s+35) + 24p(4s+17) - 16(s(s+16)+45)) \\ &\quad + 12n^2p^2[3p^6 - 6p^5(4s+25) + 12p^4(4s^2+70s+231) - 24p^3(s(44s+423)+994) \\ &\quad + 96p^2(s(s(4s+89)+553)+1035) - 1152p(s(s(s+18)+97)+162) + 512(3s(s(s+14)+63)+274)] \\ &\quad - 6np(3p-4(s+5))[3p^6 - 24p^5(s+4) + 12p^4(2s+9)(2s+11) \\ &\quad - 48p^3(2s+9)(4s+17) + 96p^2(s(15s+122)+245) - 768p(s(3s+23)+43) + 1024(s+3)(s+4)] \\ &\quad - (p-4)p[p^7 - 4p^6(3s+11) + 4p^5(3s(4s+33)+220) - 16p^4(2s(s(2s+33)+181)+641) \\ &\quad + 16p^3(s(44s^2+630s+2941)+4483) - 128p^2(s(s(31s+390)+1625)+2248) \\ &\quad + 128p(s+4)(s+5)(71s+237) - 9216(s+3)(s+4)(s+5)] , \\ f_{s,4} &= \dots \end{aligned} \quad (\text{C.14})$$

For $s = k = 0$ we reproduced the $O(\varepsilon)$ correction predicted by (B.19).

From the last two lines of (C.9) we obtain $O(\varepsilon)$ corrections to the (squared) tree-level bulk-defect OPE coefficients, i.e.

$$(b_{s,k}^{S_n,1\text{-loop}})^2 = (b_{s,k}^{S_n})^2 + \varepsilon(\delta b_{s,k}^{S_n})^2 + O(\varepsilon^2) , \quad (\text{C.15})$$

We find (here and below we are taking the external operators, as well as $\psi_{s,k}$ to be unit-

normalized)

$$\begin{aligned}
(\delta b_{s,0}^{S_n})^2 &= \frac{2^s n(6n + N - 4) \left(\frac{1}{2}(n-1)p\right)_s (\psi_2 + \gamma)}{(N+8)s!} , \\
(\delta b_{s,1}^{S_n})^2 &= \frac{2^{s-1} n(6n + N - 4) \left(\frac{1}{2}(n-1)p\right)_{s+1} (\psi_2 + \gamma)}{(N+8)s!(4s+4-p)(np-p+2s+2)} \left[f_{s,1} + \frac{g_{s,1}}{(np-p+2s+2)(\psi_2 + \gamma)} \right] , \\
(\delta b_{s,2}^{S_n})^2 &= \frac{2^{s-4} n(6n + N - 4) \left(\frac{1}{2}(n-1)p\right)_{s+2} (\psi_2 + \gamma)}{(N+8)s!(p-4(s+1))(p-4(s+2))((n-1)p+2(s+2))((n-1)p+2(s+3))} \\
&\quad \times \left[f_{s,2} + \frac{g_{s,2}}{2(np-p+2s+4)(np-p+2s+6)(\psi_2 + \gamma)} \right] , \\
(\delta b_{s,k}^{S_n})^2 &= \left(\frac{1}{2}(n-1)p \right)_{s+k} (\dots) \tag{C.16}
\end{aligned}$$

with $f_{s,k}$ given in (C.14), $\psi_k \equiv \psi(p/k)$, and

$$\begin{aligned}
g_{s,1} &= (p-2)p(p-4s-4)(np-p+2s+4) , \\
g_{s,2} &= (p-2)p(p-4s-8)(np-p+2s+8) [3(n-1)p^4 \\
&\quad + 2p^3(-n(8n(2n-5)+6s+41)+9s+24) \\
&\quad - 4p^2(16n^2(2s+5)-2n(27s+64)+6s^2+45s+69) \\
&\quad - 16p(n(8s^2+42s+58)-s(7s+33)-42)-64(s+3)^2] . \tag{C.17}
\end{aligned}$$

The special case of $n = 1$

The $O(\varepsilon)$ correction to the bulk two-point function of S_1 has a particularly simple defect block expansion. Eq. (C.9) does not depend on the transverse angle when $n = 1$, which means that it can be expanded into scalar defect blocks only. The anomalous dimensions of the defect operators, as well as their OPE coefficients, turn out to be simply (see (C.13) and (C.16))

$$\hat{\gamma}_{0,0} = \frac{N+2}{N+8} \delta_{s,0} \delta_{k,0} , \quad (\delta b_{s,k}^{S_n})^2 = \hat{\gamma}_{0,0} (\psi_2 + \gamma) \delta_{s,0} \delta_{k,0} . \tag{C.18}$$

The bulk channel expansion is even simpler. It only features the bulk identity, as well as the operator S_2 with coefficient

$$a_{S_2} C_{SSS_2} = -\frac{\varepsilon \hat{\gamma}_{0,0}}{2} \frac{\Gamma\left(\frac{p}{2}\right)^2}{\Gamma(p)} + O(\varepsilon^2) , \tag{C.19}$$

where $C_{SSS_2} = \sqrt{\frac{2(2+N)}{N}}$ (for unit-normalized bulk operators).

References

- [1] M. F. Paulos, J. Penedones, J. Toledo, B. C. van Rees, and P. Vieira, *The S-matrix bootstrap. Part I: QFT in AdS*, *JHEP* **11** (2017) 133, [[arXiv:1607.06109](#)].

- [2] M. Billò, V. Gonçalves, E. Lauria, and M. Meineri, *Defects in conformal field theory*, *JHEP* **04** (2016) 091, [[arXiv:1601.02883](#)].
- [3] R. Rattazzi, V. S. Rychkov, E. Tonni, and A. Vichi, *Bounding scalar operator dimensions in 4D CFT*, *JHEP* **12** (2008) 031, [[arXiv:0807.0004](#)].
- [4] S. El-Showk, M. F. Paulos, D. Poland, S. Rychkov, D. Simmons-Duffin, and A. Vichi, *Solving the 3D Ising model with the conformal bootstrap*, *Phys. Rev. D* **86** (Jul, 2012) 025022, [[arXiv:1203.6064](#)].
- [5] S. El-Showk, M. F. Paulos, D. Poland, S. Rychkov, D. Simmons-Duffin, and A. Vichi, *Solving the 3d Ising Model with the Conformal Bootstrap II. c-Minimization and Precise Critical Exponents*, *J. Stat. Phys.* **157** (2014) 869–914, [[arXiv:1403.4545](#)].
- [6] A. Dymarsky, F. Kos, P. Kravchuk, D. Poland, and D. Simmons-Duffin, *The 3d stress-tensor bootstrap*, *JHEP* **02** (2018) 164, [[arXiv:1708.05718](#)].
- [7] F. J. Dyson, *Existence of a phase-transition in a one-dimensional Ising ferromagnet*, *Commun. Math. Phys.* **12** (1969) 91–107.
- [8] M. E. Fisher, S.-K. Ma, and B. G. Nickel, *Critical exponents for long-range interactions*, *Phys. Rev. Lett.* **29** (1972) 917–920.
- [9] K. G. Wilson and M. E. Fisher, *Critical exponents in 3.99 dimensions*, *Phys. Rev. Lett.* **28** (1972) 240–243.
- [10] M. Lohmann, G. Slade, and B. C. Wallace, *Critical two-point function for long-range $O(n)$ models below the upper critical dimension*, *J. Stat. Phys.* **169** (2017) 1132–1161, [[arXiv:1705.08540](#)].
- [11] M. F. Paulos, S. Rychkov, B. C. van Rees, and B. Zan, *Conformal Invariance in the Long-Range Ising Model*, *Nucl. Phys. B* **902** (2016) 246–291, [[arXiv:1509.00008](#)].
- [12] J. Sak, *Recursion relations and fixed points for ferromagnets with long-range interactions*, *Phys. Rev.* **B8** (1973) 281–285.
- [13] C. Behan, L. Rastelli, S. Rychkov, and B. Zan, *Long-range critical exponents near the short-range crossover*, *Phys. Rev. Lett.* **118** (2017), no. 24 241601, [[arXiv:1703.03430](#)].
- [14] C. Behan, L. Rastelli, S. Rychkov, and B. Zan, *A scaling theory for the long-range to short-range crossover and an infrared duality*, *J. Phys.* **A50** (2017), no. 35 354002, [[arXiv:1703.05325](#)].

- [15] C. Behan, *Bootstrapping the long-range Ising model in three dimensions*, *J. Phys.* **A52** (2019), no. 7 075401, [[arXiv:1810.07199](#)].
- [16] E. Lauria, P. Liendo, B. C. van Rees, and X. Zhao, *Line and surface defects for the free scalar field*, [arXiv:2005.02413](#).
- [17] N. Levine and M. F. Paulos, *Bootstrapping bulk locality. Part I: Sum rules for AdS form factors*, [arXiv:2305.07078](#).
- [18] C. Behan, L. Di Pietro, E. Lauria, and B. C. Van Rees, *Bootstrapping boundary-localized interactions*, [arXiv:2009.03336](#).
- [19] C. Behan, L. Di Pietro, E. Lauria, and B. C. van Rees, *Bootstrapping boundary-localized interactions II. Minimal models at the boundary*, *JHEP* **03** (2022) 146, [[arXiv:2111.04747](#)].
- [20] D. Benedetti, R. Gurau, S. Harribey, and K. Suzuki, *Long-range multi-scalar models at three loops*, *J. Phys. A* **53** (2020), no. 44 445008, [[arXiv:2007.04603](#)].
- [21] L. F. Alday, J. Henriksson, and M. van Loon, *Taming the ε -expansion with large spin perturbation theory*, *JHEP* **07** (2018) 131, [[arXiv:1712.02314](#)].
- [22] S. Caron-Huot, *Analyticity in Spin in Conformal Theories*, *JHEP* **09** (2017) 078, [[arXiv:1703.00278](#)].
- [23] M. Hogervorst, S. Rychkov, and B. C. van Rees, *Unitarity violation at the Wilson-Fisher fixed point in $4-\epsilon$ dimensions*, *Phys. Rev. D* **93** (2016), no. 12 125025, [[arXiv:1512.00013](#)].
- [24] E. Lauria, M. Meineri, and E. Trevisani, *Radial coordinates for defect CFTs*, *JHEP* **11** (2018) 148, [[arXiv:1712.07668](#)].
- [25] D. Gaiotto, D. Mazac, and M. F. Paulos, *Bootstrapping the 3d Ising twist defect*, *JHEP* **03** (2014) 100, [[arXiv:1310.5078](#)].
- [26] P. Liendo, L. Rastelli, and B. C. van Rees, *The Bootstrap Program for Boundary CFT_d*, *JHEP* **07** (2013) 113, [[arXiv:1210.4258](#)].
- [27] F. Gliozzi, P. Liendo, M. Meineri, and A. Rago, *Boundary and Interface CFTs from the Conformal Bootstrap*, *JHEP* **05** (2015) 036, [[arXiv:1502.07217](#)].
- [28] S. Giombi and H. Khanchandani, *$O(N)$ Models with Boundary Interactions and their Long Range Generalizations*, [arXiv:1912.08169](#).

- [29] D. Simmons-Duffin, *The lightcone bootstrap and the spectrum of the 3d Ising CFT*, *JHEP* **03** (2017) 086, [[arXiv:1612.08471](#)].
- [30] M. Reehorst, *Rigorous bounds on irrelevant operators in the 3d Ising model CFT*, *JHEP* **09** (2022) 177, [[arXiv:2111.12093](#)].
- [31] A. B. Zamolodchikov, *Renormalization Group and Perturbation Theory Near Fixed Points in Two-Dimensional Field Theory*, *Sov. J. Nucl. Phys.* **46** (1987) 1090.
- [32] N. Chai, M. Goykhman, and R. Sinha, *Long-range vector models at large N* , *JHEP* **09** (2021) 194, [[arXiv:2107.08052](#)].
- [33] L. Di Pietro, E. Lauria, and P. Niro, *3d large N vector models at the boundary*, *SciPost Phys.* **11** (2021), no. 3 050, [[arXiv:2012.07733](#)].
- [34] L. Di Pietro, E. Lauria, and P. Niro, *Vacuum stability, fixed points, and phases of QED_3 at large N_f* , [arXiv:2301.04611](#).
- [35] M. E. Fisher, S.-k. Ma, and B. G. Nickel, *Critical Exponents for Long-Range Interactions*, *Phys. Rev. Lett.* **29** (1972) 917–920.
- [36] C. C. Behan, *Bootstrapping some continuous families of conformal field theories*. PhD thesis, Stony Brook U., 2019.
- [37] S. Rychkov and Z. M. Tan, *The ϵ -expansion from conformal field theory*, *J. Phys. A* **48** (2015), no. 29 29FT01, [[arXiv:1505.00963](#)].
- [38] S. Giombi and V. Kirilin, *Anomalous dimensions in CFT with weakly broken higher spin symmetry*, *JHEP* **11** (2016) 068, [[arXiv:1601.01310](#)].
- [39] A. Antunes and C. Behan, *Coupled Minimal Conformal Field Theory Models Revisited*, *Phys. Rev. Lett.* **130** (2023), no. 7 071602, [[arXiv:2211.16503](#)].
- [40] D. Simmons-Duffin, *Projectors, Shadows, and Conformal Blocks*, *JHEP* **04** (2014) 146, [[arXiv:1204.3894](#)].
- [41] J. Liu, D. Meltzer, D. Poland, and D. Simmons-Duffin, *The Lorentzian inversion formula and the spectrum of the 3d $O(2)$ CFT*, *JHEP* **09** (2020) 115, [[arXiv:2007.07914](#)].
- [42] S. M. Chester, W. Landry, J. Liu, D. Poland, D. Simmons-Duffin, N. Su, and A. Vichi, *Carving out OPE space and precise $O(2)$ model critical exponents*, *JHEP* **06** (2020) 142, [[arXiv:1912.03324](#)].

- [43] L. F. Alday and A. Bissi, *Loop corrections to supergravity on $AdS_5 \times S^5$* , *Phys. Rev. Lett.* **119** (2017) 171601, [[arXiv:1706.02388](#)].
- [44] F. Aprile, J. M. Drummon, P. Heslop, and H. Paul, *Quantum gravity from conformal field theory*, *JHEP* **01** (2018) 035, [[arXiv:1706.02822](#)].
- [45] F. Aprile, J. M. Drummond, P. Heslop, and H. Paul, *Unmixing supergravity*, *JHEP* **02** (2018) 133, [[arXiv:1706.08456](#)].
- [46] L. F. Alday and S. Caron-Huot, *Gravitational S-matrix from CFT dispersion relations*, *JHEP* **12** (2018) 017, [[arXiv:1711.02031](#)].
- [47] I. Heemskerk, J. Penedones, J. Polchinski, and J. Sully, *Holography from conformal field theory*, *JHEP* **10** (2009) 079, [[arXiv:0907.0151](#)].
- [48] M. Hogervorst and B. C. van Rees, *Crossing symmetry in alpha space*, *JHEP* **11** (2017) 193, [[arXiv:1702.08471](#)].
- [49] J. Liu, E. Perlmutter, V. Rosenhaus, and D. Simmons-Duffin, *d-dimensional SYK, AdS loops, and 6j symbols*, *JHEP* **03** (2019) 052, [[arXiv:1808.00612](#)].
- [50] R. Gopakumar and A. Sinha, *On the Polyakov Mellin bootstrap*, *JHEP* **12** (2018) 040, [[arXiv:1809.10975](#)].
- [51] C. Behan, P. Ferrero, and X. Zhou, *More on holographic correlators: Twisted and dimensionally reduced structures*, *JHEP* **04** (2021) 008, [[arXiv:2101.04114](#)].
- [52] C. Behan, *Holographic S-fold theories at one-loop*, *SciPost Phys.* **12** (2022) 149, [[arXiv:2202.05261](#)].
- [53] L. F. Alday, *Large spin perturbation theory for conformal field theories*, *Phys. Rev. Lett.* **119** (2017) 111601, [[arXiv:1611.01500](#)].
- [54] E. Witten, *Multi-trace operators, boundary conditions, and AdS/CFT correspondence*, [hep-th/0112258](#).
- [55] F. Kos, D. Poland, and D. Simmons-Duffin, *Bootstrapping Mixed Correlators in the 3D Ising Model*, *JHEP* **11** (2014) 109, [[arXiv:1406.4858](#)].
- [56] D. Simmons-Duffin, *A semidefinite program solver for the conformal bootstrap*, *JHEP* **06** (2015) 174, [[arXiv:1502.02033](#)].

- [57] F. Kos, D. Poland, D. Simmons-Duffin, and A. Vichi, *Bootstrapping the $O(N)$ archipelago*, *JHEP* **11** (2015) 106, [[arXiv:1504.07997](#)].
- [58] F. Kos, D. Poland, D. Simmons-Duffin, and A. Vichi, *Precision islands in the Ising and $O(N)$ models*, *JHEP* **08** (2016) 036, [[arXiv:1603.04436](#)].
- [59] J. Rong and N. Su, *Bootstrapping the minimal $\mathcal{N} = 1$ superconformal theory in three dimensions*, *JHEP* **06** (2021) 154, [[arXiv:1807.04434](#)].
- [60] A. Atanasov, A. Hillman, and D. Poland, *Bootstrapping the minimal 3D SCFT*, *JHEP* **11** (2018) 140, [[arXiv:1807.05702](#)].
- [61] S. M. Chester, W. Landry, J. Liu, D. Poland, D. Simmons-Duffin, N. Su, and A. Vichi, *Bootstrapping Heisenberg magnets and their cubic instability*, *Phys. Rev.* **D104** (2021) 105013, [[arXiv:2011.14647](#)].
- [62] R. S. Erramilli, L. V. Iliesiu, P. Kravchuk, A. Liu, D. Poland, and D. Simmons-Duffin, *The Gross-Neveu-Yukawa archipelago*, *JHEP* **02** (2023) 036, [[arXiv:2210.02492](#)].
- [63] A. de la Fuente, *Bootstrapping mixed correlators in the 2d ising model*, [arXiv:1904.09801](#).
- [64] N. B. Agmon, S. M. Chester, and S. S. Pufu, *The M-theory archipelago*, *JHEP* **02** (2020) 010, [[arXiv:1907.13222](#)].
- [65] A. Chalabi, C. P. Herzog, K. Ray, B. Robinson, J. Sisti, and A. Stergiou, *Boundaries in free higher derivative conformal field theories*, *JHEP* **04** (2023) 098, [[arXiv:2211.14335](#)].
- [66] M. Picco, *Critical behavior of the Ising model with long range interactions*, [arXiv:1207.1018](#).
- [67] M. C. Angelini, G. Parisi, and F. Ricci-Tersenghi, *Relations between short-range and long-range Ising models*, *Phys. Rev.* **E89** (2014) 062120, [[arXiv:1401.6805](#)].
- [68] C. Behan, *Unitary subsector of generalized minimal models*, *Phys. Rev. D* **97** (May, 2018) 094020, [[arXiv:1712.06622](#)].
- [69] D. Poland, V. Prilepina, and P. Tadić, *The five-point bootstrap*, [arXiv:2305.08914](#).
- [70] M. Reehorst, S. Rychkov, D. Simmons-Duffin, B. Sirois, N. Su, and B. van Rees, *Navigator function for the conformal bootstrap*, *SciPost Phys.* **11** (2021) 072, [[arXiv:2104.09518](#)].
- [71] A. Liu, D. Simmons-Duffin, N. Su, and B. C. van Rees, *Skydiving to bootstrap islands*, [arXiv:2307.13046](#).

- [72] K. Ghosh and Z. Zheng, *Numerical conformal bootstrap with analytic functionals and outer approximation*, [arXiv:2307.11144](#).
- [73] S. El-Showk and M. F. Paulos, *Bootstrapping conformal field theories with the extremal functional method*, *Phys. Rev. Lett.* **111** (Dec, 2013) 241601, [[arXiv:1211.2810](#)].
- [74] L. Bianchi, A. Chalabi, V. Procházka, B. Robinson, and J. Sisti, *Monodromy defects in free field theories*, *JHEP* **08** (2021) 013, [[arXiv:2104.01220](#)].
- [75] J. Henriksson, S. R. Kousvos, and M. Reehorst, *Spectrum continuity and level repulsion: the Ising CFT from infinitesimal to finite ε* , *JHEP* **02** (2023) 218, [[arXiv:2207.10118](#)].
- [76] A. Richards, *University of Oxford Advanced Research Computing, Zendo* (2015).
- [77] W. Landry and D. Simmons-Duffin, *Scaling the semidefinite program solver SDPB*, [arXiv:1909.09745](#).
- [78] K. Symanzik, *On calculations in conformal invariant theories*, *Lett. Nuovo Cim.* **3** (1972) 734–738.
- [79] F. A. Dolan and H. Osborn, *Conformal four point functions and the operator product expansion*, *Nucl. Phys.* **B599** (2001) 459–496, [[hep-th/0011040](#)].
- [80] M. Lemos, P. Liendo, M. Meineri, and S. Sarkar, *Universality at large transverse spin in defect CFT*, *JHEP* **09** (2018) 091, [[arXiv:1712.08185](#)].